A spectral-domain approach for the calibration of shot noise-based models of daily streamflows

UNIVERSITÀ DEGLI STUDI DI NAPOLI
FEDERICO II

Francesco Morlando

Dipartimento di Ingegneria Civile, Edile e Ambientale

A thesis submitted for the degree of

Ph.D. in Hydraulic and Environmental Engineering

Napoli, April 2015

Supervisors:

Prof. Domenico Pianese

Dr. Luigi Cimorelli

Dr. Luca Cozzolino

Ph.D. Coordinator:

Prof. Elvira Petroncelli

A Giuliano, Gianna, Maddalena, Alessia, Valeria ed Enrico
Siete stati sempre presenti. Vi voglio bene

Acknowledgements

The last three years at the Dipartimento di Ingegneria Civile, Edile e Ambientale at the University of Napoli *Federico II* have been a fascinating experience and I want to express my gratitude to some people that had a key role in the development of my work.

First of all, I would like to thank Prof. Domenico Pianese, who has been more than a mentor during the last years, teaching me the basics of being a researcher and giving me the chance to express my capacities and aptitudes autonomously.

A special thanks is needed to Dr. Luigi Cimorelli, who has been fundamental in my growing process, supporting me in the resolution of a multitude of complex problems until the night. Today we are friends and, as a friend, I wish his dream of becoming a professor come true. He deserves the best.

I would also like to express my gratitude to Dr. Giovanni Mancini, member of the Dipartimento di Ingegneria Elettrica e Tecnologie dell'Informazione at the University of Napoli *Federico II*, who introduced me to a completely new scientific field, that of the system identification, with patient and high competence.

Moreover, I would like to offer a special and sincere thanks to Prof. Alberto Montanari. It was a honour for me to be guest, for a short period, of the Dipartimento di Ingegneria Civile, Chimica, Ambientale e dei Materiali of the University of Bologna and to have started such a stimulating

collaboration with one of the world's most notorious researcher in the hydrologic field. I really hope to continue our research activities in the next future and I would like, in particular, to thank him for his words of appreciation for my skills and technical background.

A last, but not least, special thanks is for all my colleagues, friends and especially my family, for all those laughs and for all the support that have relieved my hardest days. Thank you all, guys.

Abstract

Since 50's the scientific community has been strongly interested in the modeling of several classes of stochastic processes, among which a particular attention has been attracted by hydro-meteorological phenomena. Indeed, both their synthetic reproduction and forecasting is a central point in the resolution of a wide class of problems, as the design and management of water resources systems and flood risk analysis.

Concerning the modeling of generic stochastic variables, there are two crucial aspects to be addressed: the identification of the most appropriate model able to correctly reproduce the statistical features of the real process (i.e., model selection), and the estimation of the parameters of the selected model (i.e., model calibration) from available data, concerning both input and output processes of the system to be identified.

During the last decades, considerable efforts have been undertaken by researchers to provide the scientific community with suitable calibration techniques of several class of models, resulting in the current availability of numerous procedures for the estimation of the selected model parameters. A general distinction can be made between time-domain and frequency-domain (or spectral-domain) calibration approaches, whose main difference consists in the typology of information adopted in the parameters estimation. Indeed, while the former are usually based on a numerical comparison between historical and synthetic series of the output process, spectral-domain

procedures adopt, in several ways, the frequency information content of recorded input and output series. Such a substantial difference results in some considerable advantages for frequency-domain techniques, especially in the case of unavailability of sufficiently long and simultaneous records of both input and output variables. This latter condition, in particular, is not rare in the case of hydrologic model calibration problems, since the model input sequences (e.g., rainfall and air temperature series) and the output sequence (e.g., the streamflow series) can be usually both available but not simultaneously or even unavailable (i.e., poorly gauged or ungauged basins). These considerations make recommendable the adoption of frequency-domain calibration techniques in hydrologic applications.

Starting from this proposed framework, in this thesis the author focuses on the spectral-domain calibration problem of a widely developed class of models for the modeling of daily streamflow processes, the so-called shot noise models. These models consider the river flow process as the result of a convolution of Poisson-distributed occurrences, representing the rainfall process, and a linear response function, depending on the parameters to be estimated, representing the natural basin transformations.

The technical literature provides several techniques for the calibration of this class of models, both in the time and in the frequency domain. Nevertheless, none of the existing procedures is found to take advantage of a remarkable property of shot noise models, i.e. the impulsive nature of the autocorrelation function of the input process. On the contrary, starting from this relevant feature, the proposed calibration technique allow the estimation of the basin response function parameters only through the knowledge of the power spectral density of the recorded streamflow series. Hence, on the one hand, the main drawbacks of classical time-domain calibration approaches are

solved and, on the other hand, the dependence of existing frequency-domain techniques on the availability of both input and output data is overcome.

The effectiveness of the proposed procedure is widely proved through its application to three daily streamflow series, associated to three watersheds located in the Italian territory. In particular, performances of the approach in the reproduction of the recorded flow series statistical properties are ascertained through a simulation analysis.

Table of contents

List of figures

List of tables

1. Introduction

Stochastic modeling of hydro-meteorological phenomena has always been attracting a great interest among the scientific hydrologic community, especially given the relevant interest in the generation of synthetic data that represent non-deterministic inputs to the generic system under study, thus providing a basis for undertaking a variety of water-related design, operation, and diagnostic studies. Indeed, synthetic data generation allows accounting for uncertainty and large variability of input into the related process. Several technical fields are strongly suitable for the implementation of such approaches, due to the intrinsically uncertain nature of hydro-meteorological phenomena involved, as input processes, into the problem to be solved. Moreover, the use of synthetic time series, instead of historical records, is essential for providing sufficiently large samples (e.g., with length of hundreds or thousands of years) in order to evaluate a wide range of possible outcomes [*Efstratiadis et al.*, 2014].

One could think, for instance, to design and management problems of water resources systems, as the necessity of determining the most effective scheduling of an artificial reservoir over a fixed time period, in terms of maximization of system reliability (namely the probability of satisfying the associated water uses and constraints). In these cases the generation of

streamflow series from weekly to monthly aggregation scale is usually required. Moreover, for the representation of streamflows, finer time steps are also adopted (e.g., daily), for taking into account reservoir spills [*Ilich*, 2014] and small-scale regulations. Another field of application of stochastic approaches involves the evaluation of flood risk, which requires even more detailed temporal resolutions (e.g., hourly). In particular, during the last years, a considerable attention has been paid to continuous flood modeling which makes use of synthetic rainfall [*Boughton and Droop*, 2003]. Synthetic weather data (i.e., temperature, potential evapotranspiration, solar radiation, wind velocity, etc.), can result particularly interesting in a wide range of water, energy and environmental applications, including the design and management of renewable energy systems [*Tsekouras and Koutsoyiannis*, 2014]. Furthermore, other several technical problems can be thought to be solved by the adoption of synthetic generator of river flows, as the evaluation of the long-time effects of erosion phenomena of river banks in a given section of interest, or the evaluation of the most convenient nominal power of a new hydropower system to be designed.

The basic features of hydrologic time series that a stochastic model should be able to correctly reproduce can be summarized as [*Efstratiadis et al*., 2014]:

(1) asymmetric and marginal probability distribution;

(2) persistent large amplitude variations at irregular time intervals and frequency-dependent amplitude variations;

(3) periodicity, which appears at the sub-annual scale (e.g., monthly) and is due to the Earth motion;

(4) intermittency, which is a key feature of several processes at fine temporal scales (e.g., daily rainfall and discharges) and which is quantified by the probability that the value of the process within a time interval is zero (often

referred to as probability dry). Intermittency also results in significant variability and high positive skewness, which are difficult to reproduce by most generators.

Starting from these relevant properties, the scientific literature has provided, during the last decades, several models for the generation of synthetic hydrologic time series. Among others, it is worth reporting the following: shot noise model [*Weiss*, 1977], fragment model [*Srikanthan and McMahon*, 1980], AutoRegressive Moving Average (ARMA) model [*Box et al*., 1994], Artificial Neural Networks (ANNs) [*Raman and Sunilkumar*, 1995], stochastic disaggregation model [*Valencia and Schaake*, 1973], Markov chain model [*Aksoy*, 2003], bootstrapping method [*Lall and Sharma*, 1996] and wavelets [*Bayazit and Aksoy*, 2001].

A considerable ability in the reproduction of hydrologic series, in particular river flow time series, considering a short-time scale (from daily to weekly), belongs to the aforementioned shot noise models, introduced by *Bernier* [1970]. Several hydrologic literature works have dealt with the adoption of this class of models for the reproduction of streamflow process main features [*Weiss*, 1977; *Murrone et al*., 1997; *Xu et al*., 1997; *Xu et al*., 2002; *Claps and Laio*, 2003 etc.], considering a shot noise process as input of a linear system that represents the watershed physical features.

Furthermore, several techniques have been introduced for the calibration (i.e., the estimation of the model parameters value) of shot noise-based models [*Kelman*, 1980; *Koch*, 1985; *Murrone et al*., 1997; *Xu et al*., 2002; *Claps et al.*, 2005]. Most of the existing approaches, in particular, are based on a time-domain procedure, consisting in a minimization of a cost function given by the sum of the differences between recorded and generated streamflow values. Such an approach, however, is conditioned by the high

availability of input/output recorded data, which can limit their adoption in the so-called *ungauged basins* (i.e., those basins with a limited availability of input and/or output data).

Several recent contributions have dealt with calibration problems in case of ungauged basins. Some authors have discussed about the regionalization of rare hydrologic information [*Bloeschl and Sivapalan*, 1995; *Post and Jakeman*, 1999 and *Parajka et al*., 2005, among others]. *Seibert and McDonnell* [2002], instead, investigated on the adoption of *soft-data*, which are qualitative and/or scattered records.

A further valid alternative to time-domain approaches is that offered by frequency-analysis of available input and output records, since spectral features contain information that are not obtainable by raw time series and that can be adopted to simplify the calibration procedure. A recent interesting contribution in this direction was that of *Quets et al*. [2010], who provided an interesting comparison between time and frequency-domain approaches. In general, several frequency-domain techniques have been introduced in the last years for the calibration of conceptual hydrologic models [*Labat et al*., 2000; *Kirchner et al*., 2000; *Islam and Sivakumar*, 2002; *Schaefli and Zehe*, 2009 etc.]. Among them, a great interest has been attracted by the methodology introduced by *Montanari and Toth* [2007] (and subsequently adopted by *Castiglioni et al.* [2010]), who adopted the maximum likelihood estimator introduced by *Whittle* [1953], for the estimation of non-linear hydrologic models, from the only knowledge of input and output data power spectral density estimations. In particular the authors underlined how power spectral estimates could be achieved in absence of numerous and simultaneous input/output data records., thus assessing the usefulness of spectral-domain calibration techniques also in

presence of ungauged basins. Furthermore, starting from the pioneering work of *Pegram* [1980], in the last decades a relevant contribution to the spectral calibration of shot-noise based models has been developed [*Diskin and Pegram*, 1987]. In this Ph.D. thesis, the parameters, of a hydrologic conceptual linear model, were estimated through the minimization of a cost function, given by the difference between the Laplace transform of the historical and simulated streamflow series. However, to allow the application of the whole procedure, the authors clearly took into account the different structures of input and output sequences, following the previous contribution of *Diskin* [1964].

Starting from this framework, the main aim of the present dissertation is the description of a spectral-domain approach for the calibration of shot noise-based models of streamflow processes. The whole work has to be intended as an advance of the works of *Murrone et al*., 1997 and *Claps et al*., 2005, who both adopted different time-domain procedures for the calibration of a lumped-conceptual effective rainfall-runoff model, for streamflow modeling, given by the series/parallel linear combination of linear reservoirs. The same simplified hydrological model has been adopted in the present thesis, since the central issue deals with the introduced calibration procedure, which, by taking advantage of a relevant spectral property of shot noise-based models, can allow the model calibration only by the availability of streamflow data (so, useful in the case of ungauged basins).

The thesis has been structured as follows.

In Section 2 (i.e., State of the Art), a comprehensive, but also synthetic, overview of time and frequency-domain, continuous time, calibration techniques of linear time invariant systems is provided.

Section 3 (i.e, Identification of shot noise process-based models) firstly provides a survey on the available models for the reproduction of short time scale discharge series. Among them, subsequently, a focus on the main properties of shot noise-based models is given, with the successive description of their classical calibration techniques, both in the *time* and in the *frequency domain*. Finally, the proposed calibration technique is deeply described, providing details on the techniques for the estimation of the power spectral density of the streamflow process and, moreover, on the selection and the estimation of the effective rainfall model, fundamental for the simulation analysis to be undertaken for the model validation and testing phase.

In Section 4 (i.e., Application and testing), the overall calibration procedure is applied to three case-study Italian watersheds, whose characteristics, both in physical and climate terms, are provided in the first part of the section. Subsequently, once estimated the unknown response function parameters, results of several validation tests are provided, both in numerical and graphical form, in order to assess the effectiveness of the whole procedure.

In Section 5 (i.e., Conclusions), the most important achieved results are synthetically provided.

Eventually, the author provides the reader with an appendix, in order to allow the complete understanding of the numerous spectral analysis concepts that have been introduced in the whole thesis.

2. State of the art

2.1. General aspects

The main goal of the present Ph.D. dissertation deals with the development of a spectral-domain identification technique of linear dynamic, conceptually based, continuous and time invariant models of daily river flows. In particular, the author focused his work on shot noise process-based models, deeply discussed in Section 3 of the present thesis.
In order to give to the reader the tools to understand the developed topic, in the present section a complete and synthetic description of time-domain identification techniques of linear Continuous Time (CT) invariant models is firstly provided. Secondly, frequency-domain identification procedures are analyzed in detail.

In the system identification field, the identification of linear CT Time Invariant (TI) models was one of the first objectives pursued by the scientific community. In particular, in order to assess the parameters value of a generic CT model, the technical literature provides two distinct class of approach: an *indirect* and a *direct* technique. In the former, the sampled data of input and output processes are adopted in the identification procedure of a Discrete

Time (DT) model, which is after converted in an equivalent CT model. In the latter, instead, a direct estimate of the CT model parameters is undertaken, without considering the equivalent DT model.

Several authors have discussed about advantages and disadvantages of the two approaches. In particular, *Rao and Unbehauen* [2006] and *Young and Garnier* [2006] propose an interesting survey about this topic, providing some highlights, summarized hereinafter, on the reasons why one should prefer a CT modeling to a DT one.

First of all, CT will always remain the natural basis of our understanding of the physical world, because all the physical laws (Newton's, Faraday's etc.) are in CT, with no chances of being rewritten in DT.

Secondly, the process of discretization itself is associated with some undesirable consequences. In general, a strictly proper CT rational Transfer Function (TF), $G(s)$, with n poles, transformed into its equivalent discrete expression, $G(z)$, through the well-known relations between the Laplace plane (represented by the Laplace variable, s) and the z-transform plane, remains rational and possesses generically $n-1$ zeros that cannot be expressed in closed form in terms of the s-plane parameters and the sampling time T_S (for further details the reader can refers to *Rao and Unbehauen* [2006]).

Thirdly, discretization may turn a native minimum phase CT model into a problematic one with non-minimum phase properties. As a matter of fact, as deeply described in Section 3, the identification procedure for the latter class of models is more problematic if compared to the former class.

Furthermore, the fourth problem, listed by *Rao and Unbehauen* [2006] in their work, deals with the fact that discretization gives rise to undesirable sensitivity problems at high sampling rates, that is parameters value are dependent on the adopted sampling intervals of the input and output data.

Finally, and perhaps most importantly, CT models can be identified and estimated from rapidly sampled data, whereas DT models encounter difficulties when the sampling frequency is too high in relation to the dominant frequencies of the system under study [*Astrom*, 1969]. In this situation, the eigenvalues lie too close to the unit circle in the complex domain and the discrete-time model parameter estimates become statistically ill-defined. The practical consequences of this are:

- either that the discrete-time estimation fails to converge properly, thus providing an erroneous explanation of the data;
- or that even if convergence is achieved, the continuous-time model, as obtained by standard conversion from the estimated discrete-time model, does not provide the correct continuous-time model.

From these considerations it should be evident the convenience of the adoption of the direct procedure in the identification of a CT and TI models, avoiding, in this manner, the step corresponding to the identification of an equivalent DT model. As a consequence, in the following part of the present section, a detailed review of only CT identification techniques, available in the scientific literature, is provided.

It is worth noticing that for further details on some of the concepts treated in this section (e.g., the concept of TF of a linear model, poles and zeros of the TF etc.), the interested reader can refer to Appendix.

2.2. Brief survey of CT models identification methods

The theoretical basis for the statistical identification and estimation of linear, continuous-time models from DT sampled data can be outlined by considering the following Single-Input, Single-Output (SISO) system:

$$x(t) = \frac{B(s)}{A(s)}u(t-\tau) \tag{2.1}$$

$$y(t) = x(t) + e(t) \tag{2.2}$$

where τ is any pure time delay in time units, the ratio $G(s) = B(s)/A(s)$ is the system TF, and $A(s)$ e $B(s)$ are the following polynomials in the derivative operator $s = d/dt$:

$$A(s) = s^n + a_1 s^{n-1} + \cdots + a_{n-1}s + a_n \tag{2.3}$$

$$B(s) = b_0 s^m + b_1 s^{m-1} + \cdots + b_{m-1}s + b_m \tag{2.4}$$

This transfer function model (TFM) structure is denoted by the triad [n, m, τ]. In Eq. (2.1), $u(t)$ is the input signal, $x(t)$ is the 'noise free' output signal and $y(t)$ is the noisy output signal. In the following of the dissertation, the assumption of zero mean White Noise (WN) with Gaussian amplitude distribution for the noise term $e(t)$ is considered, for the sake of simplicity, even though this is not a restrictive assumption. The two series of coefficients a_i and b_i are the sets of the model parameters to estimate.

By the principle of superposition for linear systems, $e(t)$ is a vector of stochastic disturbances which accounts for the combined effect of the input and output disturbances at the output of the system. Although the nature of this disturbance vector is not necessarily specified, it is often considered, for analytical purposes, to have rational spectral density and so to be described by the following Auto Regressive-Moving Average (ARMA) model:

$$C(s)e(t) = D(s)\xi(t) \tag{2.5}$$

where the ratio between the two polynomials $D(s)$ and $C(s)$ is the disturbance TF, $G_n(s)$, while $\xi(t)$ is a zero mean, serially uncorrelated, WN CT process.

Once analytically defined the model M structure, given by Eqs. (2.1) and (2.2), it now possible to provide the model identification approach. The most obvious approach to the estimation of the parameters in a mathematical model, of a dynamic system, is to minimise a scalar cost (or loss) function J, which is formulated in terms of some norm in an error function, $\varepsilon(t)$, which reflects the discrepancy between the output of the model M and the real system S [*Young*, 1981]. It is the choice of $\varepsilon(t)$ which most differentiates the various estimation methodologies which have been developed over the past fifty years and this is discussed in detail in this subsection.

Concerning the choice of the cost function J, instead, the most common is given by the following relation:

$$J = \sum_{i=1}^{N} \|\boldsymbol{\varepsilon}_i\|_w^2 \tag{2.6}$$

where the subscript i indicates the value of the vector $\boldsymbol{\varepsilon}(t)$ at the *i*th sampling instant, N denotes the number of samples available in the observational interval and W is the vector of the weights to associate to each of the components of the vector $\boldsymbol{\varepsilon}(t)$.

Starting from previous considerations, the following part of the present subsection is aimed at the short description of the several approaches for the CT model identification. It is worth noticing that following procedures differ, between each other, for the error function $\varepsilon(t)$ chosen in the definition of the cost function of Eq. (2.6).

The first proposed approach is known as Output Error (OE) or Response Error (RE) method and it is probably the most intuitively one to the problem of system parameter estimation. Here, the parameters are chosen so that they minimise either an instantaneous (in the purely deterministic case corresponding to the condition $e(t) = 0$) or an integral (in the stochastic case) norm in the error between the model output, denoted by $\hat{y}(t)$, and the observed output $y(t)$, i.e. with the following model error expression $\varepsilon(t) = y(t) - \hat{y}(t)$. In the SISO case system of Eqs. (2.1) and (2.2), for instance, the error function is defined as:

$$\varepsilon(t) = y(t) - \frac{\hat{B}}{\hat{A}}u(t) \tag{2.7}$$

where $\hat{B}$ and $\hat{A}$ are, respectively, the estimates of the polynomials $B(s)$ and $A(s)$ that define together the TF of the system to be identified.

The second approach is known as Equation Error (EE) method and clearly derives from an analogy with statistic regression analysis. Here, the error function is generated directly from the input-output equations of the model. In particular, considering the previously defined model M, a scalar error function is involved and it is defined as follows:

$$\varepsilon(t) = \hat{A}y(t) - \hat{B}u(t) \tag{2.8}$$

The reader will certainly note that such a definition of the error function implies the time derivatives of the input and output process [*Eykhoff*, 1974]. See, for evidence, Eqs. (2.3) and (2.4) defining expressions of the polynomials $A(s)$ and $B(s)$. It is worth noticing that in the deterministic case

(i.e. when the noise level of the measured input and output signals is low, that means with a noise/signal ratio < 5%), the (2.8) is a linear algebraic function of the unknown parameters; as a consequence, its minimization is much more straightforward than in the OE case. For this particular case, several EE schemes have been proposed in the scientific literature both for linear and nonlinear systems, and most are mentioned by [*Eykhoff*, 1974].

Nevertheless, the inherent limitations of the deterministic approach soon became apparent and many researchers suggested different solutions which were not so sensitive to stochastic disturbances of the signals. In particular, two were the main problems deriving from a deterministic approach applied to noisy signals:

- the differentiation of signals possibly affected by noise ("noisy signal");
- the asymptotic bias in the parameters estimation.

An alternative Generalized Equation Error (GEE) method is often defined to avoid the obvious problems that arise from the differentiation of noisy signal. Here, the input and output signal are passed through a State Variable Filter (SVF) set, denoted by $F(s)$, which simultaneously filters the signal and provides filtered time derivatives [*Young*, 1964], which replace the exact but unobtainable derivatives in the definition of a modified version of $\varepsilon(t)$. Furthermore, the simplest solution to the asymptotic bias problem associated with the basic EE approach is the Instrumental Variable (IV) method. Here the least squares solution is modified to include a vector of instrumental variables, $\hat{\boldsymbol{x}}$, which are chosen in order to be highly correlated with the noise-free output x of the system, but totally uncorrelated with the noise on the measurements of the system variables [*Young*, 1981].

Subsequently, the Refined IV (RIV) method, suggested by *Young* [1976], was introduced. It is a similar but more sophisticated IV procedure, which is

able to achieve asymptotic statistical efficiency by the introduction of adaptive "prefilters" on all the measured signals [*Young*, 1981].

The third reported approach is the Prediction Error (PE) method. Here, as in the OE case, the error function is usually defined as $\varepsilon(t) = y(t) - \hat{y}(t)$, but with $\hat{y}(t) = \hat{y}(t|\widehat{\boldsymbol{a}})$. As a matter of fact, in this case $\hat{y}(t)$ is defined as some best prediction of $y(t)$, given the current estimates of the parameters $\boldsymbol{a}$ that characterize the system and the noise models. In other words, $\hat{y}(t|\widehat{\boldsymbol{a}})$ is the conditional mean of $y(t)$ given all current and past information on the system. In the SISO case of model M, the most obvious PE method involves the minimization of a norm in $\varepsilon(t)$, defined as:

$$\varepsilon(t) = \frac{\hat{C}}{\hat{D}}\left[y(t) - \frac{\hat{B}}{\hat{A}}u(t)\right] \tag{2.9}$$

where polynomials $\hat{C}$ and $\widehat{D}$ define the noise model to sum to the output of the real system [*Solo*, 1978].
Of course other arrangements are possible for a PE error function definition, for example defining the error function within an EE context. For the sake of conciseness this scheme is not reported here, but one can surely state that the solution of the PE minimization problem is generally more complex than the OE and EE equivalents, since the formulation of the PE norm implies the concurrent estimation of the noise model parameters [*Young*, 1981].

The fourth reported approach can be considered as a particular case of the PE minimization and it is known as Maximum Likelihood (ML) method. It is considered separately here, however, because of its importance as a motivating concept in research. The ML approach is based on the definition

of a PE type error function, but the formulation is restricted by the additional assumption that the stochastic disturbances to the system have specified amplitude probability distribution functions [*Stepner and Mehra*, 1973; *Kallstrom et al*., 1976]. In particular, in most applications, this assumption is restricted further for analytical tractability to the case of a Gaussian distribution, in which case, the ML formulation coincides with certain PE formulations.

The ML method can often be extended so that *a priori* information on the probability distributions is included in the formulation of the problem. This is termed the Bayesian (B) approach, since it arises from Bayes rule for linking *a priori* to *a posteriori* probability statements and, so, allows for the inclusion of *a priori* information into the solutions of the estimation problem. Further details about this approach can be found in *Young* [1981].

2.3. Parameter identification of linear CT models in the frequency-domain

Model parameters estimation in the frequency-domain is of considerable interest because of its convenience in many practical situations. Information on the system behaviour under the influence of periodic test signals is the main input to spectral-domain identification algorithms. Identification in frequency-domain is discussed, in the present subsection, with reference to linear CT systems of the typology shown in Fig. 2.1., where $u(t)$ and $y(t)$ are measurable input and output signals respectively, with the output signal corrupted by the coloured immeasurable noise signal $n(t)$.

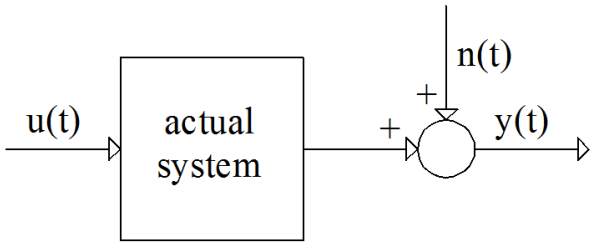

Fig. 2.1. Identification environment

A system is generally represented by its frequency-response characteristic (*Nyquist plot* or its equivalent *Bode plot*):

$$G_0(j\omega) = \frac{Y(j\omega)}{U(j\omega)} = R_0(\omega) + jI_0(\omega) \tag{2.10}$$

This information may be available at discrete frequency values, $\omega = \omega_i$, distributed, for example, logarithmically over the frequency range of interest, from computation or by direct measurement. $U(j\omega)$ and $Y(j\omega)$ are the Fourier transforms of $u(t)$ and $y(t)$, respectively, while $R_0(\omega)$ and $I_0(\omega)$ are, respectively, real and imaginary part of the complex system response function.

Measurements (or equivalently estimates) of $G_0(j\omega_i)$, for discrete values of ω_i covering the whole frequency range, can be obtained either [*Rao e Unbehauen*, 2006]:

(a) from a discrete set of measured input-output spectra $U(\omega_i)$ and $Y(\omega_i)$ for $i = 1,2 \ldots N$, or

(b) from direct excitation by periodic test signals, or

(c) indirectly from arbitrary time-domain measurements of $u(t)$ and $y(t)$, which, by Fourier transformation, convert the information into the frequency-domain.

Concerning the latter case, in particular, two main TF estimation methods are available in the literature, starting from recorded input and output signal. The first one deals with the so called Empirical Transfer Function Estimate (ETFE), given by the quotient between the Fourier transform of output and input signal [*Ljung*, 1987, Subsection 6.3]. The second one, instead, consists in the ratio between the input/output Cross-Power Spectral Density (CPSD) and the input Power Spectral Density (PSD) estimations [*Broersen*, 1995]. Even though the aim of the author is not that of focusing on a detailed description of TF estimator, it is worth noticing a fundamental feature of CPSD estimators, that is their ability in preserving both magnitude and phase information of the system frequency response. As a consequence, such an estimator can be successfully adopted both in the identification of linear TI minimum and nonminimum phase systems (for more details see, for reference, *Nikias and Mendel* [1993]).

Starting from previous considerations, assume that the system is modelled by the following expression, corresponding to the scheme reported in Fig. 2.2 (where $y_S(t)$ and $y_M(t)$ are, respectively, the output from the deterministic part of the model and the whole model output, both in the time domain):

$$Y_M(s) = G_M(s, \boldsymbol{\theta})U(s) + G_n(s, \boldsymbol{\theta})W(s) \tag{2.11}$$

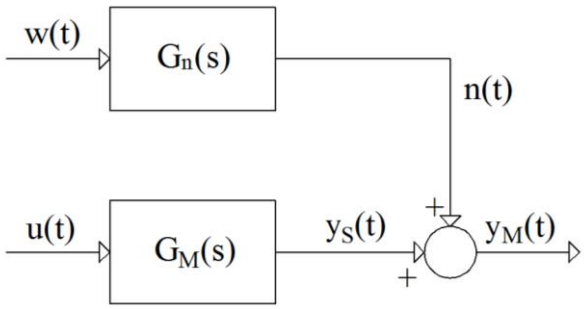

Fig. 2.2. Model of actual system

where the TF, $G_n(s,\boldsymbol{\theta})$, represents the model for the stochastic component which determines a coloured noise signal $n(t)$, from a normally distributed zero-mean WN signal $w(t)$, while the deterministic model part is described by the rational TF, $G_M(s,\boldsymbol{\theta})$, defined as follows:

$$G_M(s,\boldsymbol{\theta}) = \frac{Y_S(s)}{U(s)} = \frac{b_0+b_1 s+\cdots+b_n s^n}{a_0+a_1 s+\cdots+a_n s^n} = \frac{B(s,\boldsymbol{\theta})}{A(s,\boldsymbol{\theta})} \tag{2.12}$$

In Eq. (2.12) $Y_S(s)$ is the output, in the Laplace domain, corresponding to the considered model due to the input signal $u(t)$, with $U(s)$ its Laplace domain expression.

The parameter vector is given by:

$$\boldsymbol{\theta} = [b_0\ b_1 \dots b_n \vdots\ a_0\ a_1 \dots a_n]^T \tag{2.13}$$

The identification problem deals with the estimation of the vector $\boldsymbol{\theta}$ of the real parameters a_i and b_i $(i = 1,2 \dots n,)$. For this purpose, generally, the Laplace transform, E^*, of the output error, e^*, is introduced (as defined in Fig. 2.3):

$$E^*(s,\theta) = G_n^{-1}(s,\theta)[Y(s) - Y_S(s,\theta)] \tag{2.14}$$

where $Y(s)$ is the Laplace transform of the actual system output, $y(t)$.

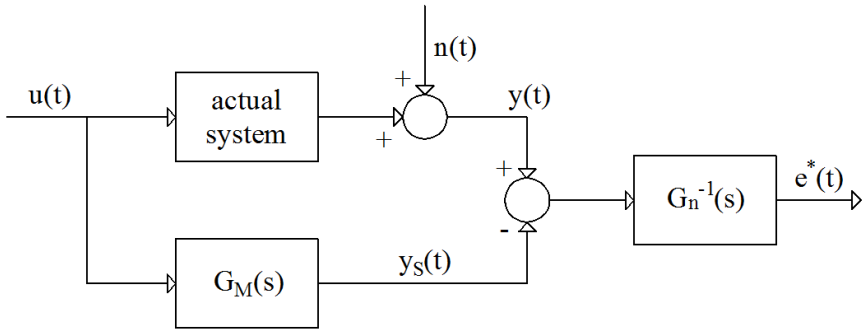

Fig. 2.3. Definition of the general form of the output error $e^*(t)$

The best approximation for $G_0(j\omega)$, that is the real system TF, by the model $G_M(j\omega, \boldsymbol{\theta})$ is thus obtained by minimizing the quadratic cost function of the model output error $e^*(t, \boldsymbol{\theta})$, i.e.:

$$J(\boldsymbol{\theta}) = \boldsymbol{e}^{*T}\boldsymbol{e}^* \tag{2.15}$$

where $\boldsymbol{e}$ is the vector containing the L sampled values, in equidistant intervals equal to the sampling time interval T_S, of the continuous error function $e^*(t, \boldsymbol{\theta})$.

The estimated parameter vector is finally computed from:

$$\widehat{\boldsymbol{\theta}}_L = \arg min[\textstyle\sum_{k=0}^{L} \boldsymbol{e}^{*2}(k, \boldsymbol{\theta})] \tag{2.16}$$

Using Parseval's theorem in the frequency-domain, that is not reported here for the sake of conciseness, and introducing in Eq. (2.16) the Eq. (2.10), the parameter vector estimation finally becomes:

$$\widehat{\boldsymbol{\theta}}_L = \arg min \left[\frac{1}{N}\sum_{i=1}^{N} \frac{|U(j\omega_i)|^2}{|G_n(j\omega_i,\boldsymbol{\theta})|^2} |G_0(j\omega_i) - G_M(j\omega_i,\boldsymbol{\theta})|^2\right] \quad (2.17)$$

where the Laplace variable, $s = \sigma + j\omega$ (with σ and ω, respectively, its real and imaginary parts), is replaced by its imaginary contribution, thus allowing the transition from the Laplace to the Fourier domain in order to allow the summation in the frequency domain reported by Eq. (2.17).

In particular, if the $G_n(j\omega)$ is independent of $\boldsymbol{\theta}$ then the parameter estimation will be consistent. This is usually the case in which $G_n(j\omega)$ is given or fixed, but it should be noted that in many practical cases the parameters of the noise model are unknown and, thus, they have to be included in $\boldsymbol{\theta}$. Furthermore, some authors have shown that Eq. (2.17) leads to a nonlinear least-squares problem [*Unbehauen and Rao*, 1997].

An alternative to the least-squares estimation, according to (2.17), is provided by the *Maximum Likelihood* (ML) estimation method [*Pintelon et al*., 1994]. According to this method, the negative logarithm of the likelihood function becomes:

$$L_L(\boldsymbol{\theta}) = \sum_{k=1}^{N} \left\{log|G_n(j\omega_i,\boldsymbol{\theta})|^2 + \frac{1}{\sigma_{e^*}^2}\frac{|U(j\omega_i)|^2}{|G_n(j\omega_i,\boldsymbol{\theta})|^2}|G_0(j\omega_i) - G_M(j\omega_i,\boldsymbol{\theta})|^2\right\} + Nlog\sigma_{e^*}^2 \quad (2.18)$$

where $\sigma_{e^*}^2$ is the variance of $e^*(t,\boldsymbol{\theta})$, according to Fig. 2.3. Of course, the estimate of the parameter vector is given by:

$$\widehat{\boldsymbol{\theta}}_L = \arg min L_L(\boldsymbol{\theta}) \quad (2.19)$$

Owing to its numerical treatment, the ML-method is one of the most efficient identification methods. For this reason, many scientific works belonging to different scientific fields, which have been produced in the last fifty years, are based on this latter approach to solve the identification problem (for an example concerning the hydrologic field one could refer to *Montanari and Toth* [2006]).

Up to this points, the author has assumed the "true" input $u(t)$ to be observable and, therefore, measurable. This, however, can result in a biased parameter estimation when the real measured input, $u_m(t)$, is corrupted by a noise signal $n_2(t)$, as shown in the following figure (where, $n_1(t)$ is the noise on the output signal from the actual system and $y_m(t)$ is the real measured output):

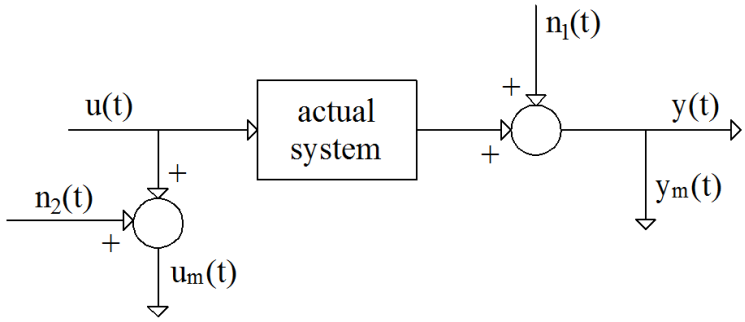

Fig. 2.4. Errors-Invariable (EV) model structure

Such an assumption can be overtaken by means of the application of the Errors-Invariable (EV) model structure [*Soderstrom and Stoica*, 1989] or the IV method, already proposed in Subsection 2.2, concerning time-domain identification approaches. In particular, it has been shown that estimators based on the EV model structure are consistent when the 'true' spectral density matrix of the I/O noise is known a priori [*Anderson*, 1985].

Once presented, in this subsection, the most adopted estimators, in the frequency-domain, of the parameters vector of CT linear models, the intention of the author is to finally underline an important aspect concerning the system identification theory and the two main advantages of the frequency-domain identification approaches compared to time-domain ones.

First of all, identification of a CT linear dynamic SISO systems usually starts with a discrete set of measurements of the input and output signals, sampled at equal time intervals. It is well known that discrete measurements do not contain all the information about the CT signals unless additional assumptions are made. In *Schoukens et al*. [1994] two very important assumptions were considered:

(1) the *Zero-Order Hold* (ZOH) assumption;

(2) the *Band Limited* (BL) assumption.

In case (1), it is assumed that the excitation signal value, $u(k)$, remains constant during the sampling interval (T_S). In case (2), instead, it is assumed that the sampled signals, $u(k)$ and $y(k)$, each have limited bandwidths. Both assumptions lead to an exact description of the CT system. However, it should be noted that the obtained models are only valid if their signals obey both the corresponding assumptions.

Secondly, it is worth noticing that, for system identification problems in time-domain, large data sets are usually required. In particular, the record length is given by:

$$T_m = LT_S \tag{2.20}$$

where L is the number of data points. On the other hand, the sampling frequency ω_S should be selected according to Shannon's sampling theorem:

$$\omega_S = \frac{2\pi}{T_S} \geq 2\omega_{max} \tag{2.21}$$

where ω_{max} is the frequency of the band-limited input or output signal, above which the signal spectrum vanishes. The lowest frequency of interest, ω_{min}, determines the minimum record length:

$$T_m > \frac{2\pi}{\omega_{min}} \tag{2.22}$$

From (2.20) – (2.22), it is clear that an interesting information about the minimum number of data points in the time-domain is given by the following expression:

$$L > \frac{2\omega_{max}}{\omega_{min}} \tag{2.23}$$

So, if the frequency range of interest covers, for instance, 3 decades (that is, such that the ratio between the maximum and the minimum frequency of interest is equal to 1000), it is necessary a number of time-domain data points ad-hoc sampled of about L = 2000.

Given these considerations, the aim of the author is to highlight that the large data sets, usually necessary in time-domain, can be replaced for identification in frequency-domain by a considerably reduced set of approximately logarithmically distributed frequency points, ω_i, covering the frequency range of interest [*Schoukens et al*., 1994].

Furthermore, another relevant advantage of frequency-domain approaches consists in the fact that, given that the frequency response data (such as Fourier coefficients at different frequencies ω_i) may be obtained from different experiments, an experimental simplification is possible by

combining data from different experiments, which is not so easily possible in time-domain identification procedures.

Finally, it is worth highlighting that all the symbols adopted in Section 2 are those usually adopted in the technical literature in the specific field of system identification. This is due to a specific author's decision, who preferred to avoid confusion in interested readers, who could refer to the numerous papers cited in the present section in order to acquire more detailed information on the identification of CT linear systems. For the same reason, some of the symbols adopted in Section 2 will be provided also in following sections but with a completely different meaning, in order to assure a continuity with the existing literature works concerning the study of stochastic shot noise modeling of daily streamflows.

3. Calibration of shot noise process-based models

3.1. Introduction

In Section 2 the more frequently adopted identification techniques of CT and TI models, both in the time-domain and in the frequency-domain, have been reported. Nevertheless, the main subject developed in this Ph.D. dissertation deals with a spectral domain-based identification approach of a particular class of models for daily streamflows reproduction and generation, known as *shot noise process based-models* (for the sake of brevity, from this moment the author will refer to this class of models as *shot noise models*).

In the present section, a brief description of the scientific background concerning those models intended to the reproduction, forecasting and simulation of short-time discharge data will be firstly provided. At a later stage, general time and spectral-domain properties of the shot noise process will be described, and, eventually, a comprehensive description of shot noise models identification techniques will be provided.

3.2. Reproduction of short time scale discharge series: a survey

Nowadays it is well recognized the difficulty in the use of limited streamflow time series in water resources planning and management problems. As a consequence, during the last decades, stochastic streamflow simulation has been attracting great interest among the scientific community, in particular thanks to its utility in optimization techniques [e.g., *Karamouz and Houck*, 1987; *Karamouz et al*., 1992; *Chang and Chang*, 2001; *Ahmed and Sarma*, 2005]. As a matter of fact, these methods produce synthetic streamflow traces that reflect the statistical properties of the historic data.

Depending on the particular problem, the reproduction of the streamflow process is desired at different time resolution. In the past forty years, several classes of stochastic models were proposed, which generally looked at each time scale of aggregation individually. But in order to deal with water resources planning and management problems on a daily scale, the reproduction of short-time (that is, from daily to weekly) discharge data is needed. In particular, short time streamflow series are characterized by the presence of the intermittent pattern of dry/wet periods and by the skewed nature of the hydrographs, with sudden discharge increases and slow recessions [*Murrone et al*., 1997]. These features prevent the use of parametric and non-parametric methods (e.g., Auto Regressive Moving Average K-Nearest Neighbor, etc.) [see, e.g., *Lall and Sharma*, 1996; *Ouarda et al*., 1997; *Prairie et al*., 2006], which, instead, are successfully applied to monthly and annual data.

The aptitude to reproduce the presence of peaks and recessions in daily discharge time series belongs to the *filtered point processes* [*Bernier*, 1970], also known as *Shot Noise* (SN) processes, that have received considerable attention in hydrologic literature [*Weiss*, 1977; *Koch*, 1985; *Xu et al*., 2002].

The structure of this process consists of a *point process* that reproduces the occurrence (that is the sequence of effective rainfall events) which acts as the input of a system that is representative of the watershed transformations. Runoff is obtained by filtering the input through the system response function.

The first comprehensive work on SN models of runoff was due to *Weiss* [1973; 1977], who introduced a model in which effective rainfall events were reproduced through a Poisson process of occurrences coupled to exponentially-distributed intensities. A two-component SN process results from this scheme, and the method of moments was proposed for parameter estimation. A more recent improved variant of Weiss' model was instead due to *Cowpertwait and O'ConnelI* [1992], who proposed the Neyman-Scott model to reproduce the effective rainfall process. Between *Weiss* [1973] and *Cowpertwait and O'ConnelI* [1992], several approaches, often based on SN formulation, were proposed for short-time runoff modeling (please refer to *Murrone et al*. [1997] for a comprehensive literature review). In particular, among them, it is worth underlining the contribution of *Treiber and Plate* [1977], *Yakowitz* [1979], *Pegram* [1980], *Hino and Hasebe* [1981], *Vandewiele and Dom* [1989], who proposed different linear or non-linear conceptual scheme of the watershed based on a SN formulation.

A central point in the use of SN process-based methods is the calibration procedure adopted for the evaluation of the parameters on which the selected form of the system response function is based. In particular, most of the existing, and most recent, literature works are based on a time-domain iterative identification approach that consists of the minimization of the squared differences between the observed discharge values and those obtained by the convolution of the response function (to be identified) and

the input series [*Murrone et al*., 1997; *Claps and Laio*, 2003; *Claps et al*., 2005; Xu et al., 2001].

A crucial aspect in the application of a time-domain approach concerns the generation of the occurrences (or effective rainfall) to be convolved with the watershed response function of a given form but with unknown parameters. As a matter of fact, the model parameters estimation is deeply dependent on the method chosen for the effective rainfalls modeling. For this reason, hereinafter, the authors will provide a thorough description of the main approaches available in the scientific literature for the effective rainfall occurrences and intensities determination.

3.3. Shot noise models: main statistical properties

Given a set of Poisson distributed points t_i (i.e. the time of occurrence of the *i*th input pulse) with average density λ, the following process is given:

$$x(t) = \sum_{i=1}^{n(t)} c_i \tag{3.1}$$

where t is the time variable, c_i is a sequence of independent and identically distributed (*i.i.d.*) random variables, independent of the points τ_i (i.e. the instant values corresponding to the effective rainfall occurrences), with mean η_c and variance σ_c^2 [*Papoulis and Pillai*, 2002, Subsection 10.2]. Hence the process $x(t)$ is a staircase function with jumps at points τ_i, equal to c_i. The process $n(t)$ is the number of Poisson points in the interval $(0, t)$, hence its expected value is $E\{n(t)\} = \lambda t$ and its second order moment is $E\{n^2(t)\} = \lambda^2 + \lambda t$. From this, it follows that:

$$E\{x(t)\} = \eta_c E\{n(t)\} = \eta_c \lambda t \tag{3.2}$$

$$E\{x^2(t)\} = \eta_c^2 E\{n^2(t)\} + \sigma_c^2 E\{n(t)\} = \eta_c^2(\lambda t + \lambda^2 t^2) + \sigma_c^2 \lambda t \quad (3.3)$$

It could be now possible to demonstrate that (but it is here avoided for the sake of conciseness):

$$C_{xx}(t_1, t_2) = (\eta_c^2 + \sigma_c^2)\lambda min(t_1, t_2) \quad (3.4)$$

where $C_{xx}(t_1, t_2)$ is the autocovariance function of the process $x(t)$.
The next step is to consider the impulse train, given by the following expression, which determines the so called Shot Noise (SN) process and that can be adopted to model the entire rainfall process:

$$z(t) = x'(t) = \sum_i c_i \delta(t - \tau_i) \quad (3.5)$$

where δ is the Dirac delta function.
Given Eq. (3.4), it follows that:

$$E\{z(t)\} = \frac{d}{dt} E\{x(t)\} = \eta_c \lambda \quad (3.6)$$

$$C_{zz}(t_1, t_2) = \frac{d^2 C_{xx}(t_1, t_2)}{dt_1 dt_2} = (\eta_c^2 + \sigma_c^2)\lambda \delta(t_2 - t_1) \quad (3.7)$$

Convolving the SN process, i.e. the impulse train (3.5), with a function $h(t)$ (that, in the hydrologic application, is representative of the watershed response function) the Generalized Shot Noise (GSN) process is obtained:

$$q(t) = \sum_i c_i h(t - \tau_i) = z(t) * h(t) \quad (3.8)$$

where $q(t)$ is the streamflow variable, intended as a continuous time variable. Its main statistical properties are provided by the following expressions:

$$E\{q(t)\} = E\{z(t)\} * h(t) = \eta_c \lambda \int_{-\infty}^{\infty} h(t)dt \tag{3.9}$$

$$C_{qq}(t_1, t_2) = C_{zz}(t_1, t_2) * h(t) * h(-t) = (\eta_c^2 + \sigma_c^2)\lambda\rho(t_1, t_2) \tag{3.10}$$

$$Var\{q(t)\} = C_{qq}(0) = (\eta_c^2 + \sigma_c^2)\lambda \int_{-\infty}^{\infty} h^2(t)dt \tag{3.11}$$

where $Var\{q(t)\}$ is the streamflow variable variance.

Given the general formulation of SN processes, the intention of the author is now to highlight some of their properties that are necessary for the comprehension and the application of the frequency domain identification procedure proposed in this thesis.

In particular, as revealed by Eq. (3.7), it is fundamental to underline the impulsive nature of the input process autocovariance function $C_{zz}(t_1, t_2)$. While the commonly adopted time-domain identification approaches, that will be discussed in Subsection 3.4, do not take any advantage from this powerful property, it is the basic principle on which the spectral-domain identification procedure here proposed was built. In particular, it is well known that the *power spectrum* $S(\omega)$, or, more concisely, the *spectrum*, of a real or complex process $y(t)$ is the Fourier transform of its autocovariance function $C_{yy}(t)$. Hence the following relation is valid:

$$S_{yy}(\omega) = \int_{-\infty}^{\infty} C_{yy}(t)\, e^{-j\omega t} dt \tag{3.12}$$

where j is the imaginary unit and ω is the angular frequency. Similarly, it is worth underlining that the well-known Power Spectral Density (PSD) of the generic process $y(t)$, or, more simply, its *spectral density*, is defined as the Fourier transform of the autocorrelation function of the process itself, suggesting that it is obtainable dividing the spectrum (3.12) by the variance of the process [*Jenkins and Watts*, 1968, p. 218]. This is the reason why it is not rare, in a system identification environment, to talk about the PSD instead of the spectrum of a given process. Thus, for the sake of simplicity, hereinafter the author will refer to the functions defined as in the equation (3.12) as PSDs.

Given the above considerations and starting from Eq. (3.7), which shows the autocovariance expression of the impulse train process $z(t)$, it should be evident that the PSD of $z(t)$ is equal to a constant, as provided by the following equation:

$$S_{zz}(\omega) = (\eta_c^2 + \sigma_c^2)\lambda \tag{3.13}$$

Thus, considering that in case of linear systems the following relation is valid [*Papoulis and Pillai*, 2002, p. 412]:

$$S_{qq}(\omega) = S_{zz}(\omega)H(\omega)H^*(\omega) = S_{zz}(\omega)|H(\omega)|^2 \tag{3.14}$$

where S_{qq} and S_{zz} are, respectively, the PSDs of the system response, $q(t)$, and of the input process, $z(t)$, *H(ω)* is the linear system TF and $H^*(\omega)$ its complex conjugate, it is clear that, given the Eq. (3.13) and the superposition effect valid for linear systems, in case of SN model the following equation holds:

$$S_{qq}(\omega) = S_{zz}(\omega)|H(\omega)|^2 = [(\eta_c^2 + \sigma_c^2)\lambda]|H(\omega)|^2 = G|H(\omega)|^2 \qquad (3.15)$$

From Eq. (3.15) it is evident how the contribution of the impulse train spectral density, S_{zz}, is only that of a scale factor, G, between the spectral density of the system response, S_{qq}, and the linear system TF, $H(\omega)$. Hence, starting from the knowledge of the output process, i.e. when river flow data are available, one can estimate the parameters of the watershed response function (model calibration) only by matching the PSD amplitudes, estimated at several frequencies, of the observed river flow records with the squared module of the linear system TF.

However, it is worth noticing that, as outlined by *Montanari and Toth* [2007], the PSD of a process does not convey any information about the mean of the process itself. As a consequence, in this work, in order to allow the correct reproduction of the recorded streamflow series mean characteristics, obviously affected by seasonality, the author decided to include all the information on the mean of the output process, $q(t)$, in the input process, $z(t)$, also known as effective rainfall process [see, for reference, *Murrone et al.*, 1997]. Hence, the TF parameters estimation was undertaken, following the aforementioned Eq. (3.15), on the PSD, $S_{\overline{qq}}$, of the deseasonalized streamflow process, $\bar{q}(t)$, in order to avoid that the seasonality of the streamflow process mean level affected the form of the PSD and, thus, the estimated values of the parameters. More details about the deseasonalization processes are provided in following sections.

As outlined in following Subsection 3.5, the main advantage of the proposed spectral-domain calibration procedure consists in the possibility to estimate the values of the TF parameters independently from the knowledge of input process data information, provided that, in the case of SN assumption, the PSD of the input process contributes to each frequency value with the same

amplitude. As a consequence, the procedure here presented is particularly suitable for the resolution of model calibration problems in the case of ungauged basins [see, for reference, *Montanari and Toth*, 2007] (i.e., those watersheds that are not provided with systems aimed at the recording of hydro-meteorological processes), which is a really common situation in developing countries where the demand of simulation tools, for design and management of new hydro-power systems, is increasing.

Moreover, thanks to this remarkable characteristic of the calibration approach, the whole proposed methodology differentiates itself from the limited number of other frequency-domain approaches, for the calibration of SN models, available in the scientific literature. A relevant contribution to this topic was that by *Diskin and Pegram* [1987], who dealt with the spectral-domain calibration of a cell model for storm-runoff modeling, with available records of a particular storm and flood hydrograph event. In particular, the whole calibration procedure, once defined a model made by a proper combination of linear reservoirs, was based on the minimization of an objective function given by the sum of the differences between the Laplace transforms (estimated at several frequency values) of the recorded output sequence and that of the model output. The overall approach, however, was based on the analytical knowledge of Laplace transforms of the output and input signal (other than that of the basin response function), starting from the knowledge of the structures of input and output sequences (i.e., respectively, a histogram structure and a polygon structure). It is thus clear the advance that the calibration approach here described introduces, in the scientific literature, in the field of spectral identification approaches of shot noise-based models.

In order to complete the position of SN process, some other few properties need to be provided. Since the density of the Poisson points and the distribution of the amplitudes c_i are assumed independent of time, the SN process results stationary, with a mean, as shown in *Papoulis and Pillai* [2002, p. 461], reported in the following equation:

$$E[z(t)] = \eta_c \lambda \tag{3.16}$$

The non-stationarity of the SN, that is useful for example to model seasonality, may arise from two different sources:
(a) the dependence of λ on time;
(b) the dependence of c_i distribution on time.
However, in both cases, following *Roberts* [1965], a useful equation that relates the mean of the streamflow process to properties of the rainfall process can be established as follows:

$$E[q(t)] = h(t) * [\lambda(t) \cdot \bar{c}(t)] \tag{3.17}$$

In Eq. (3.17), $\lambda(t)$ is the time-varying density of the Poisson points and $\bar{c}(t)$ is the time varying (conditional) expected value of the pulse amplitude, given that there is a pulse in the interval $[t, t + dt]$.
Starting from the assumptions and the considerations about the SN process presented in the present section, in Subsection 3.4 the author will firstly provide a detailed description of the most adopted calibration approaches, in the scientific literature, of SN-based hydrological models. At a later stage, moreover, the effectiveness of spectral calibration methods will be shown, assuming stationarity of the SN process, thus leaving to future works the exploitation of non-stationarity.

3.4. Shot noise models: classical calibration approaches

The procedure for parameters estimation of SN models is strictly related to the approach followed for the parameters estimation of the model of effective rainfall. In particular, for this latter goal, two alternatives are essentially available in the technical literature.

In the first one, common to most of the SN models in literature [see, for reference, *Weiss*, 1973, 1977; *O'Connell and Jones*, 1979; *Cowpertwait and O'Connell*, 1992], the form of the underlying input process is pre-determined and its parameters are estimated through the *method of moments* applied to the streamflow statistics [*Murrone et al*., 1997]. The main drawback of this procedure are:

(a) the fact that it does not allow the users to verify the hypothesis made on the input process;

(b) the impossibility to evaluate the influence of the effects of the watershed transformations on the estimation of the effective rainfall model parameters.

In the alternative approach these problems are overcome since the input series is reconstructed by inverse estimation. On the obtained series, parameters of the stochastic input model are thus evaluated. Several authors followed this latter procedure, each with a different ad-hoc introduced technique [see, among others, *Treiber and Plat*e, 1977; *Hino and Hasebe*, 1981, 1984; *Battaglia*, 1986; *Wang and Vandewiele*, 1994].

Concerning this latter procedure, a relevant scientific contribution was that of *Murrone et al.* [1997]. In this paper, the authors firstly defined the form of the basin response function $h(t)$. In particular, it was assumed linear and given by the linear combination, through coefficients α_i, of the individual responses of its components. Each component was modelled as a linear

reservoir, with a corresponding Instantaneous Unitary Hydrograph (IUH) of exponential negative form. In order to test the procedure in various case studies, the authors decided for a basin response function given by the combination of 3 linear reservoirs (each representing one among the sub-daily, over-month and over-year groundwater contributions). Moreover, the response function contribution corresponding to the surface component was modelled as an additional Dirac delta function, since the basin surface response lag was enough smaller than the time interval of data aggregation (considered from daily to weekly).

Starting from these considerations, the estimation of the model parameters (i.e. linear combination coefficients, α_i, and storage coefficients, k_i, for each of watershed contribution) was undertaken, through minimization of the squared differences between recorded flow values and those obtained through convolution of the effective occurrences and the basin function. For this purpose, an iterative procedure resulted necessary, since the input intensities (hereafter defined as *effective rainfall*), in turn, were obtained by deconvolution of the recorded streamflow series through the system response function with unknown parameters.

Finally, for the generation of synthetic streamflow series, fundamental for the statistical verifications, a Poisson White Noise Exponential Model (PWNE) [*Eagleson*, 1978] was fitted on the final effective rainfall series. In this manner, the generation of synthetic effective rainfall series, to convolve with the identified response function, was allowed.

It is worth noticing the approach followed by the authors in the selection of rainfall occurrences and intensities at the first iteration, that is when no estimates of the response function parameters are available. Indeed, the net rainfall occurrence was assumed in each time instant presenting a discharge increase. However, in order to account for errors in discharge measurements,

a threshold value, L, was considered. In particular, only when the condition $q_{t+1} > q_t + L$ was met, a trial value of the rainfall amount was assumed equal to $Y_t = q_{t+1} - q_t$ [*Battaglia*, 1986]. The choice of the threshold level was thus critical because of its direct influence on the number of input events.

The main drawback in the adoption of such a procedure dealt with the necessity of several iterations to obtain the final parameters estimation, resulting in a lack of robustness of the overall approach. Moreover, few details were given by *Murrone et al*. [1997] about the selection of the threshold, L, value in the estimation of effective rainfall occurrences and intensities at the very first iteration. For the sake of conciseness, from this moment the author will refer to this method, for the selection of effective rainfalls, as Discharge Increments Pulses (DIP) approach [see *Claps and Laio*, 2003]. Even though frequently adopted, the DIP approach presented two relevant drawbacks [*Claps et al*., 2005]. First of all, the presence of noise in the daily streamflow measurements could result in small rises in the flow process records, resulting, in turn, in an overestimation of the mean number of rainfall events per year. Secondly, the basic hypotheses of mutually independent and Poisson-distributed pulses were often not respected by the estimated sequences.

In order to overcome these two main drawbacks, *Claps and Laio* [2003] presented an evolution of the DIP approach. The Filtered Peak Over Threshold (FPOT) method was introduced in order to derive a more appropriate pulse sequence. Its main steps can be summarized as follows:

(a) given the recorded daily discharge series, the occurrences are found in correspondence of all the local maxima of the series itself;

(b) given the local maxima values, a sequence of Filtered Peaks (FP) is determined by subtracting the first local minimum preceding the considered peak;
(c) a threshold filter is increasingly applied to the FP series, in order to retain only significant peaks, until the peaks independence test of Kendall and the peaks Poisson distribution test of Cunnane are jointly met.
As stated by the authors themselves, the adoption of the FPOT approach guarantees the following advantages if compared to the DIP one:
(1) it allows one to avoid the deconvolution step in the peaks identification procedure, with considerable advantages in terms of procedure simplicity and robustness;
(2) it returns an effective rainfall series that automatically meets both the independence and Poissonianity requirements of the PWNE model.
Nevertheless, they also noticed that, as major drawback, the number of selected peaks is reduced to 5-20 per year [*Claps et al*., 2005], which underestimates the actual number of effective rainfall events. Such a consideration would suggest the inadequacy of the Poisson independent model in the correct reproduction of the effective rainfall behaviour.

Another notable contribution to the identification of SN models was that of *Xu et al*. [2001; 2002], in which the daily streamflow process was regarded as a sum of two components with different characteristics, i.e. the direct surface runoff and the baseflow. In particular, the former, responsible of the short-term variations, was considered as an intermittent process with a Gamma response function. The latter was instead characterized by the conventional negative exponential response function (that of subsurface and groundwater storages) and was considered responsible for the long-term persistence displayed by the recorded streamflow series. Both the

components to the total streamflow process were calibrated by means of physical considerations on the case study watershed considered in the application, that are not reported here because not relevant according to the main goal of the present thesis.

However, the notable contribution of the authors consisted in the procedure introduced for the estimation of pulse intensities necessary in the synthetic streamflows generation. Indeed, as in the previously described works, they referred to a sequence of uncorrelated rainfall pulses but following a Gamma probability distribution. In order to estimate the distribution parameters, starting from the recorded streamflow series, the authors followed these two steps:

(a) to determine the occurrences, they assumed that pulses occur only on those days when streamflow increases;

(b) to estimate pulses intensity, they made a least-squares fit of the reconstructed streamflow series (obtained through convolution of the input sequence with the known time response function) and the recorded one, assuming, of course, the unknown input intensities as the variable to be determined. Subsequently, in order to test the assumption of storm events compatible with a non-homogeneous Poisson point process (i.e. defining a different Poisson process, of a given parameter, for each month), the χ^2 goodness-of-fit test was made for each month.

Although the calibration approach presented in this work, that takes advantage of the SN model spectral properties described in Subsection 3.3, is completely independent from the technique adopted in the parameters estimation of the model of effective rainfall, it is of considerable interest due to its importance in the synthetic streamflow generation. As a matter of fact, a simulation analysis is necessary to assess the effectiveness of the model in

the reproduction of the main statistical features of the recorded series. For this purpose, in this thesis the author has selected the latter approach described, i.e. *Xu et al*. [2001; 2002], given its better performances, in terms of effective rainfalls features reproduction, verified in the following subsections.

3.5. A spectral domain calibration procedure

3.5.1. Model structure: the watershed response function

Given the aforementioned modification of Eq. (3.15), in which, for each angular frequency ω, the PSD of the deseasonalized streamflow process ($S_{\overline{q}\overline{q}}(\omega)$) is equal to the squared module of the watershed TF ($H(\omega)$), in order to allow its application to a general case study, the definition of the shape of the basin response function $h(t)$ is needed. For this purpose, a preliminary description of how effective rainfall reaches the basin outlet is needed. In particular, three main runoff components can be identified: the *baseflow* (i.e. the return flow from groundwater capacities), the *subsurface flow* (i.e. interflow, representing rapid flow through pipes, macro-pores and seepage zones in the soil) and saturated overland flow (*surface flow*). The two latter components form the *direct* runoff, also known as *quickflow*. It is worth underlying that separation of effective rainfall into the above components is non-linear, because the relative weight between direct and groundwater runoff depends on the infiltration capacity, that is function of the soil moisture state and of the intensity of rainfall. Nevertheless, this non-linearity is not considered here, essentially because it is thought that for the aims of the analysis undertaken it is more important to test how well the

proposed framework is able to reproduce main runoff process features at different frequencies.

Regarding the baseflow, *Claps et al*. [1993] demonstrated that, even in small basins, annual data can be autocorrelated, due to the presence of a groundwater contribution with very slow response time. Hence, even though in large basins the hydrogeologic scheme could be more complex, it is convenient to assume that when an annual autocorrelation is present in the considered time series this is due to the presence of a large and deep aquifer. Moreover, those authors also showed that in monthly data autocorrelation is present even when annual runoff is uncorrelated. As a consequence, the presence of a groundwater component that introduces "memory" in runoff data with a delay time of the order of few months is revealed. This over-month groundwater component is due to the presence of aquifers which run dry within the dry season.

Eventually, as regards direct runoff, if the basin is sufficiently large, even on daily data one can recognize the presence of both the subsurface and the surface runoff components.

Therefore, from these considerations it follows that one cannot exclude that all four of the above components can be identified from the streamflow dynamics on a short time scale. Consequently, the most general watershed scheme includes four conceptual elements in parallel.

Starting from the above considerations, in order to undertake, in the following subsections, some comparisons with results obtained by well-known literature works, in this thesis the author has referred to the same response function shape adopted by *Murrone et al*. [1997]. In this latter work a conceptual model of the watershed is considered, with a basin response function given by the linear combination, through coefficients α_i, of its components contributions. Each component, modelled as a linear reservoir

(hence with a negative exponential impulse response $u(t)$ given in Eq. (3.18)), is representative of a corresponding groundwater contribution to the streamflow process, each with a proper storage coefficient k_i:

$$u(t) = (\alpha_i/k_i)e^{-t/k_i} \tag{3.18}$$

The component identified by the coefficient α_0 (see Eq. (3.19)) is instead representative of that amount of effective rainfall that reaches directly the basin outlet (surface runoff), i.e. with a response time k_0 enough smaller than the interval of data aggregation and, for this reason, modeled as a Dirac delta function $\delta(t)$ [*Claps et al.*, 2005]. Thus, it is possible to assume the following form of the time response function:

$$h(t) = \alpha_0\delta(t) + \frac{\alpha_1}{k_1}e^{-t//k_1} + \frac{\alpha_2}{k_2}e^{-t//k_2} + \frac{\alpha_3}{k_3}e^{-t//k_3} \tag{3.19}$$

In the previous equation the groundwater components represented by the storage coefficients k_i are: the sub-daily (k_1, representing the sub-surface runoff); the over-month (k_2, representing the contribution of those groundwater capacities that are dry during the dry season); the over-year (k_3, representing deepest aquifers). Moreover, it is worth underlying that coefficients α_i, which are considered constant and which distribute the input volume among system elements, according to the continuity condition, have to fulfil the continuity condition: $\sum_i \alpha_i = 1$.

Given the response function shape of Eq. (3.19), in order to apply the spectral property of Eq. (3.15), the analytical determination of the corresponding TF form ($H(\omega)$) is needed. Starting from the well-known

properties of the Laplace transform, which are not reported here for the sake of conciseness, it is possible to demonstrate that the Laplace transform, $H(s)$, of the system response function of Eq. (3.19) is given by the following expression:

$$\mathcal{L}\{h(t)\} = H(s) = \alpha_0 + \frac{\alpha_1}{1+k_1 s} + \frac{\alpha_2}{1+k_2 s} + \frac{\alpha_3}{1+k_3 s} \tag{3.20}$$

where s is the complex Laplace variable ($s = \sigma + j\omega$), given by the summation of its real (σ) and imaginary ($j\omega$) parts.

Assumed the result shown in Eq. (3.20), it is now fundamental to determine the TF module. In particular, in order to make it estimable at discrete frequency values, it is needed to pass from the Laplace (s) to the Fourier ($j\omega$) domain, given that the latter is the restriction of the former to its imaginary axis (i.e., assuming that $s = j\omega$ in Eq. (3.20)). Starting from this premise, once obtained the TF real (Re) and imaginary (Im) parts, that are not analytically reported here for the sake of brevity, the TF magnitude is easily obtainable, by the definition of the module of a complex number, as $|H(j\omega)| = \sqrt{Re(j\omega)^2 + Im(j\omega)^2}$, which leads to the following expression:

$$|H(j2\pi f)| = \left[\left(\alpha_0 + \frac{\alpha_1}{1+k_1^2 f^2} + \frac{\alpha_2}{1+k_2^2 f^2} + \frac{\alpha_3}{1+k_3^2 f^2}\right)^2 + f^2\left(\frac{\alpha_1 k_1}{1+k_1^2 f^2} + \frac{\alpha_2 k_2}{1+k_2^2 f^2} + \frac{\alpha_3 k_3}{1+k_3^2 f^2}\right)^2\right]^{0.5} \tag{3.21}$$

with f the frequency value, expressed in Hertz, at which the module of the TF is estimated (which is related to the angular frequency by the following well-known relation: $f = \omega/2\pi$).

In Section 4 it will be shown that, once numerically estimated the PSD of the streamflow process at discrete frequency values (f_i), the TF module of Eq. (3.21) will be directly adopted in the estimation of the unknown watershed parameters.

A crucial aspect that needs to be underlined consists in the fact that, thanks to the shape of the watershed response function adopted in this thesis, the basin response function is that of a *minimum phase* system. In the scientific literature a minimum phase system is that corresponding to a TF with two particular features: (a) a positive gain; (b) all poles and zeros with a negative/null real part [*Bolzern et al*., 2004]. For this reason, in such a system an unique relation between the amplitude and the phase diagrams of the systems response exists. It is thus possible to neglect the phase of the streamflow signal and calibrate the watershed response function only by fitting its PSD.

According to the work of *Muratori et al*. [1992], about the minimum phase property of single-input single-output linear compartmental systems (i.e. networks of linear reservoirs), both the connection of *n* linear reservoirs in cascade and in parallel have minimum phase characteristics (see theorems 1 and 2 of the cited work). Therefore, given the form of the response function shown in Eq. (3.19), corresponding to the parallel connection of four linear reservoirs (with the one corresponding to the surface runoff characterized by a detention time k_0 enough smaller, and thus negligible, if compared to the data aggregation scale), it is possible to state that the system considered in this work possesses minimum phase properties. However, it is worth underlying that, given the minimum phase conditions reported in the cited work, several conceptual models based on the parallel and cascade connection of linear reservoirs, frequently adopted in hydrologic calibration

problems, have minimum phase properties. Hence, once clarified the minimum phase property associated to the adopted response function of Eq. (3.19), it is possible to state that, according to Eq. (3.15), in the present thesis the watershed model has been calibrated only by numerically matching, at each frequency, the squared values of Eq. (3.21) to the transformed streamflow process PSD, without paying any attention to the phase signal information.

It is worth noticing that, as stated by *Nikias and Mendel* [1993], the autocorrelation, or equivalently the spectral density, domain suppresses all phase information about the system to be identified. As a consequence, a proper system calibration by the adoption of procedures based on the use of only PSD functions is possible only if the system is minimum phase, that is only if an univocal relation between magnitude and phase features of the model exists. As a matter of fact, the adoption of PSD-based techniques allows only the identification of minimum phase systems [*Nikias and Mendel*, 1993].

3.5.2. PSD estimation techniques

3.5.2.1. A brief overview

Given the result shown in Eq. (3.15) and the expression of the TF module showed in Eq. (3.21), in the present subsection the author will provide an overview about PSDs, or equivalently power spectra, estimation techniques.

The techniques for estimating the conventional power spectrum fall into two main categories:

(a) the nonparametric or conventional methods;

(b) the parametric or model-based methods;

The first category, in turn, includes two classes: the direct methods, which are based on the FT of the observed data, and the indirect methods, which consist in the computation of the FT of the estimated autocorrelation sequence of the data (e.g., the *periodogram* technique). The second class, that of parametric methods, includes algorithms such as MA, AR, and ARMA modeling, and eigen-space based methods such as MUSIC, Min-Norm, etc., which are appropriate for harmonic models. Hereinafter the main features of the aforementioned categories of methods are described, with a particular focus on the adoption of the periodogram (widely adopted in technical literature) and of the autoregressive (AR) method, also known as maximum entropy method (MEM).

3.5.2.2. Nonparametric (or conventional) methods

The conventional estimators (or nonparametric ones) are generally easy to understand and easy to implement, but they are limited by their resolving power (the ability to separate two closely spaced harmonics), particularly when the number of samples is small. For random signals, these estimators typically require long observation intervals in order to achieve acceptably low values for the variances of the estimate.

The most adopted nonparametric estimator of the power spectrum $S_{yy}(f)$ of a generic time signal $y(t)$, about which N recorded sampled values are available, is certainly the so-called *periodogram* [see, e.g., *Montanari and Toth*, 2007], defined as the discrete FT of the autocovariance function $C_{yy}(m)$:

$$S_{yy}(f) = \sum_{m=-N-1}^{N-1} C_{yy}(m)e^{-jm2\pi f} = \frac{1}{N}\left|\sum_{t=0}^{N-1} y(t)e^{-jt2\pi f}\right|^2 \qquad (3.22)$$

As clearly showed, the periodogram can also be estimated as the squared value of the absolute value of the discrete FT of the time signal $y(t)$. It is worth noticing that the periodogram is an unbiased estimator of the spectrum, even though its variance at any frequencies does not go to zero as the number of samples goes to infinity (i.e. it is not a consistent estimator). Nevertheless, as N increases the spacing between estimates that are uncorrelated decreases as $1/N$, thus the fluctuations in the periodogram become more rapid. However, there are several ways to make consistent the periodogram estimation, among which it is possible to distinguish between:

- smoothing (or filtering) in the frequency domain (that leads to the well-known *Blackman-Tukey* spectral estimator, which can be considered as a "locally" weighted average of the periodogram [see, for reference, *Stoica and Moses*, 2005, Subsection 2.5]);
- averaging several periodogram estimates (Barlett, Welch and Daniell methods [*Stoica and Moses*, 2005, Subsection 2.7]).

For the sake of conciseness the author will not provide any description of the aforementioned techniques, thus the interested reader is referred to the numerous technical works concerning this matter (among which *Stoica and Moses* [2005] Section 2 is suggested).

3.5.2.3. Parametric (or model-based) methods

The second category is that of parametric methods, which are based on parametric models of a time series, such as autoregressive (AR) models, moving average (MA) models, and autoregressive-moving average (ARMA) models (this is the reason why they are also known as model-based methods). To estimate the spectrum of a time series $y(t)$ with parametric

methods, thus, you need to firstly select an appropriate model and, secondly, obtain the model parameters of the time series.

The AR or *all–pole* signals constitute the type that is most frequently used in applications. The AR equation may model spectra with narrow peaks, that is an important feature since narrowband spectra are quite common in practice. The estimations of AR model parameters are usually found by solving a system of linear equations, and the stability of the estimated AR polynomial can be guaranteed. In general, two techniques are considered for the estimation of AR parameters. The Yule Walker method that is base directly on the linear relationship between the covariances and the AR parameters. The Least-Square (LS) method, based on a LS solution of AR parameter from the corresponding time-domain equation [*Stoica and Moses*, 2005, Subsection 3.4].

The MA signal is obtained by filtering white noise with an *all–zero* filter. Owing to this all–zero structure, it is not possible to use an MA equation to model a spectrum with sharp peaks unless the MA order is chosen "sufficiently large". Thus this contrasts with the ability of AR model to model narrowband spectra by the adoption of low model orders. On the contrary, the MA models allow the fitting of spectra with broad peaks and sharp nulls. Such spectra are not really spread in engineering applications, thus limiting the adoption of MA models in the estimation of PSD functions. Moreover, MA parameter estimation problem is basically a nonlinear one, thus the type of difficulties one should face in MA and more complete ARMA estimation problems are quite similar, so one usually prefers the use of the latter typology [*Stoica and Moses*, 2005, Subsection 3.5].

For spectra with both sharp peaks and deep nulls a modeling by either AR or MA equations of reasonably small orders is not reasonable. In these cases the adoption of the more general ARMA model, also called the *pole-zero*

model, is suggested. Two main groups of estimators of ARMA models are available in the technical literature. The "theoretically optimal" estimators are based on iterative procedures whose global convergence is not guaranteed. The "practical estimators", on the other hand, are computationally simple and often quite reliable, but their statistical accuracy may be poor in some cases. The mainly adopted techniques in the estimation of ARMA type spectra are the so called Modified Yule-Walker method and the Two-Stage least square method. However, the intention of the author is not that of focusing on this typology of spectrum estimator, thus the interested reader is referred to *Stoica and Moses* [2005, Subsection 3.7] for more details.

Given the classical features of common power spectra in hydrologic applications, the author has opted in favour of the AR typology among parametric estimators. Hence, hereinafter, a more detailed description of the all-poles model is provided.

First of all, consider the transformation of the complex *f*-plane to a new plane, called the *z*-plane, through the relation:

$$z = e^{2\pi i f \Delta} \tag{3.23}$$

where Δ is the sampling interval of the continuous signal in the time domain (it is worth noticing that, limited to the present subsection, the reader must not confuse the z variable above defined with the one representing the impulse train process in the described shot noise structure).

A formal expression to represent the "true" spectrum is the following Laurent series that depends on the infinite number of values b_k:

$$S(f) = \left|\sum_{k=-\infty}^{\infty} b_k z^k\right|^2 \tag{3.24}$$

The (3.24) can be intuitively approximated in a general manner with a rational function with two finite series in both the numerator and the denominator. Less obviously, instead, there are some advantages in an approximation whose free parameters all lie in the denominator (all-poles approximation):

$$S(f) \approx \frac{b_0}{\left|1+\sum_{k=1}^{M} b_k z^k\right|^2} \tag{3.25}$$

As mentioned above, the approximation (3.25) of the real power spectrum goes under different names: indeed, apart from all-poles (where M is the number of poles adopted for the estimation) or autoregressive model, it is also usual to refer to Eq. (3.25) as *maximum entropy method* (MEM) approximation. Coefficients b_k can be evaluated by means of several estimation methods, among which the author has selected the Burg algorithm, developed by *Burg* [1975] and based on forward and backward prediction errors (see, for reference, *Stoica and Moses* [2005] Subsection 3.9.3).

Two main consideration need to be made concerning the all-poles spectra estimation technique.

Firstly, the author wants to justify the reason behind the name MEM of the method. As underlined by *Press et al.* [1996, Subsection 13.7], whatever is the chosen value of M in (3.25), the series expansion in the equation defines a sort of extrapolation of the autocorrelation function to lags larger than M, even to lags larger than the number of measurable data N. It results this particular extrapolation can be shown to have, among all possible

extrapolations, the *maximum entropy* in a definable information-theoretic sense. Because of this "fictitious" property, it is thought in general that it gives intrinsically better estimates if compared to other methods. Obviously, after this short explanation, one will be sure that this common assumption is totally unfounded.

The second consideration deals with the number M of poles (or *order* of the AR method) to adopt in the expansion series of Eq. (3.25). As reported by *Press et al*. [1996, Subsection 13.7], in common applications it is used to limit the order M of the MEM approximation to a few times the number of sharp spectral features that are desired to be fitted. In this way, the method tends to smooth the spectrum, that is often a desirable property to achieve. In general, however, even though exact values depend on the application considered, one might take M equal to 10 or 20 or 50 for N equal to 1000 or 10000, in order to make the MEM estimation not much slower than the Fast Fourier Transform (FFT) estimation.

3.5.3. The calibration approach

3.5.3.1. The parameters estimation

Once defined a form for the watershed TF, whose absolute value is showed in Eq. (3.21), in order to best model the behaviour of the basin forced by the effective rainfall process, the estimation of the unknown parameters vector $\boldsymbol{\theta}$ is possible by the adoption of Eq. (3.15). For this aim, the estimation of the deseasonalized streamflow process PSD ($S_{\overline{qq}}$), by the use of the aforementioned MEM method, was accomplished. Conversely, no estimation of the input process PSD was necessary (S_{zz}) since, as shown in

Eq. (3.15), its contribution in the relation between the output process PSD and the squared module of the TF is only that of a constant (G).

As widely repeated in previous sections, in order to allow the adoption of Eq. (3.15), it was necessary to deseasonalize the recorded streamflow series, $q(t)$. For this purpose, even though not reported here for the sake of conciseness, the deseasonalization method, clearly described in *Hipel and McLeod* [1994, Chapter 13], consisting in the difference between the generic series value with the mean of its corresponding season, was adopted.

Starting from these premises, the parameters estimation was conducted in a least square (LS) framework. The minimization of the sum of the squared differences between the numerical estimation of the deseasonalized streamflow process PSD, normalized in the range 0-1 ($\bar{S}_{\overline{qq}}$), and the analytic expression of the squared module of the TF (3.21), estimated in the frequency range of interest $[f_1 \dots f_N]$, was thus undertaken (refer to the following equation):

$$W(\boldsymbol{\theta}) = \sum_{i=1}^{N} \left[\bar{S}_{\overline{qq}}(f_i) - |H(f_i, \boldsymbol{\theta})|^2\right]^2 \tag{3.26}$$

Concerning the applied procedure, some important aspects need to be discussed.

First of all, it is worth noticing that the contribution of the constant PSD value (G) of the input process was neglected in the determination of the TF parameters. This was mainly due to the fact that, in order to minimize the function $W(\boldsymbol{\theta})$ of Eq. (3.26), its value must equal the value assumed by the PSD at the lowest frequency of the frequency range of interest (the so called *static gain*). This is the reason why the model calibration was performed considering the PSD normalized in the range 0-1 ($\bar{S}_{\overline{qq}}(f)$), obtained by

dividing each amplitude value by that assumed in correspondence of the lowest frequency.

Secondly, as above stated, a frequency range of interest $[f_1 \dots f_N]$ was defined in the minimization of Eq. (3.26). In order to understand such a decision of the author, consider Eq. (3.12) that defines the power spectrum (S_{yy}) as the FT of the autocovariance function (C_{yy}) of the generic time signal $y(t)$. As a matter of fact, the following inverse transform holds:

$$C_{yy}(\tau) = \int_{-\infty}^{\infty} S_{yy}(f)\, e^{j2\pi f \tau} df \tag{3.27}$$

from which it follows, setting the lag $\tau = 0$:

$$C_{yy}(0) = \sigma_y^2 = \int_{-\infty}^{\infty} S_{yy}(f)\, df \tag{3.28}$$

Eq. (3.28) demonstrates that the power spectrum shows how the variance (or mean power) of the time process is distributed over frequency [*Jenkins and Watts*, 1968, chapter 6.2]. Specifically, the variance of the process which is due to frequencies in the range f- $f + df$ is approximately $S_{yy}(f)df$. It is thus clear that by integrating the power spectrum in a certain frequency range gives the amount of the total variance (or mean power) in that range.

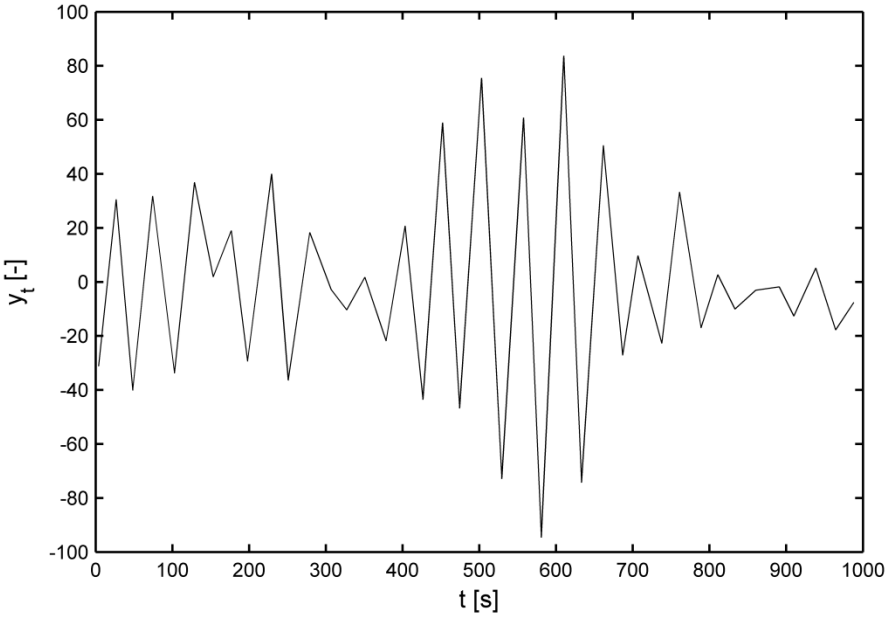

Fig. 3.1. Realization of a generic process $y(t)$

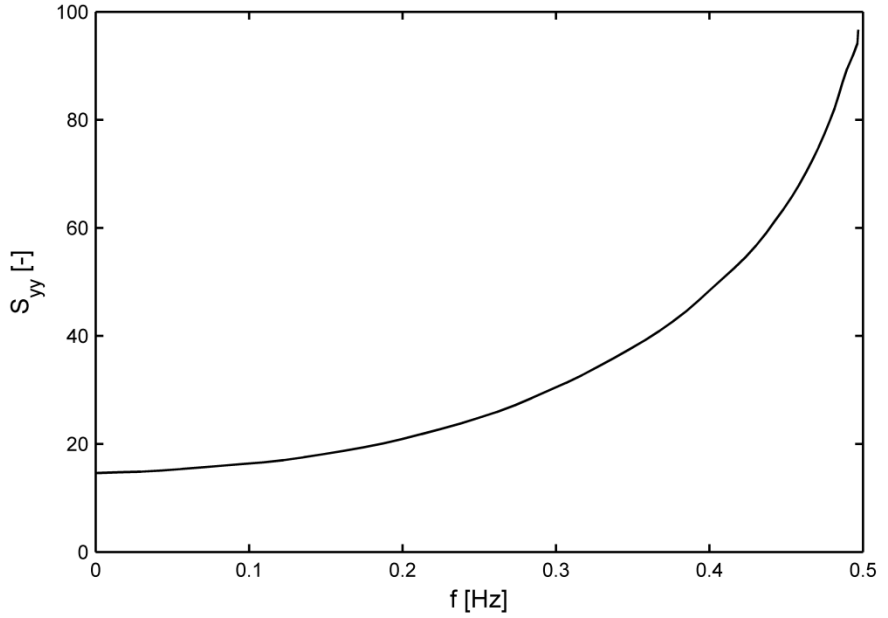

Fig. 3.2. Spectrum of the process $y(t)$ shown in Fig.3.1

For instance, consider the time process of Fig. 3.1 and the corresponding power spectrum of Fig. 3.2. It is evident that the series oscillates very quickly, with the corresponding spectrum with a large power at high frequencies and a small power at low frequencies. Hence quickly oscillating series are characterized by spectra which have most of their power at high frequencies.

Given these considerations, when results of the described procedure to three case study watersheds are provided in Section 4, it will be evident a concentration of the total variance of the process in correspondence of the lowest frequency values. As a consequence, a neglect of the higher frequencies mean power contribution was possible, by minimizing Eq. (3.26) in a fixed frequency range of interest which goes from the lowest value to a opportunely selected maximum frequency limit. In particular, several cut-off frequencies were considered, evaluating the different estimated model performances in terms of its ability to generate synthetic streamflow series compatible, in terms of main statistical features, with the historic series. As widely shown in Section 4, major problems were found in the reproduction of the second and third order moments. Finally, however, the author concluded that, independently from the riverflow series considered, a frequency range of interest limited to 2×10^{-6} Hz was sufficient to meet all the tested statistics.

Eventually, another consideration is needed concerning the PSD inability of conveying information about the phase of the system to be identified and the mean value of the process. As a matter of fact, the PSD of a time series is not affected in any manner by both a shift in the mean and a shift of the whole series in time (equivalent to a change in the phase) [see, e.g., *Montanari and Toth*, 2007]. As a consequence, when the spectral estimation of conceptual

models is undertaken by means of PSD-based estimators, researchers have adopted several techniques to cope with these two orders of problem. For instance, *Montanari and Toth* [2007] preserved the mean of the streamflow process through the assumption of zero mean for the residuals of the model, while they preserved the process phase introducing the PSD of the model error (that is connected to the system phase) in the objective function to minimize. In the present work, instead, the author solved these problems in different ways.

Concerning the preservation of the process phase, the minimum phase property of the model was adopted. Indeed, as already mentioned in Subsection 3.5.1, such a property allows one to neglect the direct adoption of phase information in the identification procedure, since they are univocally determined from the knowledge of the process output process PSD. In other words, a model calibration undertaken in the spectral density domain returns the estimation of the minimum phase system corresponding to the adopted power spectrum. So, if one could preventively verify the minimum phase property of the model to identify, he is certain that the system identified by the adoption of a PSD-based estimator corresponds to the objective one. On the contrary, if the target system is not minimum phase (see the work of *Muratori et al*. [1992] about the minimum phase property of linear compartmental systems), the identified model (minimum phase realization of the adopted PSD) is not the correct one.

The preservation of the mean, instead, was not guaranteed through the assumption of zero-mean residuals, since in the calibration approach no attention was paid to the input process, thus the estimation of model residuals was not possible. However, as deeply shown hereinafter, the ability of the model to reproduce the mean of the streamflow data was evaluated by comparing the moments of the observed and simulated discharge series

(through a simulation analysis). In particular, once the model has been calibrated, in order to generate synthetic streamflow series the preliminary generation of synthetic effective rainfalls is needed, to be subsequently convoluted in the time-domain with the time response function. For this aim, thus, the selection of a suitable effective rainfall model between several available in the literature is needed. In the following subsection the description of the selected model is provided, with a particular focus on the available techniques for the estimation of its parameters.

3.5.3.2. Effective rainfall model selection and estimation

As above highlighted, the generation of synthetic effective rainfall series is preparatory for the generation of synthetic streamflow series. In particular the first difficult task consists in the selection of an appropriate model for the representation of the effective rainfall process, given that the natural corresponding process is unobservable. At this stage, however, the author has considered that the effective rainfall process retains most of the stochastic properties of the total (observable) rainfall process, which has led to the necessity of estimating the effective rainfall series directly from the recorded streamflow series, as deeply described hereinafter.

The model class selected is that of the physically-based point processes. Among them, the classical marked Poisson white noise processes [e.g., *Eagleson*, 1978] and the ones reproducing the rainfall events as a sequence of storms made of clusters of rain cells (such as the Neyman-Scott or the Bartlett-Lewis processes [e.g., *Kavvas and Delleur*, 1981; *Rodriguez-Iturbe* et al., 1984]) have been considered in a preliminary stage. The selection of the particular model to adopt in the simulation analysis has been mainly affected by the considered scale of aggregation, given that serial correlation

decreases with the increasing aggregation scale. In particular, for scale of aggregation up to 2 days, observable rainfall data present significant autocorrelation, which is generally reproduced correctly by cluster-type models [*Bo et al.*, 1994]. However, given that in the definition of the effective rainfall process it is fundamental the adopted model of the watershed response, it is not guaranteed that the same degree of correlation exists also on the effective rainfall process. In particular, *Murrone et al.* [1997], following the procedure proposed by *Cowpertwait and O'Connell* [1992], investigated on the effectiveness of the estimation of the four-parameters Neyman-Scott model, with exponential instantaneous pulses within a SN model of daily streamflows, on the effective rainfall series obtained by inverse estimation from the recorded streamflow process. As clearly reported by the authors, it was not possible to detect the "within storm" cellular structure of the effective rainfall, thus failing in the estimation of the most peculiar feature of this kind of models. Starting from this outcome, it was judged that the two-parameter PWNE model above mentioned represents a reasonable choice for short aggregation scales.

In the PWNE model, the number N of occurrences in the time interval Δt follows a Poisson distribution, with parameter λ, while an exponential distribution, with mean $1/\beta$, is assumed for the intensity of instantaneous pulses [*Murrone et al.*, 1997]. The Probability Density Function (PDF) and the Cumulative Distribution Function (CDF) of the cumulated effective rainfall, z, over the duration Δt are given, respectively, by the following expressions (see, for reference, *Eagleson* [1978]):

$$f(z) = e^{-\lambda\Delta t}\left[\delta(z) + \frac{\sqrt{\lambda\Delta t\beta}}{z} I_1\left(2\sqrt{\lambda\Delta t\beta z}\right)e^{-\beta z}\right] \tag{3.29}$$

$$F(z) = e^{-\lambda\Delta t}\left\{1 + \sum_{\nu=1}^{\infty}\left[\frac{(\lambda\Delta t)^{\nu}}{\nu!}P(\nu, \beta z)\right]\right\} \tag{3.30}$$

where δ is the Dirac delta function, I_1 is the first order modified Bessel function and $P(\nu, \beta z)$ is the Pearson's incomplete gamma function.

Murrone et al. [1997] proposed and tested both Moments and Maximum Likelihood estimates of the couple of parameters λ and β. However, in this work only the first estimation method has been adopted, thus only method of moments formula are provided below:

$$\hat{\lambda} = \frac{2m_z^2}{s_z^2\Delta t}; \qquad \hat{\beta} = \frac{2m_z}{s_z^2} \tag{3.31}$$

where m_z and s_z are the sample mean and standard deviation of the cumulated effective rainfall series, $Y(t)$. In particular, in order to preserve the seasonal variability of the mean of the input process, and, consequently, of the output process, they were estimated on 13 different seasons of $T = 28$ days each, wherein they were supposed to remain constant.

It is worth underlying the importance of a proper estimation of the effective rainfall model parameters, since, as already pointed out in previous sections, the calibration procedure, synthesized by Eq. (3.26), does not allow the preservation of the first order moment of the record streamflow series. As a consequence, a crucial aspect in the estimation of the PWNE model, given by Eqs. (3.29) – (3.30), consists in the determination of rainfall pulses occurrences on which formula (3.31) are applied to return adequate parameters estimates. As a matter of fact, it should be noticed that the values assumed by the couples of the PWNE parameters, at each season of 28 days, directly affect the trend, given to the seasonality, of the mean of the impulse train process and, as a consequence, of the streamflow process.

In particular, in the SN modeling of occurrences, the methods for the effective rainfall model parameters estimation that have received more interest by the scientific community are those proposed by *Xu et al*. [2002] and *Claps and Laio* [2003], only briefly described in the Subsection 3.4, with the latter that has to be considered as an evolution of the aforementioned DIP approach (introduced by *Murrone et al*. [1997]). For this reason, in the following part of the present section, a comparison of their ability to reproduce the statistical properties of the observed streamflow series is provided.

The first tested procedure, the so-called FPOT (Filtered Peaks Over Threshold), was proposed by *Claps and Laio* [2003] to which the reader has to refer for more details about the algorithm steps that, however, have been summarized in Subsection 3.4. As showed in the next section, concerning the application and the validation of the proposed calibration procedure, the main drawback of the FPOT technique consists in the poor number of selected effective rainfall events per year if compared to the actual number of events of the analyzed watershed. In particular, *Claps et al*. [2005] derived the result of about 5 – 20 events per year on a large number of runoff series, suggesting a clue of inadequacy of the Poisson independent model in the correct reproduction of the effective rainfall behavior.

The second tested procedure is that originally proposed by *Xu et al*. [2001] and subsequently adopted by *Xu et al*. [2002]. As in *Claps and Laio* [2003], the unobservable pulse series is reconstructed by using observed daily streamflow data but this time it is assumed that pulses occur on all those days when streamflow increases (thus avoiding the poor number of effective rainfall occurrences of the FPOT technique). Once given the occurrences days, the pulses intensities are estimated by making a LS fit of the reproduced streamflow to the observed ones, with the former estimated by

the convolution of the *i*th iteration effective rainfall series and the time response function h with parameters given by the minimization of Eq. (3.26). Eq. (3.32) shows the aforementioned LS objective function, where $q(i)$ is the recorded daily streamflow at day i and z' is the generic reconstructed pulse height.

$$\Delta = \left\{\frac{1}{n}\sum_{i=1}^{n}\left[q(i) - \sum_{j=1}^{i} z'(\tau_j)h(i-\tau_j+1)\right]^2\right\}^{1/2} \tag{3.32}$$

Once obtained the reconstructed pulse heights series by minimization of Eq. (3.32), the non-homogeneous Poisson point assumption of the effective rainfall events is verified through a classic χ^2 goodness-of-fit test for each month of the year (see Section 4, concerning the application and the validation of the procedure, for more details). After that, the parameters of the PWNE model are estimated by the adoption of the method of moments formula of Eq. (3.31). As shown in the following section, the whole described procedure leads to a more realistic final effective pulse series if compared to the FPOT ones, in terms both of the number of occurrences and the peaks intensities. As a consequence, a more effective estimation of the PWNE model parameters is obtained, allowing, through the generation of synthetic rainfall series (following the procedure described in the next subsection), the reproduction of the streamflow recorded series first order moment in the streamflow simulation analysis.

3.6. Model validation and testing: a simulation analysis

Once firstly estimated the time response function parameters by minimizing the cost function provided by Eq. (3.26) with respect to the parameters vector $\boldsymbol{\theta}$, and once secondly estimated the effective rainfall model parameters (i.e. λ and β) on the input series obtained by the minimization of Eq. (3.32), a simulation analysis was undertaken in order to compare the synthetic streamflow series statistical features to those of the recorded one. For this purpose, a discrete time convolution (as that of Eq. (3.8)) between the time response function $h(t)$ with known parameters and the effective rainfall synthetic series was undertaken.

In particular, the generation of synthetic rainfall series was accomplished through the adoption of the *universal random variable generator* deeply described by *Hipel and McLeod* [1994, p. 302], which allows one to transform a given sequence of independent uniformly distributed random variables to a sequence belonging to another known distribution. In such a framework, the first step is to produce independent variables that follow a uniform distribution on the interval (0,1) by the adoption of a *random number generator*. In particular, as clearly stated by *Hipel and McLeod* [1994, p. 297], even though a digital computer follows a strictly deterministic process (since it exactly adheres to some precise instructions), the generation of a sequence of numbers which appear to be independent values distributed on the unit interval is possible. These numbers are referred to as *pseudo-random numbers* and are generated by a pseudo-random numbers generator. Over the year a wide range of pseudo-random numbers generators has been developed. However, both for the sake of conciseness and for the wide availability of ad hoc routines in the Matlab environment,

the author will not provide a review of these generators, referring the interested reader to the Subsection 9.2.2 of *Hipel and McLeod* [1994].

Some details will be instead provided in the following lines about the aforementioned universal random variable generator that allow the transformation of a sequence of independent uniformly distributed random variables, $\{\varepsilon_i\}$, to a new sequence, $\{w_i\}$, belonging to another distribution with known CDF, $F(w)$. The generator adopted in the present work is that introduced by *Yakowitz* [1977, p. 41] and subsequently reported in *Hipel and McLeod* [1994, p. 302]. In particular, given the sequence $\{\varepsilon_i\}$, the formula of the CDF, $F(w)$, of the distribution that one wishes the transformed variable to follow and the length, N, of the $\{w_i\}$ sequence to be generated, for each $\varepsilon = \varepsilon_i$ of the input sequence the algorithm determines $w = w_i$ such that:

$$w = minimum\{r: F(r) \geq \varepsilon\} \tag{3.33}$$

It can be proven that, if the $\{\varepsilon_i\}$ are uniform, the obtained output sequence, $\{w_i\} = w_1, w_2, \dots, w_N$, are independent and follow the required distribution $F(w)$, that in this case corresponds to Eq. (3.30).

Given that the parameters of the distribution (3.30) were estimated on 13 different seasons of $T = 28$ days each, the above described procedure was applied to each single season in order to obtain a synthetic series of effective rainfall that follows the PWNE distribution characteristic of that season. Subsequently, rearranging the obtained sequences in the proper manner, synthetic effective sequences of length $M = 364N_{sim}$ (with N_{sim} the defined number of years of the simulation and 364 the number of days in a year, considering 13 seasons of 28 days each) were obtained. In particular, in order to allow the study of mean statistical properties of synthetic

streamflow series, the generation of 1000 rainfall series of length M was executed.

Finally, synthetic streamflow series, $\{q^*(t)\}$, of equal length, were obtained through the discrete-time convolution between the generated effective rainfall series, $\{z^*(t)\}$, where each $z^*(t)$ represents the cumulated rainfall value occurring in the time interval $[(t-1)\Delta t, t\Delta t]$ (where, in turn, t represents the generic day of the whole simulation length), and the time response function, $h(t)$, of Eq. (3.19), with known parameters. The discharge value, $q^*(t)$, at time t, representing the mean daily flow in the interval $[(t-1)\Delta t, t\Delta t]$, was thus obtained by the following expression of the discrete-time convolution:

$$q^*(t) = \sum_{j=1}^{t} \left\{ z^*(t-j+1) \left[\frac{\bar{F}(j\Delta t) - 2\bar{F}\left((j-1)\Delta t\right) + \bar{F}\left((j-2)\Delta t\right)}{\Delta t} \right] \right\} \tag{3.34}$$

In Eq. (3.34), $\bar{F}$ stays for the double time-integral of the impulse response function, $h(t)$, assumed for the whole watershed given by Eq. (3.19), whose analytical expression is given by:

$$\bar{F}(t) = \alpha_0 t + \sum_{i=1}^{3} k_i \alpha_i \left(\frac{t}{k_i} + e^{-\frac{t}{k_i}} - 1 \right) \tag{3.35}$$

where k and α are, respectively, the storage coefficient and the linear combination coefficient of the generic linear reservoir characterizing the watershed response function of Eq. (3.19). Hence, the generic synthetic streamflow series was given by the sequence $\{q^*(t)\}$, with $t = 1 \dots M$ and $M = 364 N_{sim}$.

In particular, N_{sim} was selected in order to double the length of the recorded streamflow series, in terms of years (N_{rec}), to allow the removing of the first

N_{rec} years from the synthetic streamflow series, in order to avoid the influence of initial conditions of the simulated series in the statistical analysis proposed in the following section.

From the given framework, a comparison between statistical features of recorded and simulated streamflow series was thus carried out for each of the case-study riverflow series. In particular, as highlighted in Section 4, concerning the application of the proposed calibration procedure, the overall quality of the obtained solution was evaluated in terms of its ability to:

a) reproduce the first three moments, averaged on the different months, of the recorded series probability distribution;

b) return an average flow volume, in a period of length equal to N_{rec}, similar to that corresponding to the recorded series;

c) guarantee a satisfying reproduction of flow duration curves;

d) reproduce minimum and maximum values, averaged on different aggregation scales, of the recorded series.

More insight into the described analysis of the overall quality of the solution are provided in the following section.

4. Application and testing

4.1. Description of the case studies streamflow series

The identification procedure proposed in this thesis was applied to 3 time series of mean daily flows to allow the estimation of the TF parameters of the corresponding watersheds. In particular, in order to investigate on the capacity of the methodology to be adaptable in several different situations, one of the main necessities of the author was that of applying the overall procedure to case studies streamflow series belonging to different, in terms of physical characteristics, hydrologic watersheds. For this reason, the three series, related to three Italian rivers and listed in Tab. 4.1, were selected. In particular, in the cited table, for each streamflow series, the lengths of the recording periods, N_{rec}, and the following main characteristics of rivers and corresponding basins are reported: the whole basin area, A, corresponding to the position of the gauging station on the river path; the length of the river path from the corresponding headwater to the considered gauging station, $L_{g.s.}$; the height of the gauging station above the sea level, h_m. In particular, the reader should note: the relevant difference between the basin area of the Bormida River and those of the two other rivers; the fact that the height of the gauging station of the Scrivia River almost double that of the Alento

River; the relevant difference existing in terms of length of the path from the sources to the gauging stations between the considered rivers.

Tab. 4.1. Characteristic features of drainage basins and runoff series considered in the application

Series	Gauging station	A [km^2]	h_m [m a.s.l]	N_{rec} [years]	$L_{g.s.}$ [km]
(a)	Alento at Casalvelino	284	350	15	30
(b)	Scrivia at Serravalle	605	695	14	80
(c)	Bormida at Cassine	1483	493	12	150

The first recorded streamflow series is that related to the Alento River, which, with a global length of 36 km, originates in the mountain area of Monte Le Corne (894 m a.s.l.), within the Cilento National Park, and empties into the Tyrrhenian Sea. The whole path of the Alento River interests only the Campania region of Italy. The second historical series concerns the Scrivia River, which originates in the Liguria region territory, at an altitude of about 450 m a.s.l., and empties, after crossing both the territory of Piemonte and Lombardia regions, into the Po, i.e. river with the major length in Italy, with a total length of about 110 km. The third and last considered series is that related to the Bormida River, which, with a total length of about 180 km, originates in the Liguria region territory, at an altitude of about 800 m a.s.l., and empties, crossing also the Piemonte region territory, into the Tanaro river, which, in turns, empties into the aforementioned Po river.

It is worth noticing that the given length N_{rec} of the records is not intended as a continuous recording period, since, in order to deal with significant

records, the author needed to bound together two or more parts of consecutive records. However, in absence of changes in the existing natural flow regime, this necessity is not to be considered as a problem, since each year of records has to be seen as an individual and independent realization of the stochastic process of mean daily flows. Moreover, the author underlines that considered observation periods for the selected watersheds are equivalent to those adopted by *Murrone et al*. [1997] and *Claps and Laio* [2005] in the application of their previously described time-domain identification approaches to the same basins. Such a decision was due to the necessity to allow a significant comparison between the results of the spectral-domain calibration procedure, introduced in this work, and the traditional time-domain approach followed by the aforementioned works.

However, the selection of the riverflow series listed in the previous table was not suggested only by considerations on physical characteristics of the corresponding watersheds. Indeed, the intention of the author was also that of testing the methodology effectiveness on case studies basins characterized by different climate regimes. In order to make such a point comprehensible, a short framework concerning the classification of the climate regime of a region needs to be presented in the following lines.

Several criteria are available in the scientific literature to make a classification of the climate. In particular, *Thornthwaite* [1948] proposed a classification based on the so-called *climate index* ($\bar{I}$), given by the following equation:

$$\bar{I} = \frac{\bar{h} - \bar{E}_p}{\bar{E}_p} \tag{4.1}$$

where $\bar{h}$ is the mean annual rainfall depth (expressed in mm), to estimate as an arithmetic mean between the values obtained in the several recording years of observation of the phenomenon, and $\bar{E}_p$ is the mean annual potential evapotranspiration (expressed in mm), whose definition, among the several available in the technical literature, in terms of the monthly mean temperature, $\bar{t}_j$, is given by the empirical formula provided by *Thornthwaite* [1948]. Given the estimated value of the climate index according to Eq. (4.1), according to the Thornthwaite's criterion, it is possible to distinguish between:

- humid climates, i.e. those characterized by $\bar{I} \geq 0$, and the corresponding sub-classes;
- arid climates, i.e. those characterized by $\bar{I} \leq 0$, and the corresponding sub-classes.

On the Italian territory the variability of the climate index between regions is due to several factors, among which: the extension of the territory on more than 10 degree of latitude, the thermo-regulator effect of the Mediterranean sea and, eventually, its complex orography, characterized by the Alps, which protect the peninsula from cold northern winds, and the Appennine. As a matter of fact, these factors determine the geographical variability of both the mean annual temperature ($\bar{t}$) and the mean annual rainfall depth ($\bar{h}$). In particular, the first gradually increases from the north to the south of the peninsula, while the mean annual rainfall depth is strongly influenced by the orography of the territory. As a consequence, given the cited variations of $\bar{t}$, and thus of $\bar{E}_p$, and $\bar{h}$, the climate index given by Eq. (4.1) is strongly variable not only between different regions but also within the same generic region (for more details please refer to *Penta and Rossi* [1979]).

However, in order to properly characterize the climate of a given Italian region it is also useful to reasoning on quantities as the monthly mean

rainfall depths, $\bar{h}_{r,j}$ (with j the subscript representing the *j*th month of the year), and the monthly mean potential evapotranspiration ($\bar{E}_{p,j}$). As a matter of fact, it should be known that in Italy the distribution of $\bar{h}_{r,j}$ varies consistently among the different regions according to the various rainfall regimes that characterize the Italian territory. In particular, it is possible to distinguish between [see for reference *Bandini*, 1931]:

- a *continental rainfall regime*, which presents minimum values of the monthly mean rainfall depth in the winter season and maximum values in the summer season (this regime is typical of the continental Europe);
- a *maritime rainfall regime*, which is the opposite of the continental one and which is characteristic of the coastal zones of central and southern Italy;
- three different *sub-coastal rainfall regimes* (not reported here for the sake of brevity) that are intermediate between the previous ones, each characterized by two distinct maximum values, in spring and autumn, and two distinct minimum values, in winter and summer.

Given that the dry season is defined as the ensemble of months j characterized by $\bar{h}_{r,j} < \bar{E}_{p,j}$, one can recognize that the total dry season duration gradually increases passing from regions characterized by a continental to a maritime rainfall regime.

Starting from the above provided framework, the author selected the three case studies streamflows series of Tab. 4.1 in order to apply the proposed spectral-domain calibration approach to basins characterized by different rainfall regimes. As a matter of fact, Scrivia and Bormida rivers time series (shown in Fig. 4.1b,c respectively) are associated to watersheds located in the north-west Italy and are mostly influenced by the climate of the Alps (i.e. a dominant continental regime). The Alento River streamflow series (see Fig. 4.1a), instead, is related to the Apennine region of central-southern Italy, hence it is mostly characterized by a maritime rainfall regime.

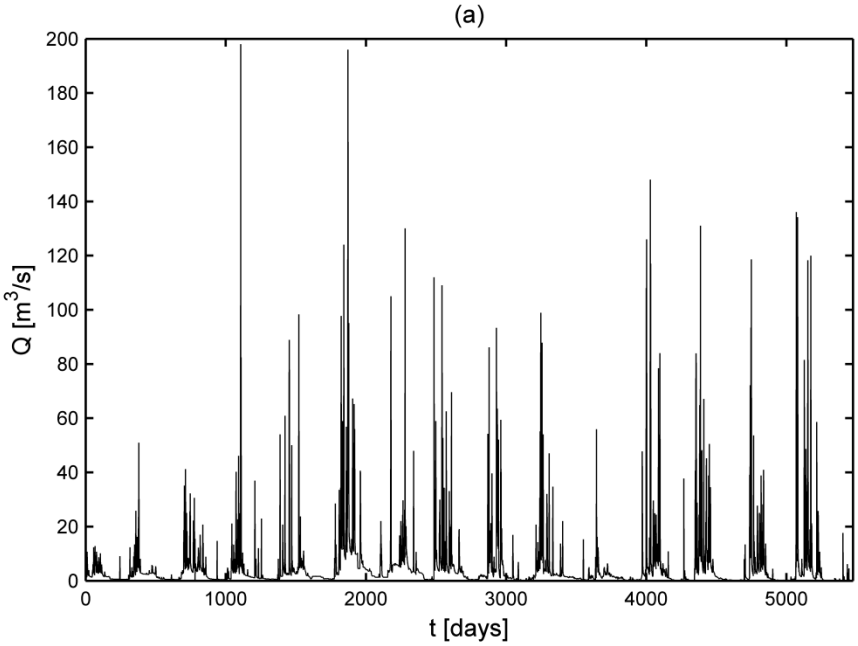
(a)
Q [m3/s]
t [days]
0
20
40
60
80
100
120
140
160
180
200
0
1000
2000
3000
4000
5000

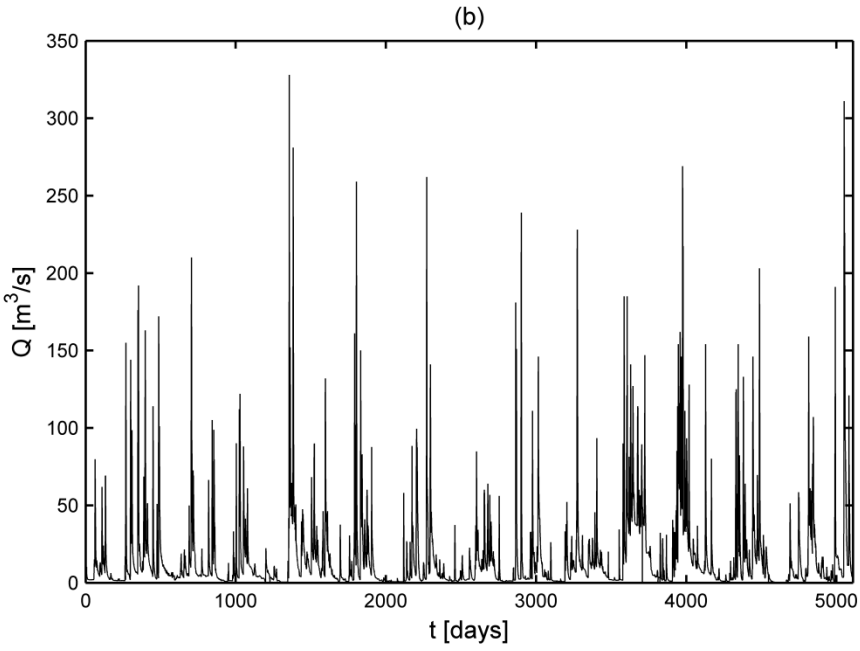
(b)
Q [m3/s]
t [days]
0
50
100
150
200
250
300
350
0
1000
2000
3000
4000
5000

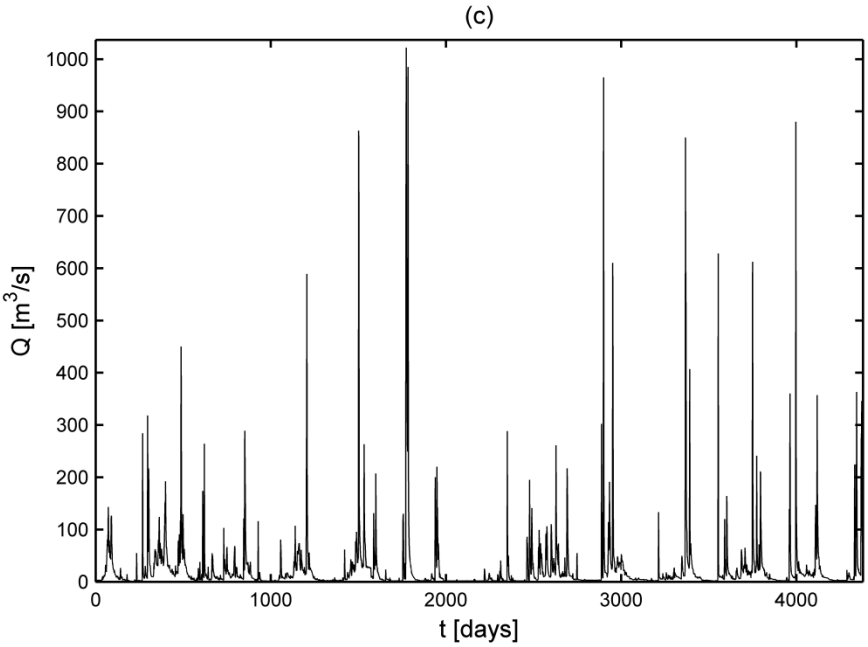

Fig. 4.1. Recorded streamflow series – (a) Alento; (b) Scrivia; (c) Bormida

4.2. Power spectral density (PSD) estimation

PSDs of the deseasonalized case studies streamflow series were estimated by the adoption of the maximum entropy method (MEM), deeply described in Subsection 3.5.2.3 dealing with parametric (or model-based) PSD estimation methods. In particular, coefficients b_k of Eq. (3.25) were evaluated by the adoption of the Burg algorithm, developed by *Burg* [1975] and based on forward and backward prediction errors (see, for reference, *Stoica and Moses* [2005], Subsection 3.9.3). For this purpose, the Matlab built-in function *psd* was adopted, selecting as *estimator* the *burg* option and setting:

- the sampling frequency to $F_s = 1/86400$ Hz, given that 86400 is the number of seconds in a day (i.e. the sampling interval, Δt, of the recorded series in the case of mean daily streamflows);

- the number of poles in the MEM approximation of the "real" PSD, or, equivalently, the number of b_k coefficients in the denominator of Eq. (3.25), to $M = 4$ (for further details concerning this choice, please refer to Subsection 4.3.2).

In the following Fig. 4.2 the PSDs estimates of the three case studies riverflow series, with the corresponding confidence interval at the 95% confidence level (represented by dash-dotted lines), are provided.

Some aspects concerning the representation of the PSD need to be highlighted. First of all, it should be noticed that the highest frequency value for which the PSD is sought, is usually equal to $1/2\Delta t$. This frequency is known as the Nyquist frequency, sometimes also called the cut-off frequency F_c. Furthermore, it is worth noticing that the PSD is usually represented with the power, i.e. vertical, axis reported in decibel (dB) and the frequency, i.e. horizontal, axis reported in Hertz (Hz), with the latter according to a logarithmic scale. In particular, it is worth noticing that in order to obtain the generic power value, P, in decibel, P_{dB}, the following transformation is needed: $P_{dB} = 20log_{10}(P)$.

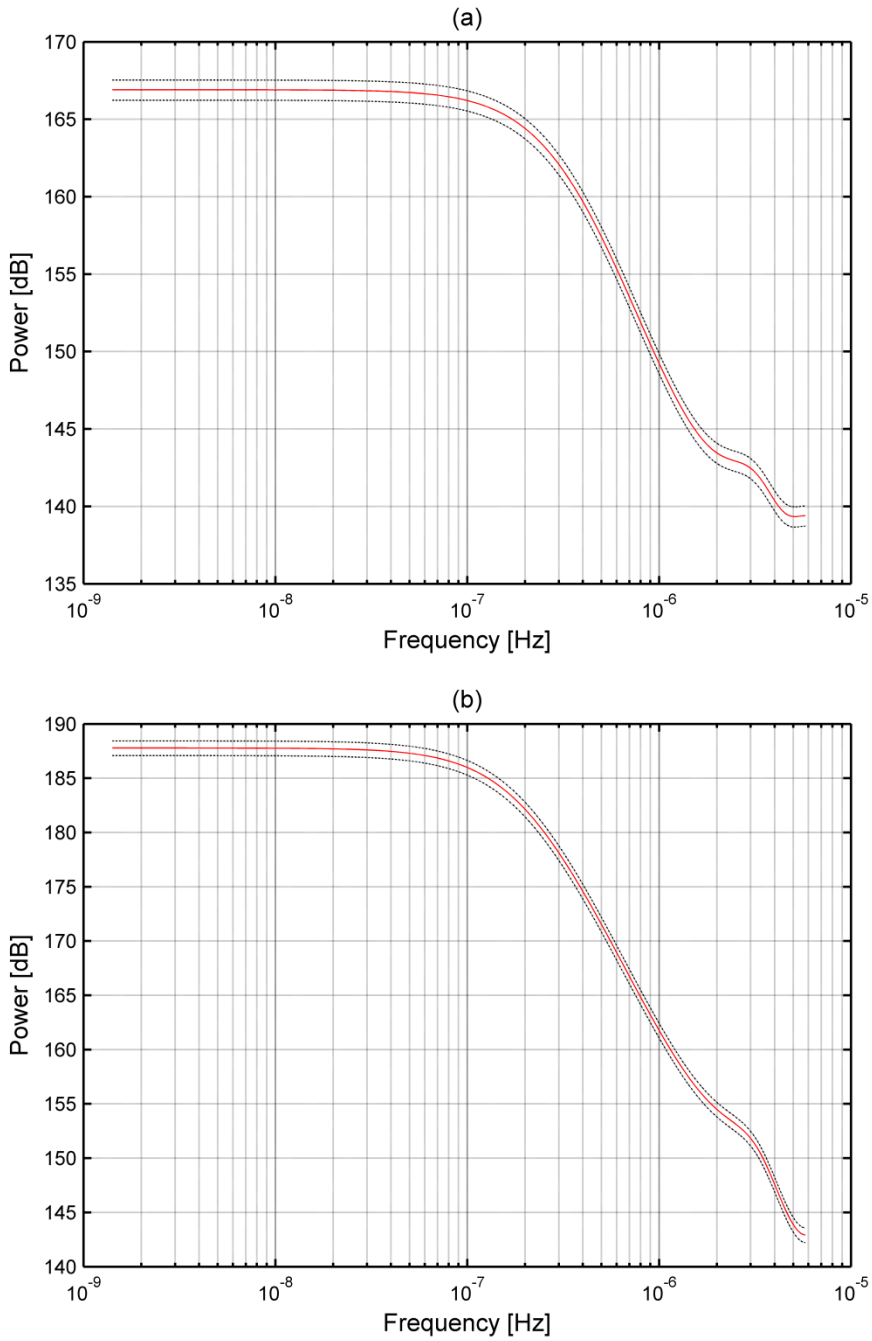
(a)
Power [dB]
Frequency [Hz]
(b)
Power [dB]
Frequency [Hz]

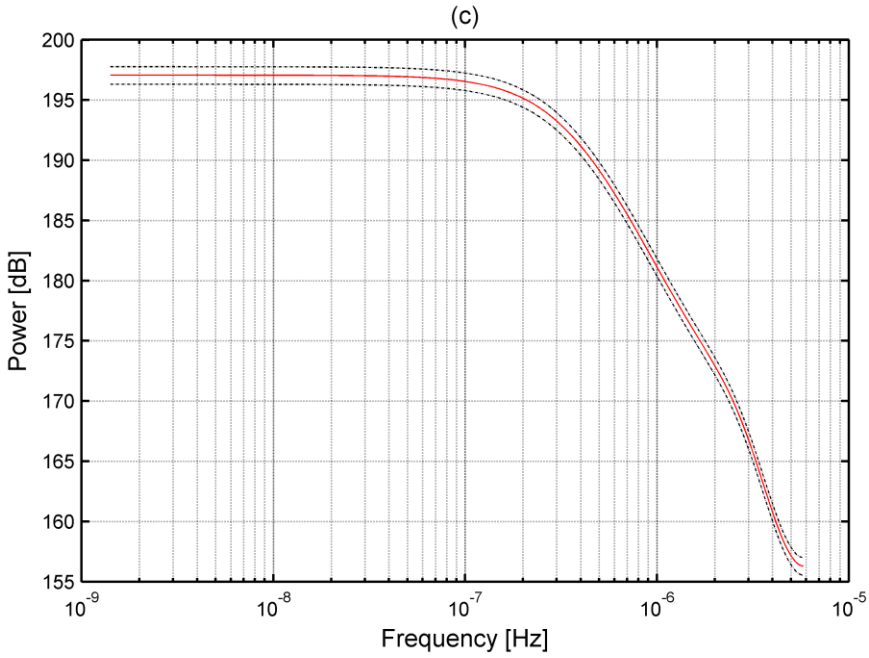

Fig. 4.2. Burg PSD estimates (95% confidence limits in dash-dotted lines); $M = 4$ – (a) Alento; (b) Scrivia; (c) Bormida

An interesting consideration is needed concerning the PSD frequency range of interest. It is well known that the total power in a time signal is the same whether one computes it either in the time domain or in the frequency domain (Parseval's theorem):

$$Total\ Power = \int_{-\infty}^{+\infty} |h(t)|^2 dt = \int_{-\infty}^{+\infty} |H(f)|^2 df \qquad (4.2)$$

where $H(f)$ is the Fourier transform of the function $h(t)$ [*Press et al.*, 1996, p. 492]. In particular, if one wants to determine the amount of power contained in a certain frequency range, the one-sided power spectral density of the function needs to be estimated, that, in case of real time function, at each frequency f is equal to:

$$P_h(f) = 2|H(f)|^2 \tag{4.3}$$

It is thus clear that the integral of the PSD over a given frequency band computes the average power in the signal over that frequency band. Starting from this consideration, given the PSD estimations of Fig. 4.2, it should be evident that, once passed a certain frequency value, the increase in the frequency band does not result in an considerable increase of the average power. As a consequence, one could define an exact frequency value (a *cut-off frequency*) above which the neglect of the PSD contribution does not result in a relevant underestimation of the total average power of the signal. To cope with this problem, the author tested the calibration procedure described in Section 3, and applied to the three streamflow series in the following subsections, by applying it several times considering different values of the aforementioned cut-off frequency. Results were evaluated in terms of the ability of the estimated time response function, given by Eq. (3.19), to properly reproduce the main statistical features of the recorded series. In particular, the author noticed that above a cut-off frequency value of $2e^{-6}$ Hz there was not an improvement of the aforementioned ability of the identified model. As a consequence, the fitting of the streamflow process PSD by means of the squared module of the TF with unknown parameters (through minimization of the cost function of Eq. (3.26)), was undertaken, for each of the case studies streamflow series, from the lowest frequency value to a maximum fixed to $2e^{-6}$ Hz.

4.3. Transfer function parameters estimation

4.3.1. A multidimensional minimization approach: Powell's method

Given the analytical TF form of Eq. (3.20), with the corresponding module formula of Eq. (3.21), and the couple of values frequency-power representing the PSDs estimation of the case studies riverflow series, in the determined frequency range of interest, the minimization of the cost function of Eq. (3.26) was undertaken in order to estimate values of the unknown response function parameters.

For this purpose, a multidimensional minimization problem was defined, i.e. finding the minimum of a function, $W(\boldsymbol{\theta})$, of more than one independent variable ($\boldsymbol{\theta} = \{\alpha_0, \alpha_1, \alpha_2, \alpha_3, k_1, k_2, k_3\}$). Several methods are available in the technical literature for the resolution of such a problem and a thorough review is provided by *Press et al*. [1996, Section 10]. However, in this thesis the *direction set* (or *Powell*'s) *method* [*Powell*, 1964] was adopted, and, in order to understand the usefulness of such a method, a brief introduction to direction set methodologies is needed.

It is known that if one starts at a point $\boldsymbol{P}$ in a *N*-dimensional space and proceeds from there in some vector direction $\boldsymbol{n}$, then any function of *N* variables $f(\boldsymbol{P})$ can be minimized along the line $\boldsymbol{n}$ by one of the one-dimensional methods described in Section 10 of *Press et al*. [1996]. Various multidimensional minimization methods consist of sequences of such *line minimization* and they differ between each other only by how, at each stage, the next trial direction $\boldsymbol{n}$ is chosen. In particular, an interesting class of methods is characterized by those whose choice of successive directions does not involve explicit computation of the cost function gradient, given

that, in many practical situations, this computation could represent a considerable limit to the application of the minimization procedure.

In such a case, thus, one might first think of a simple method. Take the unit vectors $(\boldsymbol{e_1}, \boldsymbol{e_2}, \dots, \boldsymbol{e_N})$ as a set of directions and, using one-dimensional methods, move along the first direction to its minimum, then, from there, along the second direction to the corresponding minimum, and so on, cycling through the whole set of directions, as many times as necessary, until the given cost function stop decreasing. It is thus obvious that what is mainly needed in these cases is a better set of directions than the $\boldsymbol{e_i}$'s. All direction set methods, for instance, consist of prescriptions for updating the set of directions as the method proceeds, attempting to come up with a set which either:

- includes some very good directions that will take the procedure far along narrow valleys of the solution space;
- or includes some number of *non-interfering*, or *conjugate*, directions with the special property that minimization along one is not "spoiled" by subsequent minimization along another, so that interminable cycling through the set of directions can be avoided (for further details please refer to *Press et al*. [1996, Subsection 10.5]).

In particular, the ideal direction set method would come up with a set of *N* linearly independent, mutually conjugate directions. *Powell* [1964] first discovered a direction set method that produces such directions characterized by such a property. His methodology starts from initializing the set of directions $\boldsymbol{d_i}$ to the basis vectors, that is $\boldsymbol{d_i} = \boldsymbol{e_i}, i = 1 \dots N$, and, then, repeating the following steps until the function stop decreasing:

- save the starting position as $\boldsymbol{P}_0$;
- for $i = 1 \dots N$, move $\boldsymbol{P}_{i-1}$ to the minimum along direction $\boldsymbol{d_i}$ and call this point $\boldsymbol{P}_i$;

- for $i = 1 \ldots N - 1$, set $\boldsymbol{d_i} = \boldsymbol{d_{i+1}}$;
- set $\boldsymbol{d_N} = \boldsymbol{P}_N - \boldsymbol{P}_0$;
- move $\boldsymbol{P}_N$ to the minimum along the direction $\boldsymbol{d_N}$ and call this point $\boldsymbol{P}_0$.

Powell [1964] showed that, for quadratic cost function of form similar to that of Eq. (3.26), k iterations of the above "basic procedure" produce a set of directions $\boldsymbol{d_i}$ whose last k members are mutually conjugate. Hence, N iterations of the basic procedure, amounting to $N(N+1)$ line minimizations, will exactly minimize a quadratic form cost function.

However, one of the main problem of the Powell's quadratically convergent method, consists in the fact that the procedure tends to produce sets of directions that fold up on each other and become linearly dependent. As a consequence, the procedure finds the solution only over a finite subspace of the full *N*-dimensional case. Nevertheless, there are several ways to fix up the problem of linear dependence in Powell's algorithm, among which *Press et al*. [1996, Subsection 10.5] provided three main alternatives that are not reported here for the sake of brevity. Among them, however, the one chosen by the author and implemented in the minimization algorithm consists in the introduction of a more heuristic scheme (due to Powell) which, once given up the property of quadratic convergence, tries to find some good directions along narrow valley, instead of *N* necessarily conjugate directions. The complete routine for the application of the Powell's method is reported in p. 411 by *Press et al*. [1996].

4.3.2. Calibration results

The above described almost quadratically convergent Powell's method was applied to estimate the vector parameter values, $\boldsymbol{\theta}$, through the minimization of the cost function of Eq. (3.26), reported here for the sake of clearness:

$$W(\boldsymbol{\theta}) = \sum_{i=1}^{N}\left[\bar{S}_{\overline{qq}}(f_i) - |H(f_i, \boldsymbol{\theta})|^2\right]^2 \quad (4.4)$$

where the author reminds that H is the unknown model TF, whose form is given by Eq. (3.20), and $\bar{S}_{\overline{qq}}$ is the PSD of the deseasonalized recorded streamflow series, $\bar{q}(t)$, normalized in the range 0-1 for the reasons discussed in Subsection 3.5.3.1.

Estimates of the response function parameters, for each case study, are reported in Tab. 4.2. Moreover, Fig. 4.3 graphically shows the PSDs fitting results, given the above discussed cut-off frequency value of $2e^{-6}$ Hz. The almost perfect superimposition of the fitting functions (reported in red) on the estimated PSDs (reported in black) makes really difficult their graphical distinction.

Tab. 4.2. Estimated parameters of the watershed TF of Eq. (3.20)

Series	α_0 [-]	α_1 [-]	α_2 [-]	α_3 [-]	k_1 [d]	k_2 [d]	k_2 [d]
(a)	0.157	0.045	0.550	0.249	0.9	34.4	36.2
(b)	0.020	0.070	0.170	0.740	0.5	50.7	57.2
(c)	0.122	0.039	0.571	0.268	0.4	30.8	25.9

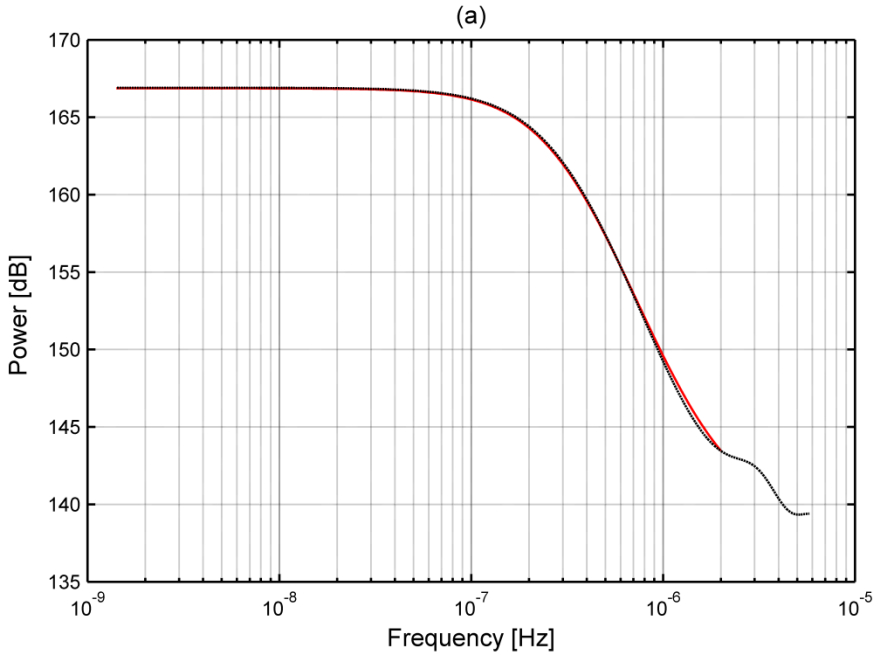
(a)
Power [dB]
170
165
160
155
150
145
140
135
10^{-9}
10^{-8}
10^{-7}
10^{-6}
10^{-5}
Frequency [Hz]

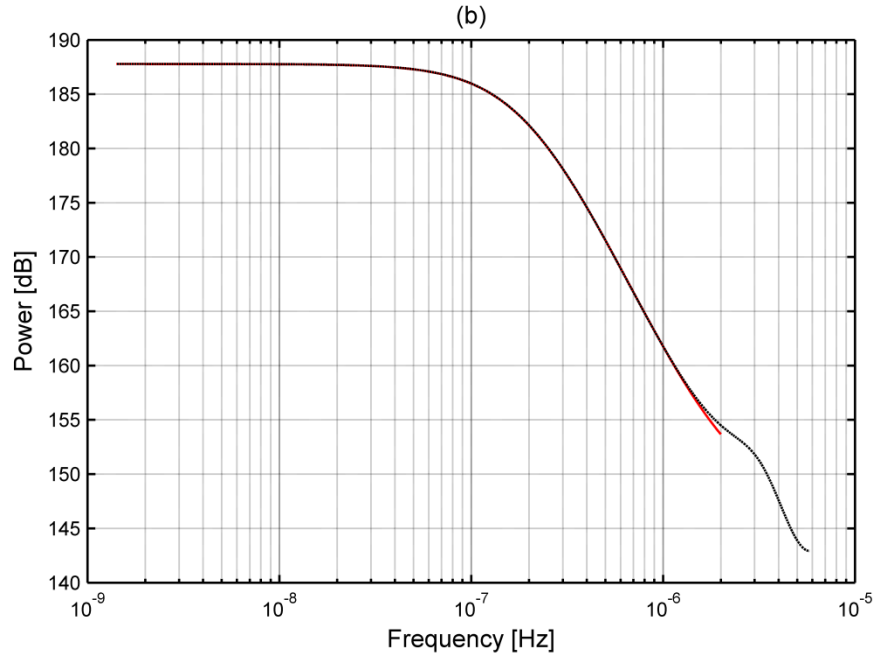
(b)
Power [dB]
190
185
180
175
170
165
160
155
150
145
140
10^{-9}
10^{-8}
10^{-7}
10^{-6}
10^{-5}
Frequency [Hz]

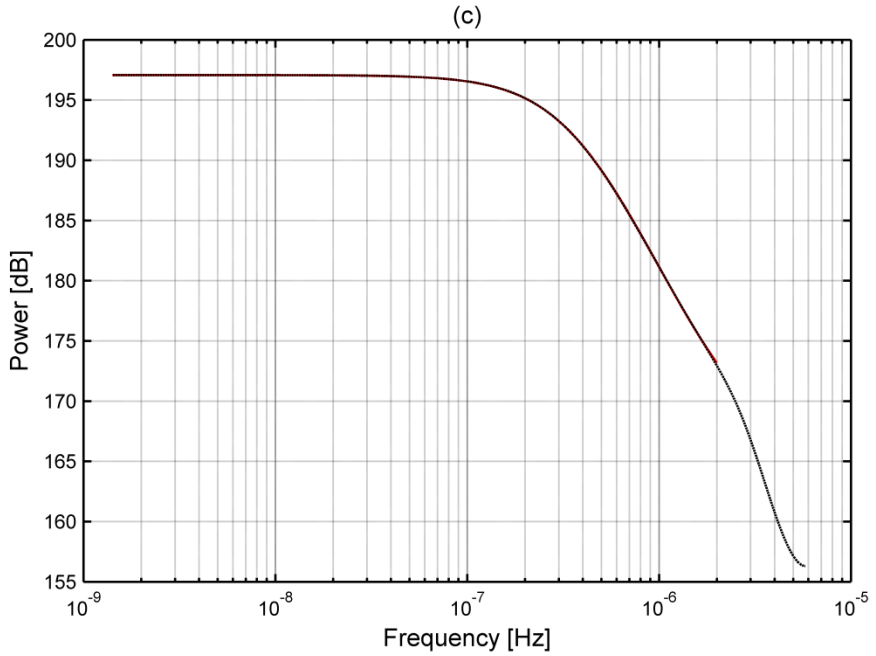

Fig. 4.3. Fitting (red line) of the Burg PSD estimate (black line); $M = 4$ – (a) Alento; (b) Scrivia; (c) Bormida

From the results provided in Tab. 4.2, it is evident the absence, for each of the identified response function, of a real over-year groundwater contribution, given that the corresponding storage coefficient (k_3) results, in each case study watershed, quite similar to the value assumed by the over-month contribution (k_2). Such a result suggests the possibility to obtain a considerable fitting of the detrendized streamflow PSD also by the adoption of a three components-response function, that is one given by the parallel linear combination of a kinematic linear channel (α_0), a sub-daily (α_1, k_1) linear reservoir and a over-month (α_2, k_2) linear reservoir. In order to test the validity of such a consideration, the author undertook the parameter estimation, for each of the case studies streamflow series, assuming a 2-poles TF watershed model given by the following expression:

$$H(s) = \alpha_0 + \frac{\alpha_1}{1+k_1 s} + \frac{\alpha_2}{1+k_2 s} \tag{4.5}$$

From the parameters estimates provided in the following Tab. 4.3, it is evident that, for each of the case studies, the over-month response time (k_2) assumes a value between those assumed by the over-month and the over-year (k_3) contributions in the case of the 3-poles TF. Furthermore, the corresponding coefficient (α_2) assumes values almost equal to the sum of α_2 and α_3 in the previous case. The possibility to obtain the same streamflow process PSD fitting, both by the adoption of a 3-poles and a 2-poles TF, is thus confirmed.

Tab. 4.3. Estimated parameters of the watershed TF of Eq. (4.5)

Series	α_0 [-]	α_1 [-]	α_2 [-]	k_1 [d]	k_2 [d]
(a)	0.145	0.059	0.796	0.7	35.1
(b)	0.080	0.000	0.920	0.8	55.8
(c)	0.100	0.020	0.880	0.7	29.8

However, starting from these considerations, the adoption of a more complex TF should be generally preferred in the proposed identification procedure, since, in case of watersheds well modelled by a lower number of parameters, the response function form is automatically simplified by the parameters estimation procedure, as clearly shown by the comparison of parameters estimates of Tab. 4.2 and 4.3.

As above mentioned, the main reason of the choice of the response function form given by Eq. (3.19) was the necessity to allow the author to perform

some comparisons with results obtained by *Murrone et al*. [1997] and *Claps et al*. [2005]. In particular, in the former paper, a time-domain calibration procedure was applied to several basins belonging to the southern Italy territory, among which the one concerning the Alento River (series (a) of the three case study applications of the present thesis). The second cited work, instead, dealt with the time-domain identification of seven northern Italy natural watersheds, among which the ones related to the Scrivia and Bormida rivers, respectively series (b) and (c) of the present applications. In particular, *Murrone et al*. [1997] adopted a response function given by the linear combination of three linear reservoirs (representing the different basin storage capacities, each with a different storage constant) and a linear kinematic channel (representing, instead, the quick contribution to the runoff process). *Claps et al*. [2005], instead, undertook the calibrations by the adoption of a simpler form of the response function, that is characterized by only two, instead of three, linear reservoirs, linearly combined with a linear kinematic channel.

However, thanks to calibration results shown in Tab 4.2 (referring to the adoption of three linear reservoirs) and Tab. 4.3 (which refers to the adoption of only two linear reservoirs), the author is able to provide a comparison between the time-domain identification approaches previously developed and the frequency-domain procedure here presented. Indeed, the following Tab. 4.4 provides the comparison of parameter estimations concerning the Alento series (a), reported from the work of *Murrone et al*. [1997], and Scrivia (b) and Bormida (c) series, reported from the paper of *Claps et al*. [2005].

Tab. 4.4. Comparison of spectral and time-domain parameters estimates

Series	Approach	c_0 [-]	c_1 [-]	c_2 [-]	c_3 [-]	k_1 [d]	k_2 [d]	k_3 [d]
(a)	spectral	0.157	0.045	0.550	0.249	0.9	34.4	36.2
	Murrone et al. [1997]	0.340	0.281	0.297	0.082	3.1	60.4	551.4
(b)	spectral	0.080	0.000	0.920	-	0.8	55.8	-
	Claps et al. [2005]	0.120	0.280	0.600	-	2.7	56.9	-
(c)	spectral	0.100	0.020	0.880	-	0.7	29.8	-
	Claps et al. [2005]	0.120	0.380	0.500	-	2.5	89.1	-

Starting from the Alento series (a), it is evident a significant difference both in terms of linear combination coefficients and storage constants values. In particular, parameters obtained by the time-domain approach reveal that about the 8% of the global runoff process was attributed to a storage capacity with a storage coefficient significantly greater than one year. This result is in contrast to coefficients obtained by the spectral procedure, since the maximum storage coefficient obtained is equal to about one month. Moreover, also the direct runoff contribution coefficient (c_0) is substantially greater than the one obtained by the proposed technique (i.e., about 35% against 16%).

Concerning the calibration of the response functions of Scrivia and Bormida rivers, instead, the results provided by *Claps et al.* [2005] are substantially more similar to those here presented, both in terms of combination coefficients and storage constants. It is believed that this difference with the Alento River calibration was mainly due to the considerable advances made by the authors with the introduction of the FPOT approach, against the

previously adopted DIP approach, in the estimation of effective rainfall occurrences, as also clearly stated by the authors themselves in their most recent contribution.

However, it is worth noticing that the slight differences concerning Scrivia and Bormida series calibrations, together with the strong differences concerning the Alento River estimates, are mainly due to the fact that, while there exists a strict dependence of the time-domain procedure on the technique adopted for the rainfall peaks identification (i.e., the previously cited DIP and FPOT), the proposed spectral approach, as widely underlined in previous sections, is completely independent from this problem.

Furthermore, a fundamental observation, concerning the number of poles, M, adopted in the all-poles approximation of the "real" PSDs, is needed. Indeed, as stated in previous subsections, the number of poles, or, equivalently, the number of b_k coefficients in the denominator of Eq. (3.25), was set equal to 4, for each of the case study streamflow series. Concerning this point, one could observe that a greater number of poles could have been adopted in order to improve the accuracy in the MEM approximation of the "real" PSD, since, as shown in the following Fig. 4.4, a greater value of the degree, M, of the denominator polynomial in the MEM formulation, would have resulted in a considerable different shape of the estimated PSD. Despite of this consideration, the reader must think that the TF $H(s)$, provided by Eq. (3.20), is characterized by a limited number of degree-of-freedom, given that the number of poles of the modeling system was set to 3 (as a matter of fact only 3 linear reservoirs were considered in the watershed time response formulation, (3.19)). As a consequence, in Eq. (3.20), the number of free parameters is limited to 6, i.e. the 3 mean storage coefficients k_i, representing the parallel linear reservoirs, and 3 of the 4 combination

coefficients α_i, given that the fourth one is estimable as a linear combination of the first three. Hence, given the limited number of free parameters of the adopted TF, the improvement in the number of poles of the MEM approximation of the PSD would have not resulted in the improvement of its fitting through the minimization of the cost function $W(\boldsymbol{\theta})$ of Eq. (3.26). For the sake of clarity, Fig. 4.4 shows the best graphical fitting results of the PSD estimation of the three case study series, obtained by setting $M = 20$, through the adoption of the TF form of Eq. (3.20).

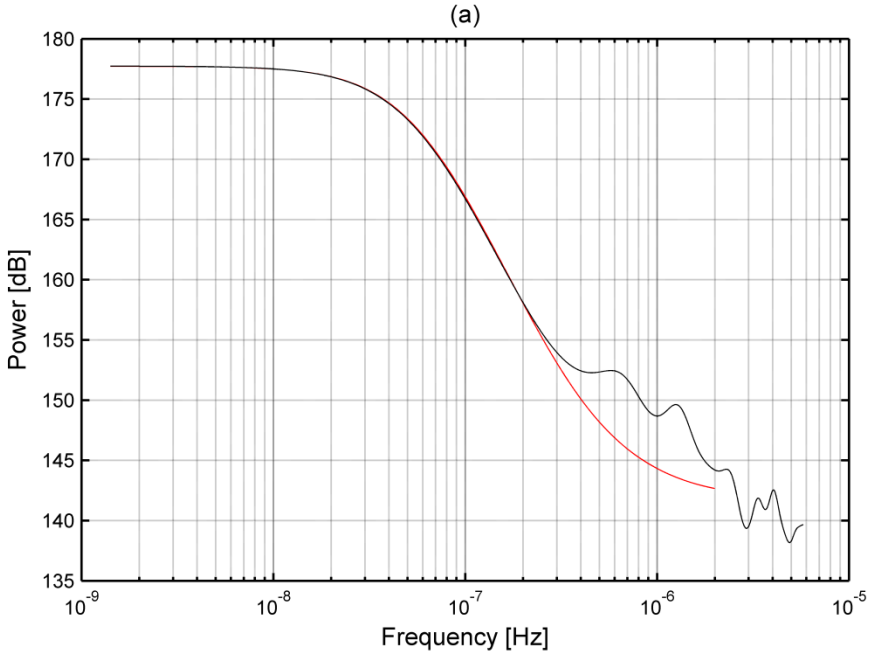

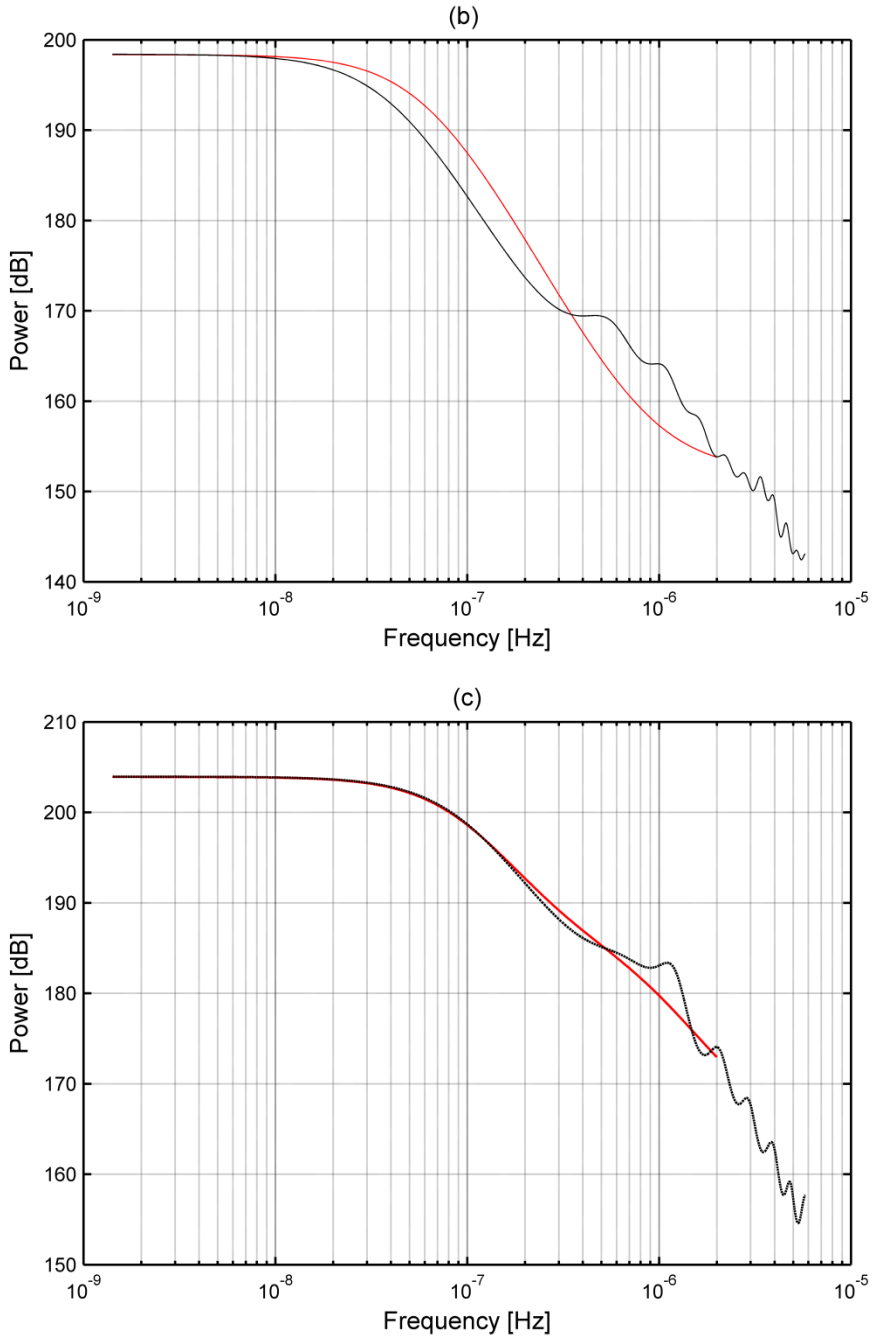

Fig. 4.4. Twenty poles ($M = 20$) MEM approximation of the streamflow series PSD (black line) and corresponding best fitting results (red line) with the TF form of Eq. (3.20) – (a) Alento; (b) Scrivia; (c) Bormida

4.4. Validation of the procedure: a simulation analysis

4.4.1. Synthetic effective rainfall series generation

4.4.1.1. Comparison between two methods for pulse sequence derivation

In order to test the performances of the proposed calibration procedure, in terms of reproduction of the main statistical features of the recorded streamflow series, the generation of synthetic flow series was required. For this purpose, the generation of synthetic effective rainfall series was preliminary necessary (through the universal random variable generator described in Section 3), to subsequently allow the discrete-time convolution of these series with the time response function of the basin. An even more necessary operation, however, consisted in the estimation of the parameters of the so-called PWNE model of effective rainfall, whose PDF and CDF are given, respectively, by Eq. (3.29) and (3.30). In Section 3 some details have been provided on the available techniques for the assessment of the sequence of rainfall pulses, starting from the recorded streamflow series, from which the parameters of the PWNE model thus estimated. In particular, the author focused on: the FPOT procedure, proposed by *Claps and Laio* [2003], and the procedure proposed by *Xu et al*. [2001], to which, from this moment, the author will refer as MA (Minimization Approach).
Starting from this general framework, in the present subsection the intention of the author is to provide the reader with a comparison between results obtained by the adoption of the FPOT and the MA procedures.

The first tested methodology is the FPOT procedure. As already mentioned in Section 3, the author highlights that, once estimated the sequence of

Filtered Peaks (FP, obtained by subtracting to each local maximum, of the streamflow series, the first previous local minimum), a threshold filter has to be increasingly applied to the FP series, until the independence test of Kendall and the Poisson distribution test of Cunnane are jointly met [*Claps and Laio*, 2003]. The author will refer to the peaks that meet these tests as *significant FPOT peaks*, which are graphically reported, for the first recording year of the streamflow process, in Fig. 4.5, for each case study series.

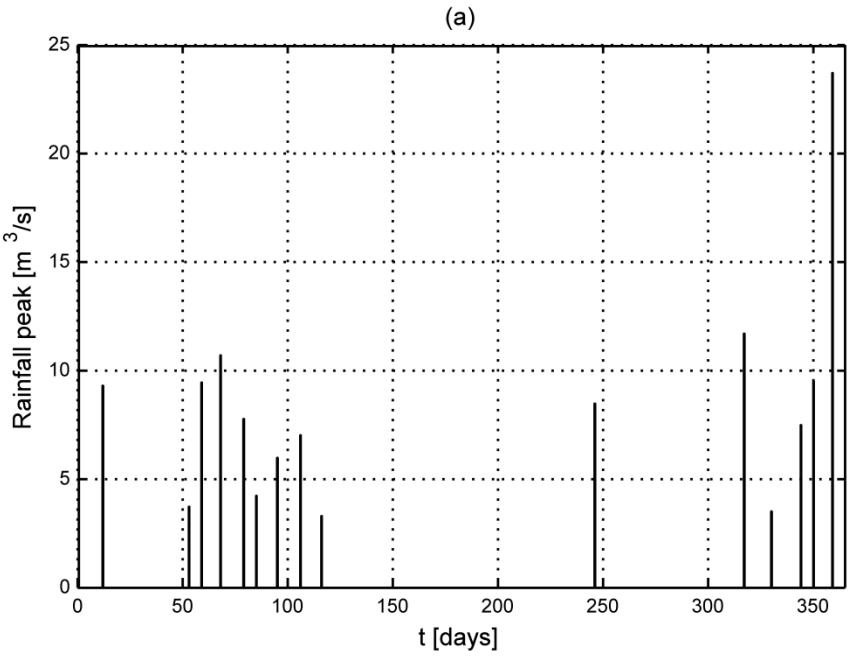

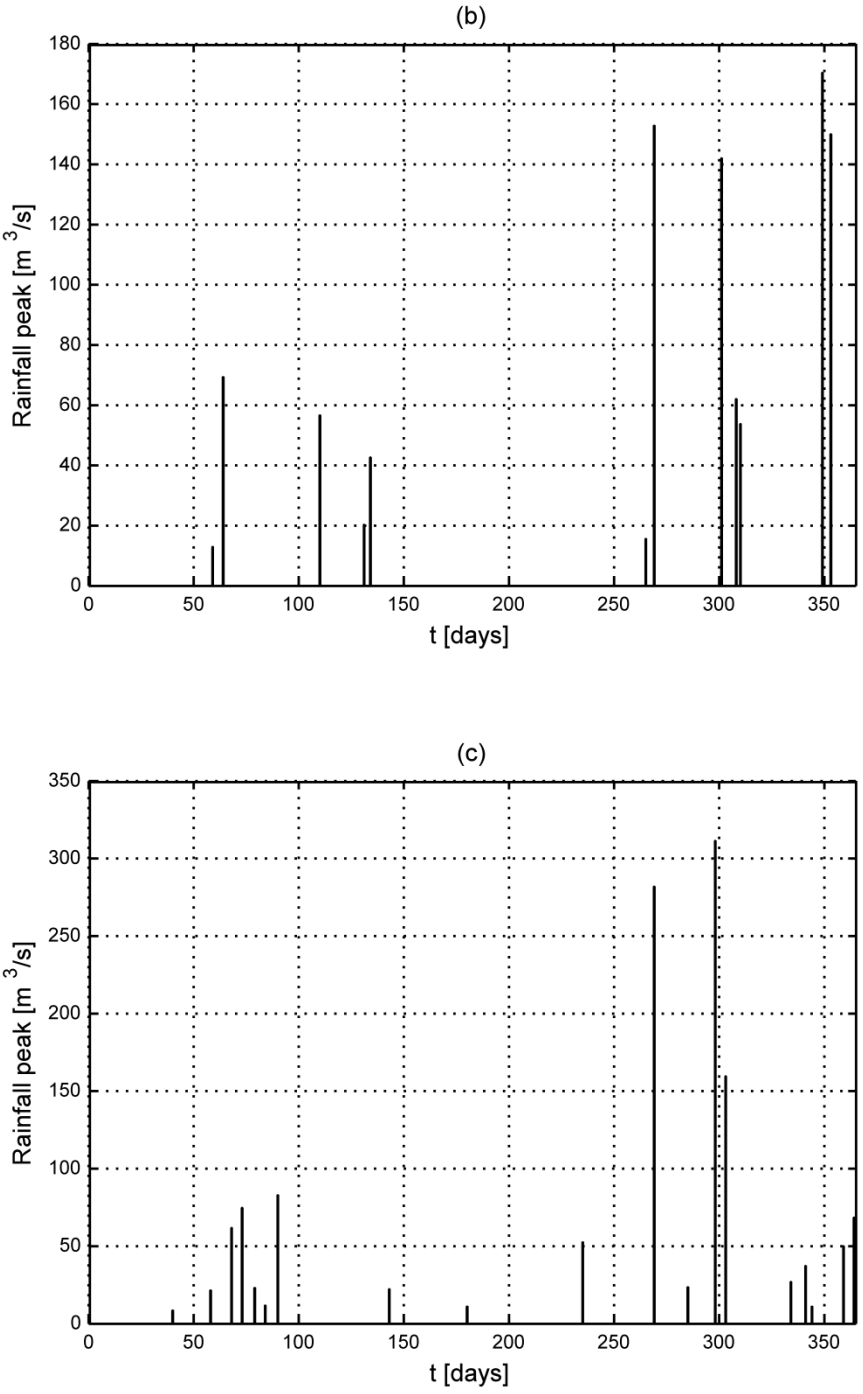

Fig. 4.5. Significant FPOT peaks in the first year of recording – (a) Alento; (b) Scrivia; (c) Bormida

The MA procedure by *Xu et al*. [2001] was also applied to each recorded streamflow series (for more details about the methodology, the interested reader may refer to Subsection 3.5.3.2). In particular, it is worth underlying that the pulse heights obtained by the application of MA procedure (from now called *significant MA peaks*) were estimated through the minimization of the cost function shown by Eq. (3.32). Given that, according to *Xu et al*. [2001], pulses occur on all those days when streamflow increases, it is obvious that the minimization of Eq. (3.32) defines a highly multidimensional minimization problem that the author solved by the adoption of the Powell's method described in Subsection 4.3.1. The estimated peak sequences, for each case study and for the first year of recording, are graphically reported in Fig. 4.6.

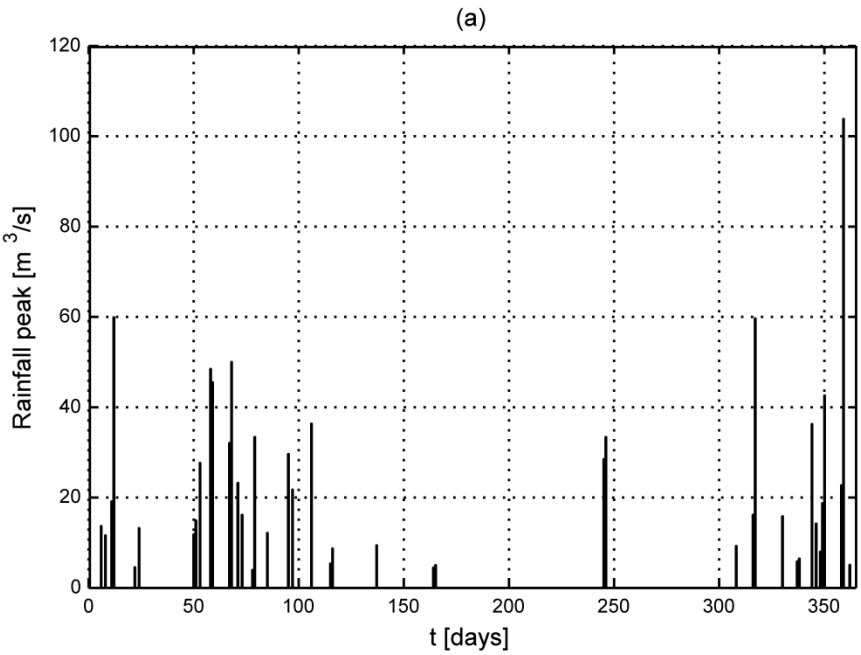

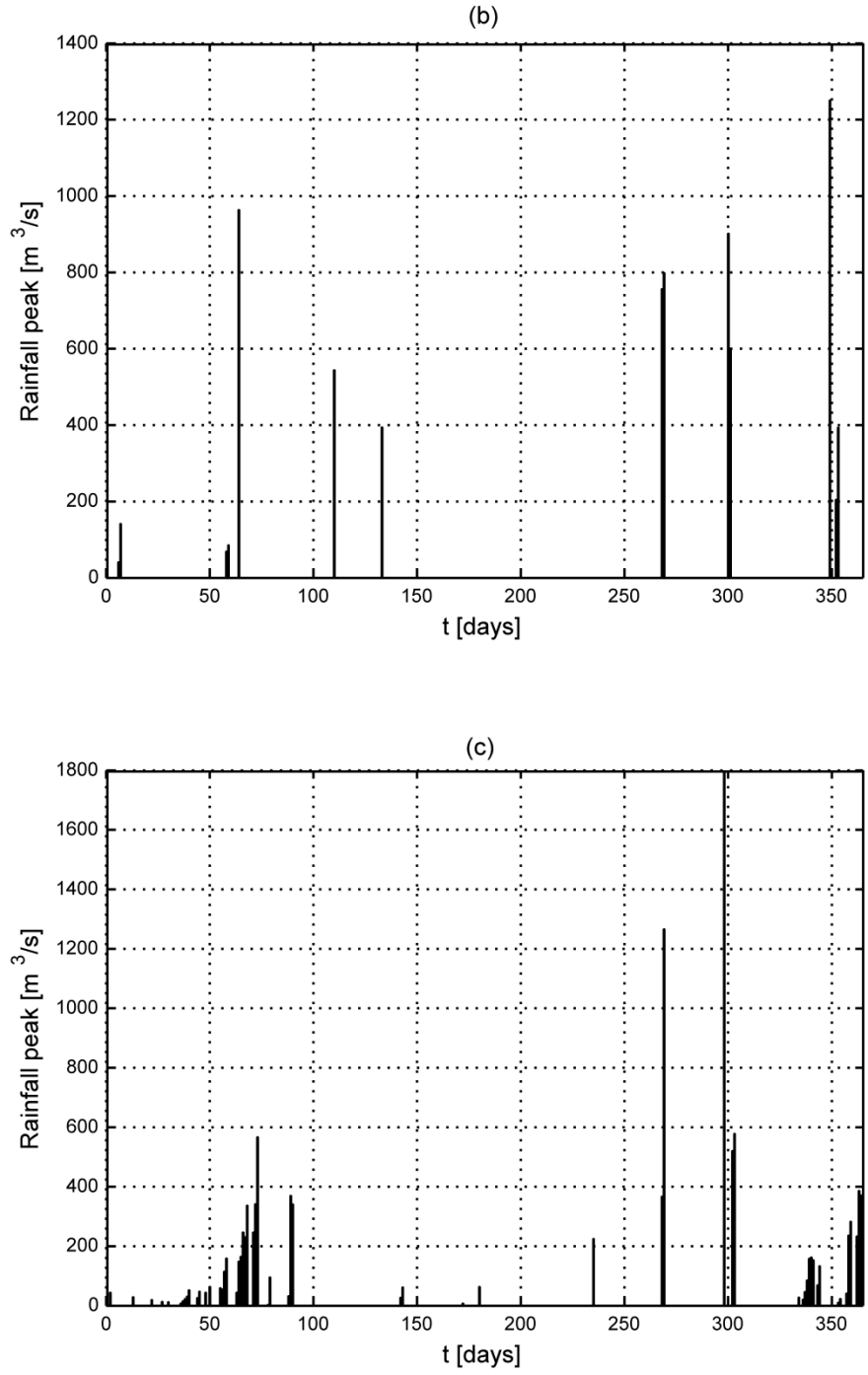

Fig. 4.6. Significant MA peaks in the first year of recording – (a) Alento; (b) Scrivia; (c) Bormida

Once estimated the significant peak sequences, the author verified that the storm events occurred along the time axis according to a non-homogeneous Poisson point process, as required by *Xu et al*. [2001]. For this purpose, a χ^2 goodness-of-fit test was undertaken for each month of the year (Tab. 4.4 provides χ^2 values for each of the 3 case study watersheds).

Tab. 4.5. χ^2 goodness-of-fit test for non-homogeneous Poisson distribution on significant MA peaks

Series	(a)	(b)	(c)
Month		χ^2 value	
January	1.335	0.318	0.923
February	0.556	1.072	0.079
March	0.013	0.747	0.616
April	0.080	0.344	0.989
May	0.279	1.802	2.486
June	1.083	0.490	3.023
July	0.538	0.008	0.436
August	0.003	0.670	0.372
September	1.309	2.472	0.088
October	0.025	0.041	0.002
November	0.024	1.469	0.148
December	0.151	0.508	0.001

Given a statistic limit of 9.488 at the 5% significance level (see *Xu et al*. [2001]), it is evident that for each basin the null hypothesis of Poisson distributed occurrences during each month cannot be rejected. The non-homogeneous Poisson point process is therefore acceptable for describing the storm occurrences. Nevertheless, as above introduced, the slight differences in the mean number of rainfall events between months allow the author to assume the input process to be stationary.

One major comment is needed about the comparison of the two effective peaks estimation procedures. As it is possible to realize also by a graphical analysis of Fig. 4.5 and 4.6, the mean number of significant rainfall events per year obtained by the MA procedure is considerably higher than that resulting from the FPOT procedure, for each of the case studies. The values reported in Tab. 4.5 confirm this consideration.

Tab. 4.6. Mean number of rainfall events per year: comparison between MA and FPOT procedures

Series	(a)	(b)	(c)
Procedures	Mean annual rainfall events		
FPOT	17.5	13.1	16.0
MA	39.4	17.9	46.7

In particular, the mean number of events per year obtained by the FPOT approach confirms the results of *Claps and Laio* [2005], who reported a rough estimate of about 5-20 peaks per year for each of the numerous analyzed runoff series. However, the main point consists in the fact that authors themselves admitted that such estimation could result in a underestimation of the actual number of effective rainfall events, suggesting a clue of the inadequacy of the Poisson independent model in the correct reproduction of the effective rainfall behavior. The mean number of events per year obtained by the MA procedure, instead, seems to be much more compatible with the actual number of events. As a matter of fact, taking the Alento River as an example, several regional studies undertaken on the

Italian territory on several uniform compartments (from a hydrological point of view) seem to confirm the result. In particular, using the Extreme Value-I (EV-I) distribution for statistical analysis of rainfall heights' annual maxima in intervals of different duration (in the area where the Alento basin is located), a mean number of events per year equal to 37 was evaluated [*Di Nunno*, 1981]. Furthermore, adopting the Two-Component Extreme Value (TCEV) distribution [*Rossi et al*., 1984] for the analysis of instantaneous discharges annual maxima at Casalvelino station (Alento River), a mean number of flood events per year equal to 44 was estimated [*Rossi and Villani*, 1995].

Starting from these considerations, the author considered the MA procedure more efficient, compared to the FPOT approach, thanks to its ability to provide a more realistic pulses sequence in terms of mean annual number of events. It is worth underlying that, on the contrary, a comparison between FPOT and MA procedures in terms of the mean annual intensity of rainfall events would be meaningless. Indeed, while the FPOT approach derives the peak sequence only by means of operation on the recorded runoff series, the MA procedure provides a sequence, through minimization of Eq. (3.32), strictly dependent on the values of the estimated parameters of the TF. Furthermore, given that TFs estimates obtained in this work are considerably different from those provided by *Murrone et al*. [1997], concerning the Alento River, and *Claps and Laio* [2005], concerning the Scrivia and Bormida rivers, a comparison between pulses sequence in terms of intensity would be practically useless.

Eventually, a first way to ascertain, on the one hand, the validity of the response function form adopted in the calibration approach, and, on the other hand, the efficiency of the selected MA procedure for the determination of the effective peaks series, is to provide the reader with a graphical

comparison between recorded and reconstructed series (Fig. 4.7). The latter one, in particular, was obtained, for each case study series, through the convolution (see Eq. 3.34) between the known response function and the corresponding input sequence. From a quick graphical analysis of the proposed comparison, it is possible to observe the almost perfect superimposition of the peak occurrences time between reconstructed and recorded series, in addition to a practical coincidence between corresponding discharge values.

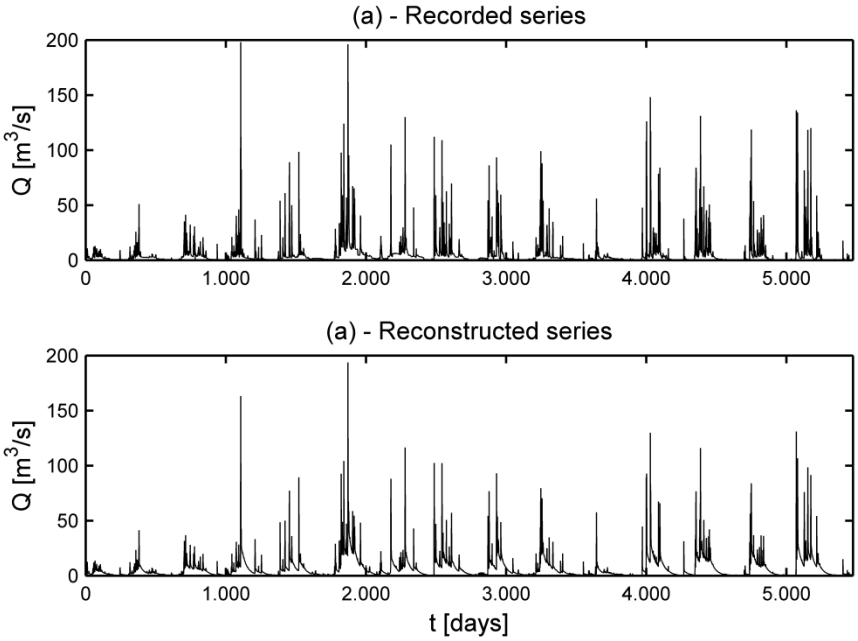

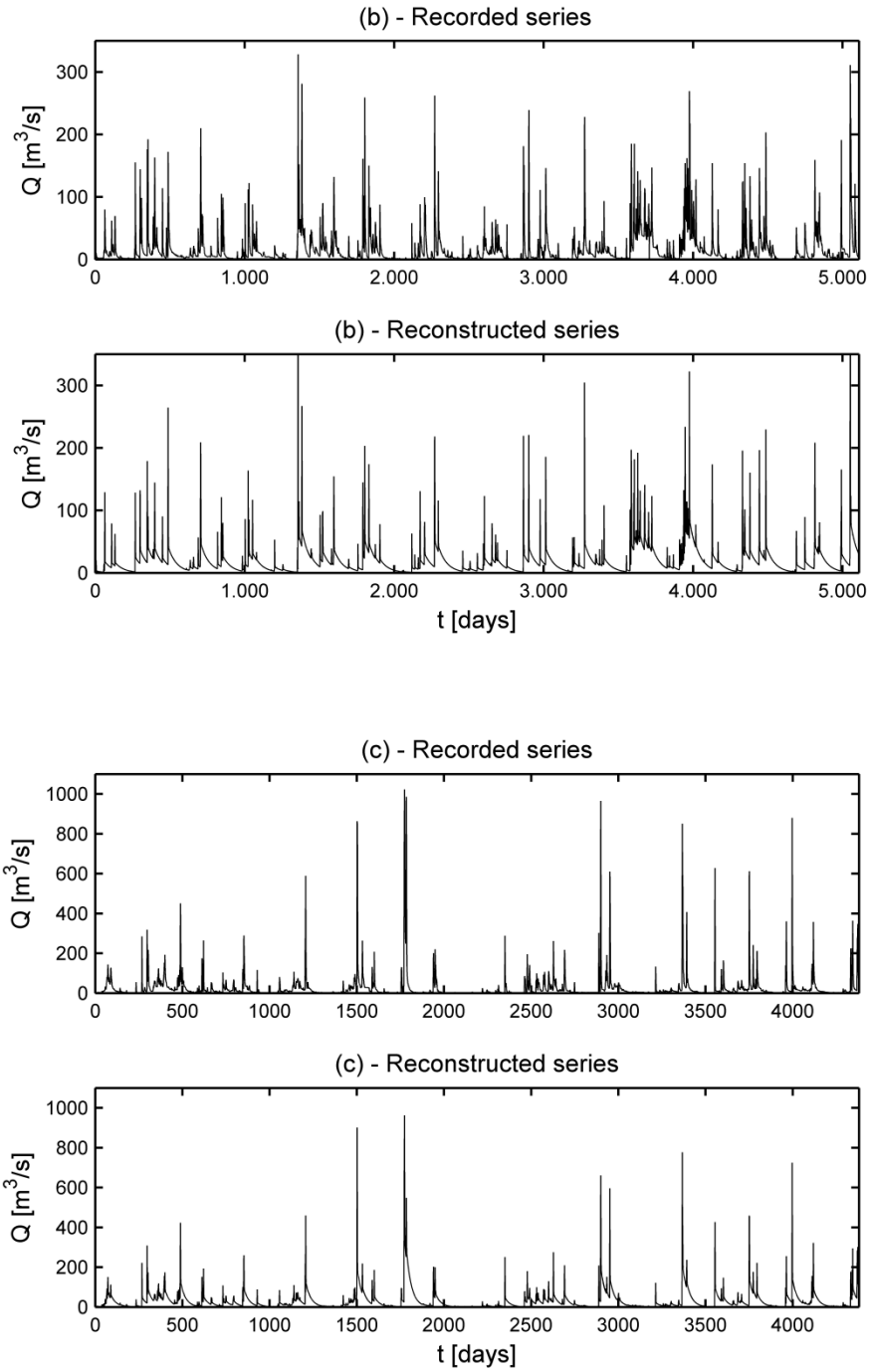

Fig. 4.7. Recorded and reconstructed runoff series comparison – (a) Alento; (b) Scrivia; (c) Bormida

4.4.1.2. PWNE model parameters estimation

Once selected the MA procedure by *Xu et al*. [2001] for the estimation of the significant values of peak rainfall events, given the consideration of Subsection 4.4.1.1, the PWNE model of effective rainfall was estimated by the adoption of the method of moments formula of Eqs. (3.31). In particular, as mentioned in Section 3, starting from the series of significant rainfall pulses, the parameter λ, of the Poisson distribution of the occurrences, and the parameter β, of the exponential distribution of the intensities, were estimated on 13 different seasons of $T = 28$ days each, wherein they are supposed to remain constant. In such a way, the intention of the author was that of preserving, in the simulated streamflow series, the first-order moment season variability. Indeed, it is worth underlying that, as stated by some recent worthy contribution about spectral calibration problems (see, e.g., *Montanari and Toth* [2007]), the PSD of a realization of a stochastic process does not convey any information about the mean value of the process itself. As a consequence, in almost all technical papers dealing with spectral calibration procedures, the authors tend to preserve the mean of the runoff process through the assumption of zero mean of the model error $e(t)$, which corresponds to imposing the equality for the mean values of observed and simulated data [*Montanari and Toth*, 2007]. However, such a framework can be easily followed when some information about the input (rainfall, evapotranspiration etc.) processes are available. When, on the contrary, no information is obtainable on the input process, the effective rainfall model parameters estimation becomes fundamental to assure the correct reproduction of the first moment of the recorded series. As a consequence, the season length T, for the estimation of PWNE parameters λ and β, was set to 28 days because it was considered the optimal value for the correct

reproduction of the seasonal variability of the recorded series first order moment.

Starting from these premises, the parameters estimates of the PWNE model, for each case study series, are provided in the following Tab. 4.6.

Tab. 4.7. PWNE model parameters estimates

Series	(a)		(b)		(c)	
Season #	λ [1/d]	$1/\beta$ [m^3/s]	λ [1/d]	$1/\beta$ [m^3/s]	λ [1/d]	$1/\beta$ [m^3/s]
1	0.109	165.9	0.054	269.5	0.174	114.7
2	0.067	154.8	0.045	258.8	0.038	1281.8
3	0.086	99.1	0.067	450.4	0.061	824.3
4	0.058	102.5	0.056	386.2	0.063	762.6
5	0.059	43.5	0.048	467.2	0.094	483.8
6	0.024	50.9	0.011	93.9	0.013	635.3
7	0.075	6.5	0.010	106.0	0.034	41.0
8	0.023	17.9	0.010	100.1	0.027	123.2
9	0.091	6.0	0.014	391.3	0.020	256.3
10	0.033	36.3	0.031	766.8	0.037	631.7
11	0.029	129.1	0.073	642.5	0.061	389.8
12	0.090	136.0	0.073	486.4	0.058	1198.8
13	0.142	124.1	0.062	589.4	0.056	1055.4

The universal random variable generator, described in Subsection 3.6, was thus applied for the generation of synthetic rainfall series, whose statistical distribution was that of Eqs. (3.29) and (3.30), which were then numerically convoluted with the discrete time response function of the watershed to generate synthetic streamflow series. For further details on the simulation analysis, the interested reader may refer to Subsection 3.6.

4.4.2. Comparison of main statistical features between recorded and synthetic streamflow series

4.4.2.1. Introduction

In the present subsection the author will provide the reader with some interesting comparisons between the generated streamflow series, according to the procedure exposed in the previous subsections, and the recorded ones, in order to ascertain the applicability and efficiency of the proposed frequency-domain calibration procedure. Even though already depicted in Section 3, it is worth underlying now that, for each case study series, the generation of 1000 streamflow series of length, in days, $M = 364N_{sim}$ was undertaken, where 364 is the number of days in a year, considering 13 seasons of 28 days each, and N_{sim} is the number of years of the simulation, assumed in order to double the length of the recorded streamflow series, in terms of years, N_{rec}. However, before the execution of the statistical analysis, the first N_{rec} years of the synthetic runoff series were removed, in order to make generated series independent on the initial conditions of the simulation.

Concerning statistical analysis, it is widely known that the real value of a stochastic model must be judged from its capacity of correctly reproducing the statistical properties of recorded series from which its parameters have been assessed. As a consequence, as already mentioned at the end of Section 3, the quality of the obtained solution (i.e. TF parameter estimates) was evaluated in terms of its ability to:

a) reproduce the first three moments, averaged on the different months, of the recorded series probability distribution;

b) return an average flow volume, in a period of length equal to N_{rec}, similar to that corresponding to the recorded series;
c) guarantee a satisfying reproduction of flow duration curves;
d) reproduce minimum and maximum values, averaged on different aggregation scales, of the recorded series.

4.4.2.2. Comparison of mean statistics

The first validation test, useful to assess the real efficacy of the estimated watershed response function, concerns the comparison of the moments of the observed and generated flows, averaged on the different months of the year. In particular, the author focused on the comparison of the first three moments of the distribution of the streamflow variable q (i.e. mean, standard deviation and skewness coefficient), whose estimators are provided, respectively, in the following formulas:

$$\bar{q} = \frac{1}{n}\sum_{i=1}^{n} q_i; \tag{4.6}$$

$$\sigma_q = \left(\frac{1}{n-1}\sum_{i=1}^{n}(q_i - \bar{q})^2\right)^{0.5}; \tag{4.7}$$

$$\gamma_q = \frac{\frac{1}{n}\sum_{i=1}^{n}(q_i-\bar{q})^3}{\left(\sqrt{\frac{1}{n}\sum_{i=1}^{n}(q_i-\bar{q})^2}\right)^3}; \tag{4.8}$$

where n is the number of elements in the considered sample and q_i is the *i*th element of the sample.
The graphical comparison of the aforementioned moments is provided in the following Fig. 4.8, where upper and lower confidence limits are also provided by adding and subtracting the standard deviation value to the corresponding statistic estimate.

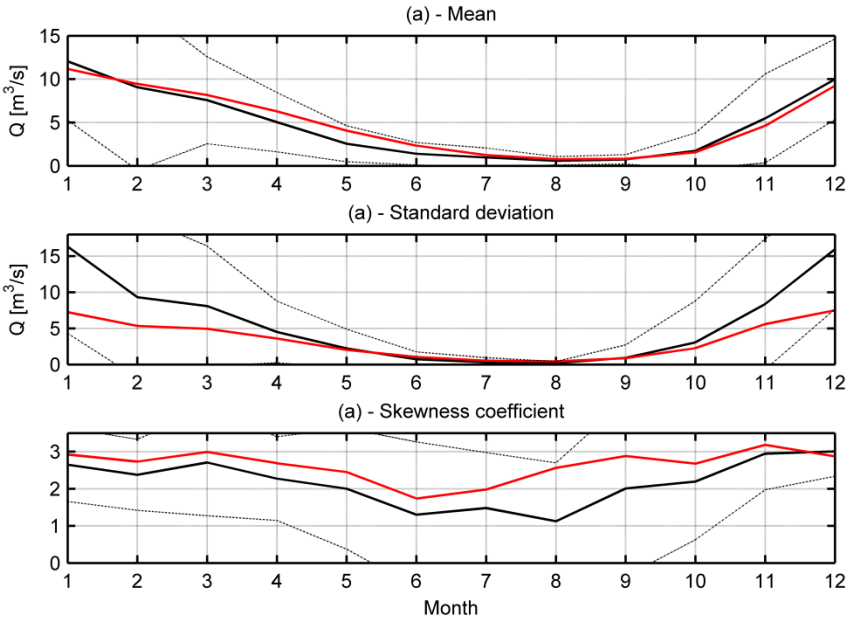
(a) - Mean
Q [m3/s]
(a) - Standard deviation
Q [m3/s]
(a) - Skewness coefficient
Month

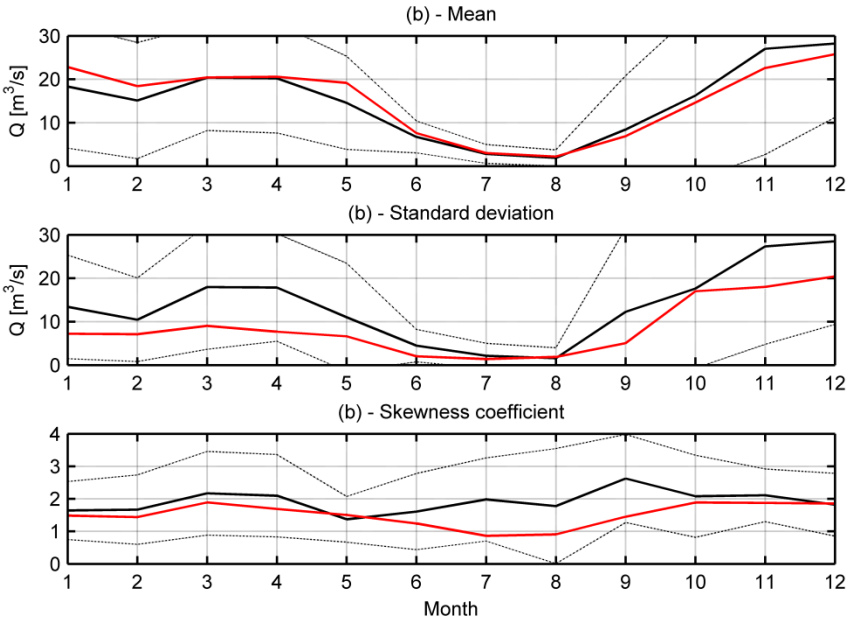
(b) - Mean
Q [m3/s]
(b) - Standard deviation
Q [m3/s]
(b) - Skewness coefficient
Month

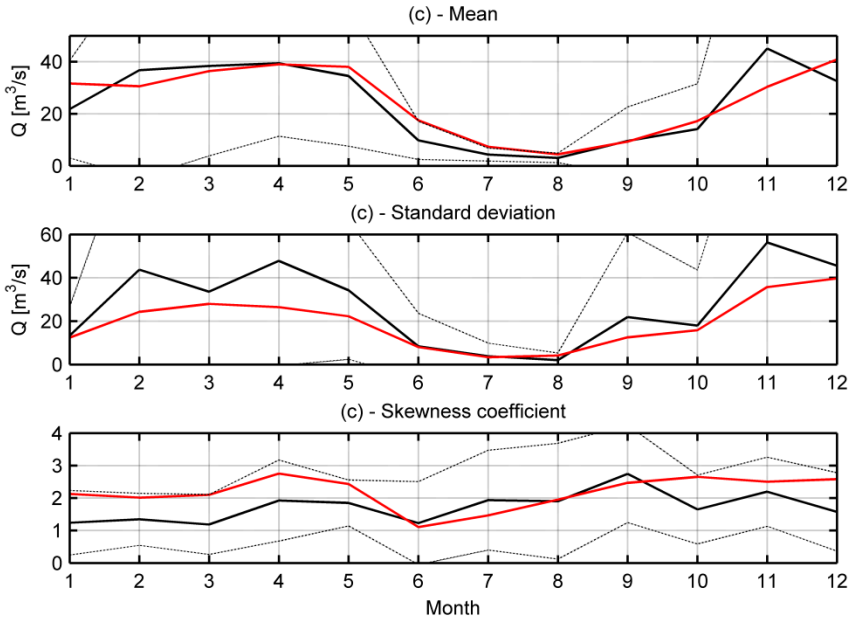

Fig. 4.8. Comparison of mean statistics of daily flows for each calendar month between recorded (solid black line) and generated series (solid red line); confidence intervals ±σ are shown in dashed line – (a) Alento; (b) Scrivia; (c) Bormida

For each of the case study time series, it can be noticed that the overall trend of the monthly averaged historical moments is quite well preserved by the generated series. In particular, the best performance concerns the reproduction of the monthly mean flow values, which confirms the efficiency of the selected model of effective rainfall. Furthermore, also the standard deviation and the skewness coefficient overall trends are quite well preserved. In particular, the former generally presents a negative bias in correspondence with the tail of the statistics, while both the central and the extreme portion of the synthetic skewness trends are characterized by a positive and negative error. Nevertheless, all the synthetic trends are included in the respective confidence interval represented by the dashed lines in Fig. 4.8.

However, in future advances of the calibration procedure here proposed, it will be attempted to considerably reduce the error in the reproduction of the mean monthly second order moment, since it is fundamental in simulation analysis aimed at the reproduction of the correct discharge trend within a month. The reader should think, for instance, to a typical water resource management problem of an artificial reservoir. As a matter of fact, in this case, in order to define the best rule for the management of water volumes stored in the reservoir during the year, it is fundamental the availability of a stochastic model for the correct reproduction of the streamflow process within the year. In particular, the shorter is the aggregation scale within which the model is able to reproduce the streamflow variability, the more detailed will be the estimated reservoir scheduling.

The second validation test, in terms of mean statistics, concerns the comparison of the total historical flow volume, that corresponds to the recorded streamflow series of length N_{rec}, with the average of the 1000 total flow volumes corresponding to the simulated runoff series of the same length (Tab. 4.7 provides the comparison for each case study series). The importance of this test is intuitive, given the evident necessity of a correct reproduction of this statistic in water resources management problems on a over-year time scale.

Tab. 4.8. Recorded and mean synthetic flow volumes comparison for each case study series

Series	Rec. flow vol. [m^3]	Mean synt. flow vol. [m^3]	% error
(a)	2.24×10^9	2.32×10^9	-3.6
(b)	6.61×10^9	7.01×10^9	-6.0
(c)	9.07×10^9	9.61×10^9	-5.9

Tab. 4.7 demonstrates the capacity of the identified watershed models to properly reproduce, with an acceptable error, the total flow volume on a period of length equal to N_{rec}. In particular, for each of the watersheds, the slightly overestimation of the recorded flow volume was probably due to the uncertainty both in the effective rainfall model parameters estimations and in the subsequent rainfall series synthetic generation.

4.4.2.3. Comparison of flow-duration curves

The flow-duration curve is a cumulative frequency curve that shows the percent of time during which specified discharges were equalled or exceeded during a given period. It combines in one curve the flow characteristics of a stream throughout the range of discharge, without regard to the sequence of occurrence. To prepare a flow-duration curve, the mean daily, weekly, or monthly flows during a given period are arranged according to their magnitude, and the percent of time during which the flow variable equals or exceeds the specified values is computed. The curve, drawn to average the plotted points of specified discharges versus the percent of time during which they were equalled or exceeded, thus represents an average for the

period considered rather than the distribution of flow within a single year [*Searcy*, 1959].

It is widely recognized the utility of flow-duration curves in several applications. In particular, in this thesis, they were adopted to properly compare the observed and synthetic cumulative distribution functions of the streamflow process, of which flow-duration curves can be considered an appropriate representation.

Estimation of flow-duration curves was undertaken by the adoption of the procedure, described by *Claps et al*. [2005], described in the following lines. Concerning the observed discharge series, the historical dataset of size N, where N is the length of the series in days, was sorted in descending order and an empirical frequency of occurrence, equal to $F_{(i)} = \frac{i}{N+1}$ was assigned to the *i*th order statistics in the sample, that is $q_{(i)} = q\left(F_{(i)}\right)$. The same procedure was followed for the whole generated runoff series, given by merging the 1000 synthetic series, each of length N, in an unique generated series. As a result, the size $\overline{N}$ of the synthetic series was much larger than N. Hence, the empirical frequency of occurrence was estimated as $F_{(j)} = \frac{j}{\overline{N}+1}$ and the *j*th order statistics in the sample was evaluated as $q^*_{(j)} = q^*\left(F_{(j)}\right)$, where the apex $*$ is used to distinguish synthetic streamflow data from recorded ones. Eventually, the flow-duration curves were given by the $F_{(i)}$ and $F_{(j)}$ values, on the abscissa, plotted versus, respectively, $q_{(i)}$ and $q^*_{(j)}$ on the ordinate. The graphical comparison between recorded and synthetic series flow-duration curves is provided in the following figure, for each case study watershed. It is worth noticing that, in order to allow the representation of the frequency axis in terms of number of days in the year, it is only needed to multiply by 365 the frequency of occurrence values on the abscissa

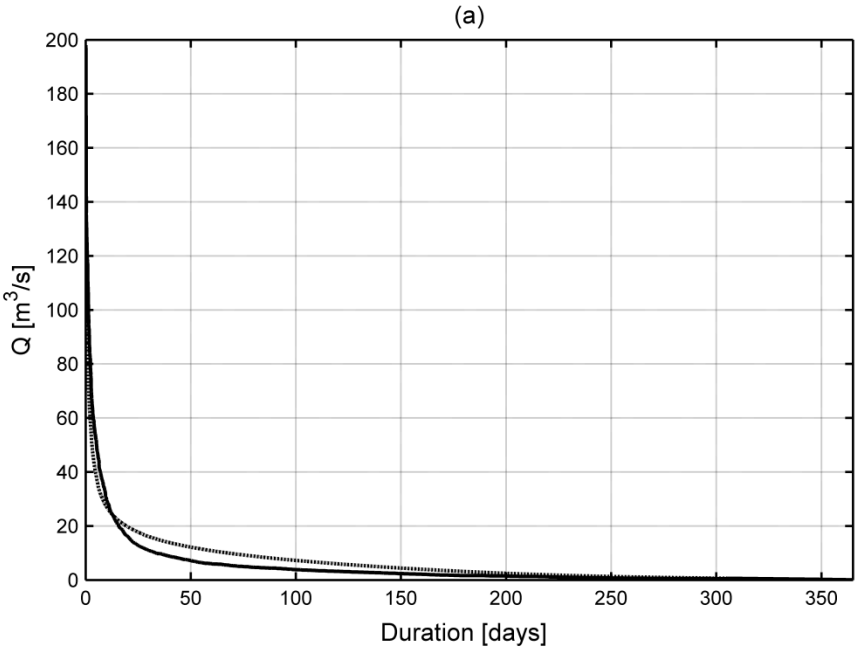
(a)
Q [m3/s]
Duration [days]
0
20
40
60
80
100
120
140
160
180
200
0
50
100
150
200
250
300
350

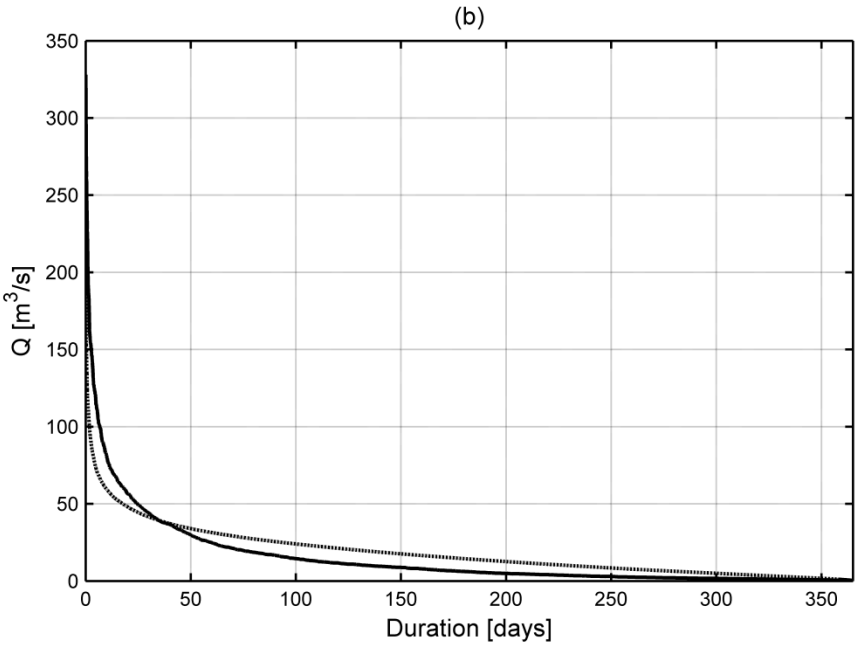
(b)
Q [m3/s]
Duration [days]
0
50
100
150
200
250
300
350
0
50
100
150
200
250
300
350

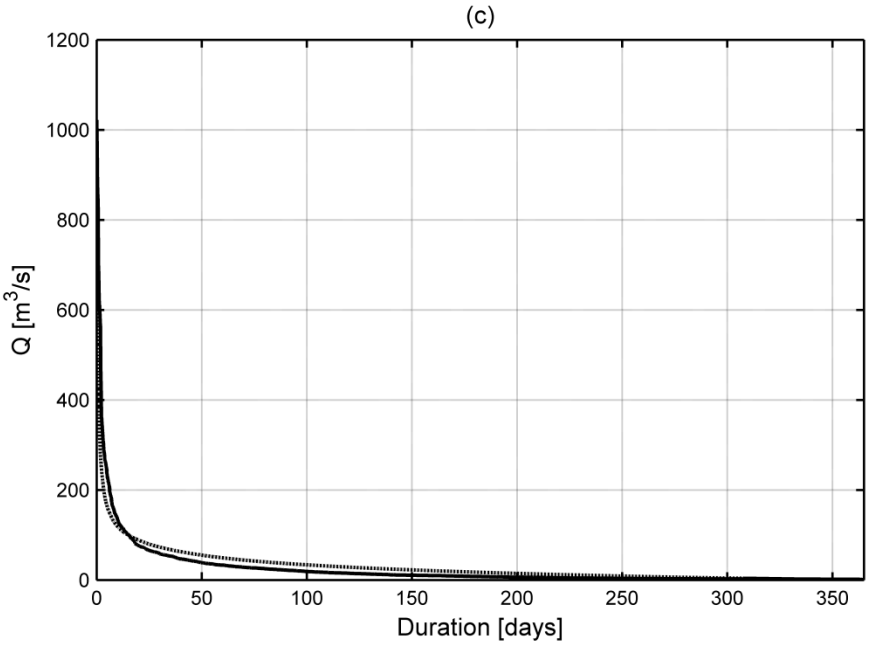

Fig. 4.9. Comparison between flow-duration curves of recorded (solid line) and simulated (dotted line) series – (a) Alento; (b) Scrivia; (c) Bormida

Figs. 4.9a-c clearly show the considerable result obtained in terms of matching of the global trend of the recorded runoff series flow-duration curves for the Alento and Bormida rivers, both for the lower (less frequent and, thus, more relevant flow events) and the upper (more frequent discharge values) tails of the frequency distribution. A certain difference, instead, can be noticed between the two curves concerning the Scrivia River (Fig. 4.9b). In particular, a low underestimation of the highest flow values (i.e. the rarest events) and a moderate overestimation of the lowest discharges (i.e. the runoff during long dry periods) is revealed. Such a difference could be addressed to the absence, in the time response function identified for the Scrivia watershed, of a strong impulsive contribution. As a matter of fact, given the results shown in Tab. 4.2, while for the Alento and Bormida rivers this component is respectively equal to about the 16% and 12% of the total

discharge, for the Scrivia River the direct runoff is only the 2% of the total. This substantial difference can particularly affect the capacity of the calibrated response function of properly reproducing both the dry periods runoff values and the rarest events. In particular, in presence of response functions similar to that of the Scrivia River, when a high intensity effective rainfall event is generated by the universal random variable generator described in Section 3, the resulting runoff value will not be characterized by a relevant magnitude, since the absence of a considerable impulsive contribution results in the fact that only a small portion of the effective rainfall feeds the runoff process. At the same time, given that the greatest amount of rainfall contribution feeds the over-month and over-year storage capacities of the watershed, the direct consequence will be an overestimation of more frequent (i.e. with minor intensity) flow values, since they are affected by that amount of previous intense rainfall events that have been preliminary stored in the several watershed capacities, and, after, slowly released to the river. Such an interesting result would suggest the adoption of a different response function form for the Scrivia River, in order to differently model the surface runoff. For instance, the Dirac delta function could be substituted by 2 or 3 identical linear reservoirs, obtaining a response function able to release in a wider time interval the quick runoff contribution [see, for reference, *Boyle*, 2000]. However, in this direction further investigation need to be pursued to improve the overall capacity of the proposed approach to properly fit the upper and lower tails of the recorded flow-duration curves.

The different performances, of the proposed calibration approach, in the reproduction of the cumulative distribution functions of the recorded streamflow processes, could result in troublesome limitations to the adoption of the methodology in water resources management problems. Indeed, for

instance, the management of an artificial reservoir at a short time-scale would require the ability of the stochastic model, for the generation of synthetic streamflow series, of correctly reproducing the high frequency values, given their importance in the definition of a short time-scale scheduling of the reservoir. However, it is also true that, as already shown in Tab. 4.7, all the calibrated response function are able to correctly reproduce, with a limited error, the global flow-volume in the recording period, suggesting the model ability in reproducing the real flow regime on an extended period. Such a result is not contrasting with the flow-duration curve of the Scrivia River (Fig. 4.9b), since the underestimation of the high frequency discharge values and the overestimation of the low frequency ones results in a global trade-off in terms of flow-volume, providing the results shown in Tab. 4.7.

4.4.2.4. Reproduction of minimum flow values over fixed durations

As already said, one of the main applications of streamflow processes stochastic models is the possibility to generate synthetic streamflow series to cope with a wide variety of water resources problems. In particular, one of the most popular class of problems, to which synthetic models have been usually applied, deals with water resources planning and management, e.g. the determination of the best artificial reservoir operating rule curve within a year or in a multi-year framework. As already stated, it is intuitive that, in this type of applications, stochastic models have to be able to correctly reproduce the main distribution properties of the recorded series from which they have been calibrated. In previous subsections, indeed, several validation tests have been provided, comparing recorded and generated series in terms of, in particular, the first three moments of the distribution, the global flow-

volume over a given period and flow-duration curves. All these tests showed satisfying results. However, it is worth underlying that, in almost all practical problems to which a stochastic streamflow model can be applied, the proper reproduction, in statistical terms, of minimum flow values would be a significant characteristic of the adopted model. For this reason, in the present subsection, the graphical comparison between recorded and simulated mean minimum flows, averaged over different durations, is provided.

For the sake of repeatability, the author will firstly describe how to estimate mean minimum flow values, given a series of mean daily flows of N_{rec} values. Defined a certain duration d (in days), a new series is obtained by averaging the M groups of flows, each characterized by d daily flow values, obtained by dividing the historic sequence in $M = N_{rec}/d$ portions. The minimum value of the series thus obtained is the mean minimum flow value for the fixed duration d. The same procedure needs to be followed both for recorded and synthetic series (that in the present work are 1000 for each case study river). In this latter case, in particular, once repeated, for the a fixed duration d, the previous procedure for each of the generated series, the mean minimum flow to be compared to that corresponding to the recorded series, for the same duration d, is evaluated by averaging the 1000 mean minimum values obtained by the synthetic series. Fig. 4.10 shows results for each case study watershed.

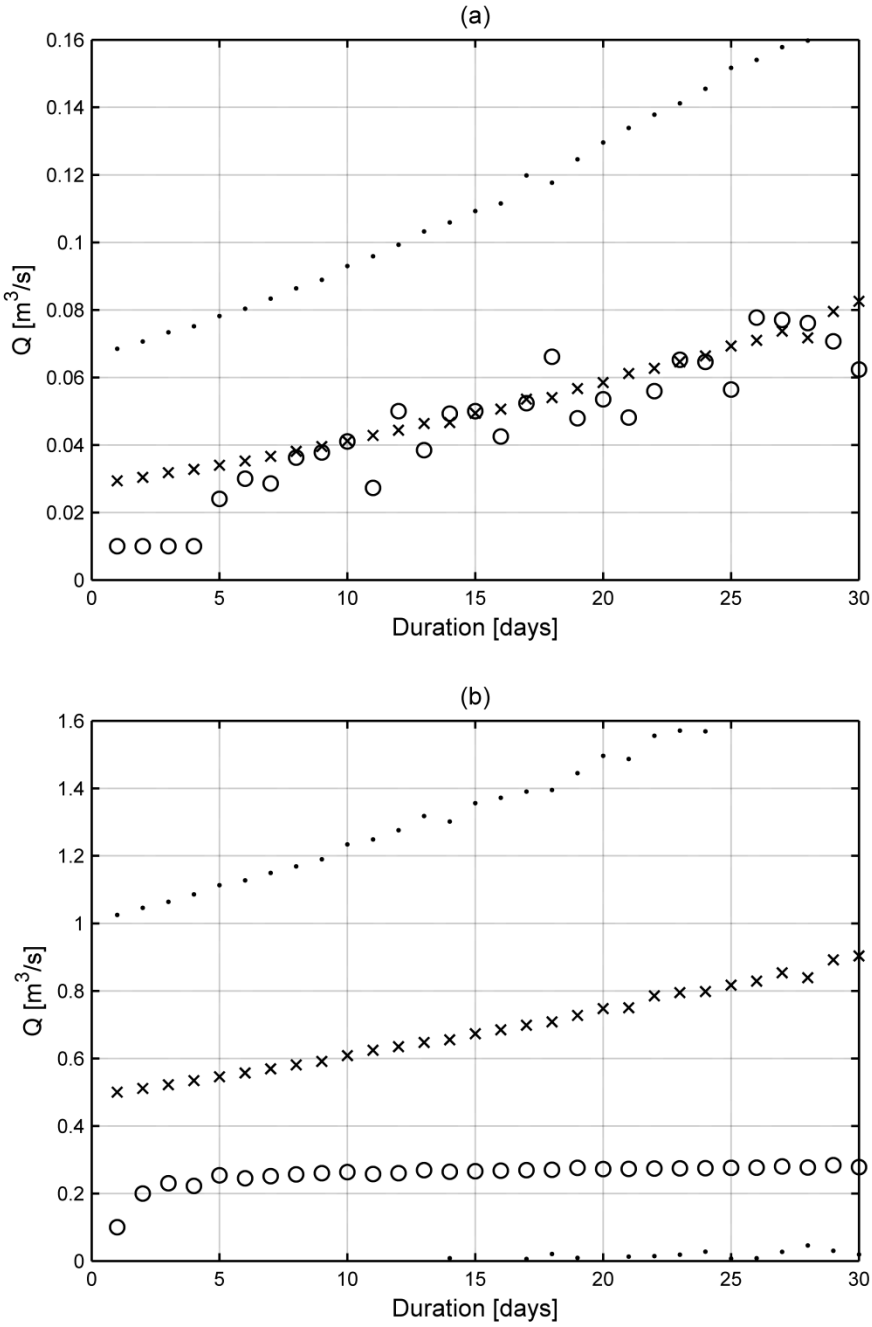
(a)
Q [m3/s]
Duration [days]
(b)
Q [m3/s]
Duration [days]

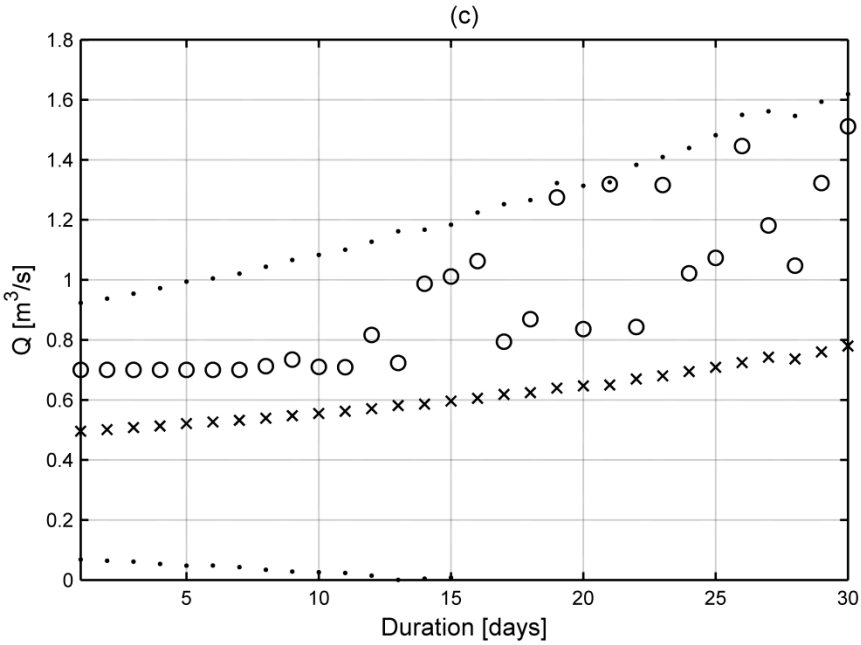

Fig. 4.10. Comparison of minimum mean discharges, averaged over different durations, between recorded (circle points) and synthetic (cross points) series with ± 2σ confidence limits (dotted points) – (a) Alento; (b) Scrivia; (c) Bormida

From a first graphical analysis of Fig. 4.10, one should notice that, for each case study, the recorded and generated series trends are both included within the 2σ confidence bands (following *Murrone et al.* [1997]). In particular, the best performance is that obtained for the Alento riverflow series, where an almost perfect superimposition of recorded and generated mean minimum flow values was obtained for each duration from 1 to 30 days. However, within the same case study, it has to be noticed the poorest results, if compared to those obtained for the other durations, are those pertinent to the shortest durations (from 1 to 4 days). The author connects this result to the adopted effective rainfall model (the so-called PWNE model) that, most likely, is not able to properly reproduce shortest-time statistical features given the limitation in the number of its parameters.

Considerably different results were instead achieved concerning the Scrivia (Fig. 4.10b) and Bormida (Fig. 4.10c) case study rivers. In the former case, indeed, it is possible to notice a certain increasing overall trend, for the synthetic streamflow series, in the mean minimum values from lowest to highest durations. On the contrary, the same trend is not recognizable for the recorded series, where, instead, the mean minimum flow value remains almost constant. This result is easily explicable by means of a detailed analysis of the Scrivia recorded streamflow series. As a matter of fact, from the corresponding 14 recording years, it is possible to notice a particularly long and anomalous dry period (that is, with a mean daily flow value minor than 0.5 m^3/s) from the second half of July to the first half of October, of the thirteenth year of the recorded sequence. As obvious, given that the parameters of the PWNE model, of the effective rainfall, had been estimated as mean values on each month of the year, they were not able to take into consideration of such an atypical occurrence, determining the evident difference in the global trend shown in Fig. 4.10b.

A considerable different situation concerns, instead, the Bormida River case study. As a matter of fact, Fig. 4.10c clearly shows an underestimation of the mean minimum flow values of the recorded series by the generated ones, for each duration d. Nevertheless, the overall increasing trend is quite similar to that of the historical sequence. However, it is evident the inability of the model in reproducing the considerable "peaks", of the mean minimum flow values, for some of the considered averaging durations, given that, as confirmed also by Fig. 4.10a-b, the model is only able to reproduce a regular increasing path of the minimum values over fixed durations. Such a limit is to be related to the aforementioned estimation procedure of the parameters of the PWNE model of the effective rainfall. As a matter of fact, the estimation of the couple of parameters λ and β on 13 "season", each of 28 days of

length, does not allow the correct reproduction of those particular streamflow events that can result in the "peaks" provided by Fig. 4.10c.

Hence, synthetically, results obtained by the comparison of mean minimum flows, averaged over different durations, between historical and generated series, provide that the calibrated model is able to satisfactory reproduce the recorded series path if two conditions are verified (see Fig. 4.10a concerning the Alento River):

- the absence, in the historical sequence, of singular long dry periods, which could be considered anomalous if compared to the standard dry periods;
- the absence of singular streamflow events, whose high intensity of the rainfall events, from which it originates, could be barely reproduced by the mean estimates of the parameter of the adopted model for the effective rainfall reproduction.

In order to overcome these limitations, the author is confident that the adoption of a more complex models for the reproduction of the effective rainfall phenomenon (e.g., the five-parameters Neyman-Scott cluster model) can be decisive. However, further analysis will be necessary in the immediate future to confirm this idea.

5. Conclusions

5.1. Thesis summary

In this thesis, a frequency-domain calibration procedure of SN-based models for streamflow modeling has been studied. It is now worthwhile to review the most important results and considerations achieved in the different sections of the thesis.

Section 2 has been devoted to provide the reader with a comprehensive and synthetic review of the techniques, available in the technical literature, aimed at the calibration of CT model. The first part of the section has been addressed to the definition of the major advantages of the application of a CT identification framework compared to a DT one, resulting in the general convenience of the former class of approaches. Subsequently, in a first subsection, a short survey of time-domain methods for the identification of CT models has been provided, while in a successive subsection the class of frequency-domain identification procedures has been dealt with. Finally, the two main advantages of the latter class of methods have been discussed, that can be summarized as:

(a) the possibility to replace large data sets, usually necessary in a time-domain framework, with a limited number of frequency-domain information on input and output signals;
(b) the possibility of combining data collected from different experiments that, on the contrary, is not easily possible in time-domain data procedures.

Section 3 has focused on that class of CT models known as *Shot Noise* (SN). In particular, in a first subsection, a comprehensive survey of the literature contributions to the topic has been provided, recognizing the model ability in the reproduction of short time scale discharge series, due to its aptitude to properly reproduce the presence of peaks and recessions, characteristic of daily discharge time series. Furthermore, a detailed mathematical description of SN processes, and relative properties, has been addressed. Particular attention has been paid to their spectral properties, which allow one to avoid the adoption of input processes data (e.g., rainfall series, evapotranspiration series etc.) in the calibration procedure presented in this thesis, which can be sees as the main contribution of the whole work, especially if compared to previous identification approach of SN models in the frequency domain.
Furthermore, after an overview on classical time-domain calibration procedures, the proposed spectral-domain calibration method has been presented. The objective response function, to be identified, is given by the linear combination of three parallel linear reservoirs, each with a different storage coefficient (representing the several groundwater contributions), and a fast surface runoff contribution. In order to estimate the response function parameters, the given procedure consists in a least-square fitting of the streamflow process PSD, through the squared module of the model TF, with unknown parameters. The form of the watershed response function has been thus provided, in order to allow proper definition of the unknown

parameters. Moreover, some details on the available techniques for the estimation of the output process PSD have been provided, focusing, in particular, on the selected maximum entropy (or all-poles) approximation.
The last part of Section 3 has dealt with the description of the PWNE model for the modeling of effective rainfalls. In particular, method of moments formulas for the estimation of its two parameters have been provided. Moreover, a description of the methods, available in the scientific literature, for the assessment of the effective pulses sequence has been addressed. Particular attention has been paid to the description of the so-called FPOT and MA procedures.

Eventually, the application and testing of the proposed calibration procedure have been addressed in Section 4. A detailed description of the three selected riverflow time series has been provided in a first subsection, highlighting the differences, in terms of climatic features, among the corresponding watersheds. In particular, two rivers associated to watersheds mostly influenced by the climate of the Alps (Scrivia and Bormida) and one characterized by a maritime rainfall regime (Alento) have been selected.
Thus, once provided some details on the multidimensional minimization approach selected for the least-square minimization of the cost function (i.e. the so-called Powell's method), estimations of the parameters value have been provided, together with the graphical result of the streamflow process PSD through the squared module of the TF.
Subsequently, in order to allow the overall quality of the obtained response function, a simulation analysis, consisting in the generation of 1000 synthetic streamflow series for each case study watershed, has been needed. For this purpose, the selection of the most suitable technique for the assessment of the sequences of effective rainfall pulses has been necessary.

Concerning this point, a detailed comparison, in terms of reproduction of the statistical features of the effective rainfall phenomenon, between the aforementioned FPOT and MA procedures has been undertaken. Obtained results have suggested the general convenience in the adoption of the latter approach, especially thanks to its capacity in the reproduction of the correct number of peak events per year.

Finally, statistical analysis on the generated series have been executed and reported in the last subsections of Section 4, in order to assess the overall quality of the obtained calibrations. In particular, the following synthetic results have been reported.

The estimated response functions have shown a certain effectiveness in the reproduction of the overall trend of the first three moments of the distribution, of the recorded streamflow series, averaged over the different months of the year. In particular, only a slight negative bias in the reproduction of the tails of the standard deviation of the distribution has been noticed, for all the case study series. Furthermore, the capacity in the reproduction of the total flow-volume in a certain period of observation has been evaluated. Results, provided in Section 4, have clearly shown a maximum overestimation equal to 6% of the total flow-volume, confirming the relevance, of the calibrated response function, in water resources management problems.

Moreover, other two statistical tests have been undertaken on the generated series. Firstly, Section 4 reports the comparison between recorded and generated series flow-duration curves, considered as an expression of their cumulative distribution functions. As clearly shown, the overall trend of the curve is quite well reproduced for all the three case studies. However, concerning the Scrivia River, a moderate underestimation (overestimation) of lowest (highest) frequency values is shown. Such a result has been

addressed to the presence, in the estimated response function, of a small direct runoff contribution, if compared to other groundwater components, which could suggest the adoption of a different modeling, in the response function form, of the direct runoff (e.g., by means of one or a cascade of identical linear reservoir).

At last, the capacity in the reproduction of minimum mean flow values, averaged over different durations (from 1 to 30 days), has been investigated. Remarkable results have been obtained for the Alento River, while some problems have arisen from the Scrivia and Bormida. As a matter of fact, in the former case, the model has not been able to "read" the presence, in the historical series, of an anomalous long dry period (which results in a constant trend of minimum mean flow values over different durations). While, concerning the Bormida River, even though the overall increasing trend has been correctly reproduced, the estimated solution has resulted unsuitable for the reproduction of the "peaks" in the minimum mean discharges, especially for the highest duration values. Both Scrivia and Bormida rivers unsatisfactory results have been related to the effective rainfall model estimation technique adopted in the thesis, which estimates the two parameter values of the PWNE model as mean values over 13 periods of 28 days each, in order to preserve the seasonal variability of the input process.

5.2. Further developments

Several aspects of the proposed work can be object of future developments to improve the quality of the presented calibration approach.

A first considerable contribution could concern the form of the response function, and thus of the corresponding TF, adopted in the frequency-domain

fitting of the streamflow process PSD. Indeed, as deeply outlined in Section 4, the poor results, in the reproduction of the historical flow-duration curve for the Scrivia River, are especially due to the absence of a strong direct runoff contribution. As a consequence, the adoption of a different response function form (e.g., with the direct runoff modeled by means of a cascade of 2 or 3 identical linear reservoirs) would result in different parameters estimate and, probably, in a better reproduction of the historical flow-duration curve.

A second relevant, and probably more effective, development could deal with the application of an alternative model for the effective rainfall process modeling. Indeed, as outlined in the previous subsection, some of the differences between recorded and simulated runoff series have been addressed to the implicit limitations in the adoption of the PWNE model. As a consequence, it appears that the adoption of a more complex model, characterized by a greater number of parameters (e.g., the five parameters-Neyman-Scott model with exponential instantaneous pulses, within a shot-noise model of daily streamflows), could result in a better reproduction of the real dynamics of the effective rainfall process, thus allowing the better fitting of the streamflow process statistics.

Eventually, the intention of the author is to adopt the know-how acquired for the development of the present thesis to the resolution of problems concerning the frequency-domain calibration of hydrologic models, not only in a SN framework.

Appendix

The aim of the present brief appendix is to clarify some fundamental issues to allow the reader a comprehensive understanding of some basilar concepts addressed in this thesis.

In the technical literature, a large variety of models is available for the description of rainfall-runoff transformations, each one suitable for the resolution of a particular class of hydrologic issue. Moreover, several authors attempted to classify rainfall-runoff models [e.g., *Todini*, 1988], even in absence of an universal criterion of classification. Among them, however, each existing classification recognizes the importance of the so-called *lumped-conceptual models*. Conceptual models are those determined by the arrangement of a small number of elements, each characterizing the simple representation of a physical relationship [*Dooge*, 1959]. Lumped models, instead, refer to the fact that the model parameters are averaged on the entire watershed [*Troutman*, 1985]. Among lumped-conceptual models, a great interest has always been received by the so-called Linear Compartmental Systems (LCSs) [*Jacquez*, 1985], given by the parallel and/or cascade connection of a certain number of linear reservoirs, i.e. subsystems characterized by a negative exponential impulse response. Some applications of this category of models within stochastic streamflows

generation problems are provided by *Murrone et al.* [1997], *Boyle* [2000] and *Claps et al*. [2005]. These models are usually characterized by two main properties:

- linearity: that is, the response of the model to a linear combination of two valid inputs is equal to the linear combination of the single response of the model to each input;
- time invariance: that is, the model parameters remain constant with the time.

The validity of the given properties leads to the definition of the so-called Linear Time Invariant (LTI) models, that can be synthetically defined as those systems where at any time instant t the current value of the output process, $Y(t)$, can be obtained as a linear combination of present and past input process, $U(t)$, values [*Priestly*, 1981, Section 1]. According to this assumption, in the case of LTI models, the relationship between input and output signals can be expressed in the following form:

$$Y(t) = \int_0^\infty h(\tau)U(t-\tau)d\tau \qquad \text{(A.1)}$$

where the function $h(\tau)$, known as *impulse response function*, describes the form of the output of the system when the input is an unit impulse function (that is a function which take a very large value at just one time point, is almost zero everywhere else, and has an unit area) centred at the origin [*Priestly*, 1981, Section 1].

From the definition (A.1), the *Transfer Function* (TF), of the LTI system, is a complex valued function obtained by the bilateral Laplace transform, $\mathcal{L}\{h(\tau)\}$, of the impulse response function [*Kailath et al.*, 2000, Chapter 6]:

$$H(s) = \mathcal{L}\{h(\tau)\} = \int_{-\infty}^{\infty} h(\tau)e^{-s\tau}d\tau \quad \text{(A.2)}$$

where $s = \sigma + j\omega$ (with j the imaginary unit), known as *complex* or *Laplace variable*, defines the complex plane (i.e. the existence domain of the TF, characterized by a x, or real-axis, σ, and a y, or imaginary-axis, $j\omega$, also known as frequency, ω, axis).

Given the TF form (A.2), the corresponding *frequency response*, $H(j\omega)$, is obtainable by the restriction of the Laplace domain to the points belonging to its positive-imaginary semi-axis (thus substituting $j\omega$ for s in the TF expression, setting the real part of the complex variable to zero) [*Sourdille and O'Dwyer*, 2004]. Hence, the frequency response function can be defined as the Fourier transform of the impulse response function [*Jenkins and Watts*, 1968, Subsection 2.3]. It is worth noticing that, in many identification problems, it is convenient to refer to the rational form of the frequency response, given by the following expression:

$$H(j\omega) = \frac{N(j\omega)}{D(j\omega)} = \frac{\sum_{k=0}^{n} \alpha_k (j\omega)^k}{\sum_{k=0}^{d} \beta_k (j\omega)^k} \quad \text{(A.3)}$$

where N and D are, respectively, numerator and denominator of the frequency response, defined as a function of the two polynomials of real parameters α_k and β_k. In particular, if these latter are coprime, i.e. they have no factors in common, the roots of N and D are called, respectively, *zeros* and *poles* of the system (also known as *singularities* of the TF) [*Kailath et al.*, 2000, Chapter 6].

The two aforementioned functions, $H(s)$ and $H(j\omega)$, are fundamental in the analysis of LTI systems. As a matter of fact, if one assumes that the input $U(t)$ consists of a sum of harmonic functions with different frequencies ω,

the output from the LTI system will similarly consists of a sum of harmonic functions with exactly the same frequencies. At each frequency, however, the harmonic functions result scaled in amplitude by a certain factor $G(\omega)$ (known as *gain* or *magnitude function*) and shifted in phase by an amount $\phi(\omega)$ (called *phase angle function*) [*Jenkins and Watts*, 1968, Subsection 2.3]. The TF of Eq. (A.2), or equivalently the corresponding frequency response function of Eq. (A.3), simply provides how, for each ω, the amplitude (and phase) of an input harmonic signal of that frequency is transformed into the amplitude (and phase) of the corresponding output wave [*Priestly*, 1981, Section 1].

In system identification theory, it is conventional to plot the gain function $G(\omega)$, expressed in decibel (that is, multiplying by 20 the decimal logarithm of the considered amount), against the logarithm of the frequency ω, and the phase function $\phi(\omega)$ against the logarithm of the frequency. These diagrams, known as *Bode plots*, allow one to graphically understand the behaviour of the system in terms of transformations of both gain and phase angle features of the harmonics that characterize the input signal $U(t)$, and their aspect is determined by the combination of poles and zeros of the TF in terms both of their typology (real or complex conjugate) and of their sign (positive or negative) (for a comprehensive description of Bode plots and their utility in system identification theory, refer to *Bolzern et al.* [2004, Subsection 6.6.1]). Furthermore, some interesting examples of Bode plots, for different types of TFs with different combinations of its poles and zeros values, are provided by *Jenkins and Watts* [1968, Subsection 2.3].

References

Ahmed, J. A., and A. K. Sarma (2005), Genetic Algorithm for Optimal Operating Policy of a Multipurpose Reservoir, Water Resources Management, Volume 19, Number 2, pp. 145-161.

Aksoy, H. (2003), Markov chain-based modeling techniques for stochastic generation of daily intermittent streamflows, Adv. Water Resour., 26, pp. 663–671.

Anderson, B. (1985), Identification of scalar errors-in-variables models with dynamics, Automatica, 21, (6), pp. 709–716.

Astrom, K. J. (1969), On the choice of sampling rates in parametric identification of time series, Information Sciences 1 (1), 273-278.

Bandini, A. (1931), Tipi pluviometrici dominanti nelle regioni italiane, Servizio Idrografico Italiano, Roma (in Italian).

Battaglia, F. (1986), Modelli stocastici per la rappresentazione e la previsione dei deflussi, Dept. of Statistics Papers, No. 3, Univ. di Roma "La

Sapienza", Dip. di Statistica, Probabilità e Statistica Applicata, Rome (in Italian).

Bayazit, M., and H. Aksoy (2001), Using wavelets for data generation. J Appl Stat, 28(2): 157–166.

Bernier, J. (1970), Inventaire des modeles de processus stochastiques applicables a la description des debits journaliers des rivieres, Revue Inst Intern Stat; 38(1): 49–61.

Bloeschl, G., and M. Sivapalan (1995), Scale issues in hydrological modelling: A review, Hydrol. Processes, 1995, 9, 251– 290.

Bo, Z., S. Islam, and E. A. B. Elthair (1994), Aggregation-disaggregation properties of a stochastic rainfall model, Water Resour. Res. 30(12), 3423-3435.

Bolzern, P., R. Scattolini, and N. Schiavoni (2004), Fondamenti di controlli automatici, II edition, McGraw Hill, Milano (Italy) (in Italian).

Boughton, W. C., and O. P. Droop (2003), Continuous simulation for design flood estimation - a review, Environ. Model. Softw., 18 (4), 309-318.

Box, G. E. P., G. M. Jenkins, and G. C. Reinsel (1994), Time Series Analysis, Forecasting and Control, (third ed.) Englewood Cliffs, New Jersey, Prentice Hall.

Boyle, D. P. (2000), Multicriteria calibration of hydrological models, Ph. D. dissertation, Dep. of Hydrol. and Water Resour., Univ. of Ariz., Tempe.

Broersen, P. M. T. (1995), A Comparison of Transfer Function Estimators, IEEE Transactions on Instrumentation and Measurements, vol. 44, no. 3, pp. 657-661.

Burg, J. P. (1975), Maximum entropy spectral analysis, Ph. D. Thesis, Stanford University, Palo Alto., California.

Castiglioni, S., L. Lombardi, E. Toth, A. Castellarin, and A. Montanari (2010), Calibration of rainfall-runoff models in ungauged basins: A regional maximum likelihood approach, Adv. Water Resour., 33,1235–1242.

Chang, L. C, and F. J Chang (2001), Intelligent control for modeling of real time reservoir operation, Hydrological Processes, 15, pp. 1621–1634.

Claps, P., A. Giordano, and F. Laio (2005), Advances in shot noise modeling of daily streamflows, Adv. Water Resour., 28: 992–1000.

Claps, P., and F. Laio (2003), Can continuous streamflow data support flood frequency analysis? An alternative to the partial duration series approach, Water Resour. Res., 39 (8), p. 1216.

Claps, P., F. Rossi, and C. Vitale (1993), Conceptual-stochastic modeling of seasonal runoff using Autoregressive Moving Average Models and different scales of aggregation, Water Resour. Res. 29(8), 2545-2559.

Cowpertwait, P. S. P. and P. E. O'Connell (1992), A Neyman-Scott shot noise model for the generation of daily streamflow time series, Advances in Theoretical Hydrology, Part A, Chap. 6. Elsevier, The Netherlands.

Di Nunno, U. (1981), Analisi statistica delle massime piogge in Campania, Unpublished thesis, University of Naples (in Italian).

Diskin, M. H. (1964), A basic study of the linearity of the rainfall-runoff process in watersheds, Ph. D. thesis, Dep. of Civ. Eng., Univ. of Ill., Urbana.

Diskin, M. H. and G. G. S. Pegram (1987), A study of cell models: 3. A pilot study on the calibration of manifold cell models in the time domain and in the Laplace domain, Water Resour. Res., Vol.23, No.4, pp.663-673.

Dooge, J. C. I. (1959), A general theory of the unit hydrograph theory, J. Geophys. Res. 64 (2), 241–256.

Eagleson, P. S. (1978), Climate, soil, and vegetation: 2. The distribution of annual precipitation derived from observed storm sequences, Water Resour. Res., 14(5), 713-721.

Efstratiadis, A., Y. G. Dialynas, S. Kozanis, and D. Koutsoyiannis (2014), A multivariate stochastic model for the generation of synthetic time series at multiple time scales reproducing long-term persistence, Environmental Modelling and Software, 62, 139–152.

Eykhoff, P. (1974), System identification, Wiley, New York.

Hino, M. and M. Hasebe (1981), Analysis of hydrologic characteristics from runoff data - A hydrologic inverse problem, Jour. of Hydrol., 49(3/4), 287-313.

Hino, M., and M. Hasebe (1984), Identification and prediction of nonlinear hydrologic systems by the filter-separation autoregressive (AR) method: extension to hourly hydrologic data, Jour. of Hydrol., 68: 181-210.

Hipel, K. W., and A. I. McLeod (1994), Time Series Modeling of Water Resources and Environmental Systems, Elsevier, Amsterdam.

Ilich, N. (2014), An effective three-step algorithm for multi-site generation of weekly stochastic hydrologic time series, Hydrol. Sci. J., 59 (1), 85-98.

Islam, M., and B. Sivakumar (2002), Characterization and prediction of runoff dynamics: a nonlinear dynamical view, Advances in Water Resources, 25(2): 179–190.

Jacquez, J.A. (1985), Compartmental analysis in biology and medicine, 2nd edition (Ann Arbor: University of Michigan Press).

Jenkins, G. M., and D. G. Watts (1968), Spectral Analysis and Its Applications. Holden-Day, 525 pp.

Kailath, T., A. H. Sayed, and B. Hassibi (2000), Linear estimation, Prentice-Hall, Upper Saddle River, NJ.

Kallstrom, C. G., T. Essebo, and K. J. Astrom (1976). A computer program for maximum likelihood identification of linear multivariable, stochastic systems, Proc. 4th IFAC, Symposium on Identification and System Parameter Estimation, Tbiliss.

Karamouz, M., and M. H. Houck (1987), Comparison of stochastic and deterministic Dynamic programming for reservoir operating rule generation, Water Resources Bulletin, Bethesda, v. 23, n. 1, p. 1-9.

Karamouz, M., M. H. Houck, and J. W. Delleur (1992), Optimization and simulation of multiple reservoir systems, Journal of Water Resources Planning and Management, Vol. 118 (1).

Kavvas, M. L. and J. W. Delleur (1981), A stochastic cluster model of daily rainfall sequences, Water Resour. Res, 17(4), 1151-1160.

Kirchner, J. W., X. Feng, and C. Neal (2000), Fractal stream chemistry and its implications for contaminant transport in catchments, Letters to Nature, 403: 524–527.

Koch, R. W. (1985), A stochastic streamflow model based on physical principles, Water Resour. Res., 21(4): 545–53.

Labat, D., R. Ababou, and A. Mangin (2000), Rainfall–runoff relations for karstic springs. Part II: Continuous wavelet transform and multiresolution analyses, J. Hydrol., 238, 149–178.

Lall, U., and A. Sharma (1996), A nearest neighbor bootstrap for resampling hydrologic time series, Water Resour. Res., 32(3), 679–693.

Ljung, L. (1987), System identification: theory for the user, Prentice-Hall, Inc, Englewood Cliffs, NJ.

Montanari, A., and E. Toth (2007), Calibration of hydrological models in the spectral domain: An opportunity for ungauged basins?, Water Resour. Res., 43, W05434.

Muratori, S., C. Piccardi, and S. Rinaldi (1992), On the minimum phase of compartmental systems, Int. J. Control., 56, pp. 23–34.

Murrone, F., F. Rossi, and P. Claps (1997), Conceptually-based shot noise modeling of streamflows at short time interval, Stoch. Hydrol. Hydrau., 11:483–510.

Nikias, C. L., and J. M. Mendel (1993), Signal processing with higher-order spectra, IEEE Signal Processing Magazine, 1053-5888.

O'Connell, P. E., and D. A. Jones (1979), Some experience with the development of models for the stochastic simulation of daily flows, Inputs for Risk Analysis in Water Resources, pp. 287-314, Water Resour. Publ., Fort Collins, CO.

Ouarda, T. B. M. J., J. W. Labadie, and D. G. Fontane (1997), Indexed sequential hydrologic modeling for hydropower capacity estimation, Journal of the American Water Resources Association, 33 (6), pp. 1337–1349.

Papoulis, A., and S. U. Pillai (2002), Probability, Random Variables, and Stochastic Processes, McGraw-Hill, New York.

Parajka, J., R. Merz, and G. Bloeschl (2005), A comparison of regionalization methods for catchment model parameters, Hydrol. Earth Syst. Sci., 9, 157–171.

Pegram, G. G. S. (1980). A continuous streamflow model, Journal of Hydrology, Vol.47, pp. 65-89.

Penta, A., and F. Rossi (1979), Appunti di idrologia – Parte I: caratteristiche dei bacini idrografici, Università di Napoli, Facoltà di Ingegneria, Istituto di Idraulica e Costruzioni Idrauliche. (in Italian).

Pintelon, R., P. Guillaume, Y. Rolain, J. Schoukens, and H. Van Hamme (1994), Parametric identification of transfer functions in the frequency domain - A survey, IEEE Trans. Autom. Control, 39, (11), pp. 2245-2260.

Post, D. A., and A. J. Jakeman (1999), Relationships between catchment attributes and hydrological response characteristics in small Australian mountain ash catchments, Hydrol. Processes, 10, 877– 892.

Powell, M. J. D. (1964), An efficient method for finding the minimum of a function of several variables without calculating derivatives, Comput. J., 7: 155-162.

Prairie, J. R., B. Rajagopalan, T. J. Fulp, and E. A. Zagona (2006), Modified K-NN model for stochastic streamflow simulation, J. Hydrol. Eng., 11(4), 371–378.

Press, W.H., S. A. Teukolsky, W. T. Vetterling, and B. P. Flannery (1996), Numerical Recipes in Fortran 77: The Art of Scientific Computing, 2nd ed., Cambridge University Press, New York.

Priestly, M. B. (1981), Spectral Analysis and Time Series, London, England, Academic Press.

Raman, H., and N. Sunilkumar (1995), Multivariate modeling of water resources time series using artificial neural network, Hydrol Sci J 40(2): 145–163.

Rao, G. P., and H. Unbehauen (2006), Identification of continuous-time systems, IEE Proc. - Control Theory Appl., 152, 185-220.

Roberts, J. B. (1965), The response of linear vibratory systems to random impulses, Journal of Sound and Vibration 2, 375-390.

Rodriguez-Iturbe, I., D. L. Cox, and V. Isham (1987), Some models for rainfall based on stochastic point processes, Proc. R. Soc. Lond. A 410, 269-288.

Rossi, F., and P. Villani (1995), Leggi regionali di crescita con il periodo di ritorno. Valutazione delle Piene in Campania, C.N.R. Report, Rossi and Villani (Eds.), 99-162 (in Italian).

Rossi, F., M. Fiorentino, and P. Versace (1984), TCEV distribution for flood frequency analysis, Water Resour. Res., 20(7): 847-856.

Schaefli, B., and E. Zehe (2009), Hydrological model performance and parameter estimation in the wavelet-domain, Hydrol Earth Syst Sci, 13:1921–36.

Schoukens, J., R. Pintelon, and H. Van Hamme (1994), Identification of linear dynamic systems using piecewise constant excitations: use, misuse and alternatives, Automatica, 30, (7), pp. 1153–1169.

Searcy, J. K. (1959), Flow duration curves, U. S. Geological Survey Water.

Seibert, J., and J. J. McDonnell (2002), On the dialog between experimentalist and modeler in catchment hydrology: use of soft data for multicriteria model calibration, Water Resour. Res., 38(11), 1241.

Soderstrom, T., and P. Stoica (1989), System identification, Prentice-Hall, Englewood Cliffs, NJ.

Solo, V. (1978), A unified approach to recursive parameter estimation, Rep. No. AS/R20, Centre for Resource and Environmental Studies, Australian National University.

Sourdille, P., and A. O'Dwyer (2004), Determination of the phase of a transfer function: theory versus practice, Proceedings of the 13th European Conference on Mathematics for Industry, Eindhoven, Netherlands.

Srikanthan, R., and T. A. McMahon (1980), Stochastic generation of monthly flows for ephemeral streams, J Hydrol, 47(2): 19–40.

Stepner, D. E., and R. K. Mehra (1973), Maximum likelihood identification and optimal input design for identifying aircraft stability and control derivates, NASA Rep. No. NASA CR-2200.

Stoica, S., and R. L. Moses (2005), Spectral Analysis of Signals, Prentice-Hall, Upper Saddle River, New Jersey, Supply Paper, 1542-A.

Thornthwaite, W. (1948), An approach toward a rational classification of climate, Geogr. Rev. Vol. 38 (1).

Todini, E. (1988), Rainfall-Runoff Modeling-Past, Present, and Future., Journal of Hydrology, 100: 341-352.

Treiber, B., and E. J. Plate (1977), A stochastic model for the simulation of daily flows, Hydrological Sciences Bulletin, XXII, 1 3/1977, 175-192.

Troutman, B.M. (1985), Errors and Parameter Estimation in Precipitation-Runoff Models, Water Resources Research 21 (8): 1195-1222.

Tsekouras, G., and D. Koutsoyiannis (2014), Stochastic analysis and simulation of hydrometeorological processes associated with wind and solar energy, Renew. Energy 63, 624-633.

Unbehauen, H., and G. P. Rao (1997), Identification of continuous-time systems - A tutorial, Proc. 11th IFAC, Symposium on Identification (SYSID'97), Fukuoka, Japan, pp. 1023–1049.

Valencia, D., and J. C. Schaake (1973), Disaggregation processes in hydrology, Water Resour. Res., 9, pp. 580–585.

Vandewiele, G. L. and A. Dom (1989), A non-Gaussian multicomponent model for river flow, Water Resour. Res., 25(a), 397-404.

Wang, Z. M., and G. L. Vandewiele (1994), Stochastic simulation of streamflow with short time interval, Coping with Floods, pp. 257-269, NATO ASI Series E, Vol. 257, Kluwer, Dordrecht, The Netherlands.

Weiss, G. (1973), Shot noise models for synthetic generation of multisite daily streamflow data, Symposium Unesco, World Meteorel. Organ., Int. Ass. Of Hydrol. Sci., Madrid.

Weiss, G. (1977), Shot noise models for the generation of synthetic streamflow data, Water Resour Res, 13(1): 101–8.

Whittle, P. (1953), Estimation and information in stationary time series, Ark Mat, 2:423–34.

Xu, Z. X., A. Schumann, and B. Carsten (2001), Markov autocorrelation pulse model for two-sites daily streamflow generation, Journal of Hydrological Engineering, American Society of Civil Engineers 6(3): 189–195.

Xu, Z. X., G. A. Schultz, and A. Schumann (2002), A conceptually based stochastic point process model for daily stream-flow generation, Hydrol. Process, 16:3003–17.

Yakowitz, S. J. (1977), Computational probability and simulation, Addison-Wesley, Reading, Massachusetts.

Yakowitz, S. J. (1979), A nonparametric Markov model for daily river flow, Water Resour. Res., 15(5), 1035-1043.

Young, P. C. (1976), Some observations on instrumental variable methods of time-series analysis, Int. J. Control 23, 593.

Young, P. C. (1981), Parameter estimation for continuous-time models - A survey, Automatica 17 (1), 23-39.

Young, P. C., and H. Garnier (2006), Identification and estimation of continuous-time, data-based mechanistic (DBM) models for environmental systems, Environ. Model. Software, 21, 1055–1072.

Young, P.C. (1964), In flight dynamic checkout e a discussion, IEEE Transactions on Aerospace 2, 1106-1111.